SUBSTRATE - LEVEL CONTROL OF GLUCOSE METABOLISM IN C2C12 MYOTUBES

A Dissertation
Presented to
The Academic Faculty

by

Chia George Hsu

In Partial Fulfillment
of the Requirements for the Degree
Doctor of Philosophy in the
School of Applied Physiology

Georgia Institute of Technology
May 2016

SUBSTRATE - LEVEL CONTROL OF GLUCOSE METABOLISM IN C2C12 MYOTUBES

Approved by:

Dr. Thomas J. Burkholder, Advisor
School of Applied Physiology
Georgia Institute of Technology

Dr. Young C. Jang
School of Applied Physiology
Georgia Institute of Technology

Dr. Mindy L. Millard-Stafford
School of Applied Physiology
Georgia Institute of Technology

Dr. S. Russ Price
School of Medicine
Emory University

Dr. Edward M. Balog
School of Applied Physiology
Georgia Institute of Technology

Date Approved: March 14, 2016

ACKNOWLEDGEMENTS

I would like to thank my advisor Dr. Burkholder for the support and guidance of my Ph.D study. Thank you for spending so much time to discuss, to answer questions and to make constructive comments. I may not remember everything you taught me, but I will never forget your attitudes toward doing science. Thank you from the bottom of my "Cell".

I would like to thank my committee members: Dr. Millard-Stafford, Dr. Balog, Dr. Jang, and Dr. Price. Particularly, I would like to thank Dr. Millard-Stafford for her care, smile and encouragement for the past few years. I want to be a teacher like her! Thank you, Dr. Balog for sharing his lab equipment with me and always being able to help. Thank you, Dr Jang for joining my committee right before my proposal and sharing with me his great postdoc experience. Thank you, Russ for his time, input and interest in my project. I appreciate you all and thank you.

I would like to thank my senior labmate, Jill for teaching me several techniques and for willing to support me even though you have graduated. Thank you to Eun Shin for your help in seahorse experiment. Thank you to Matt Mosgrove and Mike Mallow for your help in the lab running the many gels needed.

Thank you to my mother, father and stepmother for your financial and spiritual support all the time. I would like to especially thank my wife, Zona, for your support, understanding, and love for the past 6 years. Thank you to my senior friends, Dave, Philip, Bruce, Nancy, Joe, and Mei for all of your care. Thank you to all SGI members in Atlanta for your spiritual support. Thank you to president Ikeda for his daily encouragement.

I would like to thank all of the staff within School of Applied Physiology for supporting administrative operations during my Ph.D study. Finally, I would like to thank the Ministry of Education in Taiwan and School of Applied Physiology for their financial support.

TABLE OF CONTENTS

Page

ACKNOWLEDGEMENTS iv

LIST OF TABLES ix

LIST OF FIGURES x

LIST OF ABBREVIATIONS xi

SUMMARY xiii

INTRODUCTION....1

1.1 CONTRACTILE ACTIVITY IMPOSES GREAT METABOLIC LOAD....1

1.1.1 Metabolic pathways....2

1.1.2 Redox state....4

1.1.3 Phenotypic specialization....5

1.2 RESPONSE TO CONTRACTILE ACTIVITY....7

1.2.1 Immediate metabolic perturbation....7

1.2.2 Functional accommodation....9

1.2.3 Long-term metabolic adaptation....13

1.3 METABOLIC SIGNALING....14

1.3.1 AMP signaling....14

1.3.2 NAD-dependent signaling....17

1.3.3 Interaction of AMP and NAD signaling....19

1.4 PROPOSED MODEL / HYPOTHESIS....22

1.5 SPECIFIC AIMS....24

1.6 EXPERIMENTAL METHODS 25

1.6.1 C2C12 myotubes *25*

1.6.2 NAD supplementation *26*

1.6.3 Metabolic assay *27*

ACTIVATION OF P38 IN C2C12 MYOTUBES FOLLOWING ATP DEPLETION DEPENDS ON EXTRACELLULAR GLUCOSE 29

2.1 ABSTRACT 29

2.2 INTRODUCTION 30

2.3 MATERIALS AND METHODS 34

2.4 RESULTS 38

2.5 DISCUSSION 53

MODULATION OF GLUCOSE METABOLISM AND AMPK ACTIVITY THROUGH REDOX STATE AND ROS IN C2C12 MYOTUBES 58

3.1 ABSTRACT 58

3.2 INTRODUCTION 59

3.3 MATERIALS AND METHODS 61

3.4 RESULTS 64

3.5 DISCUSSION 69

INDEPENDENT AMP AND NAD SIGNALING REGULATE C2C12 DIFFERENTIATION AND METABOLIC ADAPTATION 72

4.1 ABSTRACT 72

4.2 INTRODUCTION 73

4.3 MATERIALS AND METHODS 75

4.4 RESULTS 81

4.5 Discussion 89

CONCLUSION 94

5.1 Summary 94

5.2 Implications 98

5.3 Future Directions 100

REFERENCES 102

VITA 120

LIST OF TABLES

Page

TABLE 4-1 LIST OF TARGETS AND PRIMERS USED IN QUANTITATIVE PCR 80

LIST OF FIGURES

Page

FIGURE 1-1 GLUCOSE METABOLITES AND PDH, LDH FLUX AFTER EXERCISE 12

FIGURE 1-2 PROPOSED MODEL 22

FIGURE 2-1 EFFECT OF ROTENONE ON ATP CONTENT AND KINASE ACTIVITY 39

FIGURE 2-2 THE TIME COURSE OF ATP CONTENT AND KINASE ACTIVITY 41

FIGURE 2-3 MORPHOLOGY OF C2C12 MYOTUBES 43

FIGURE 2-4 THE EFFECT OF DORS ON ROTENONE POISONING 45

FIGURE 2-5 EFFECT OF AICAR ON PHOSPHORYLATION OF ACC AND P38 46

FIGURE 2-6 THE INFLUENCE OF SB203580+ BIRB ON ROTENONE POISONING 48

FIGURE 2-7 THE EFFECT OF CYTOCHALASIN B ON THE ROTENONE POISONING 50

FIGURE 2-8 EFFECT OF GLUCOSE RESTRICTION ON ROTENONE POISONING 52

FIGURE 3-1 EFFECT OF PMS ON CELLULAR NAD AND ROS PRODUCTION 66

FIGURE 3-2 EFFECT OF PMS ON ATP AND THE PHOSPHORYLATION OF ACC AND PDH ... 67

FIGURE 3-3 EFFECT OF PMS ON OCR AND ECAR 68

FIGURE 4-1 EFFECT OF AICAR AND NMN ON AMP AND NAD SIGNALING 82

FIGURE 4-2 EFFECT OF NMN SUPPLEMENTATION ON NAD CONTENT 84

FIGURE 4-3 EFFECT OF AICAR AND NMN ON METABOLIC GENE EXPRESSION 86

FIGURE 4-4 EFFECT OF AICAR AND NMN ON DIFFERENTIATION GENE EXPRESSION 88

FIGURE 5-1 REVISED MODEL IN C2C12 MYOTUBES 97

LIST OF ABBREVIATIONS

ACC	Acetyl-CoA carboxylase
AICAR	5-Aminoimidazole-4-carboxamide ribonucleotide
AMP	Adenosine monophosphate
AMPK	AMP-activated protein kinase
ATP	Adenosine triphosphate
COX2	Cytochrome c oxidase subunit II
CS	Citrate synthase
Dors	Dorsomorphin
ECAR	Extracellular acidification rate
GLUT4	Glucose transporter type 4
H_2DCFDA	2',7' –dichlorofluorescin diacetate
H3K9	Histone H3 lysine 9
HK1	Hexokinase I
LDH	Lactate dehydrogenase
MAPK	Mitogen-activated protein kinase
MYH3	Myosin heavy chain III
NAD	Nicotinamide adenine dinucleotide
Nampt	Nicotinamide phosphoribosyltransferase
NMN	Nicotinamide mononucleotide
OCR	Oxygen consumption rate

PDH	Pyruvate dehydrogenase
PDK	Pyruvate dehydrogenase kinase
PFK	Phosphofructokinase
PGC-1α	Peroxisome proliferator-activated receptor gamma coactivator 1-alpha
PMS	Phenazine methosulfate
ROS	Reactive oxygen species
SIRT1	Silent mating type information regulation 2 homolog 1
Tfam	Mitochondrial transcription factor A

SUMMARY

Metabolic flexibility is critical for muscle to maintain proper function and overall health. Muscle adapts to metabolic stress with increasing ATP synthesis by enhancing the rate of glycolysis and mitochondrial respiration. The control of that rate is mediated by several glucose metabolites. This project is based on the conceptual model that AMP indicates the balance of ATP synthesis and degradation, and NADH indicates the balance of glucose delivery to oxygen delivery. AMP signaling facilitates all aspects of glucose metabolism, and NAD^+ signaling facilitates oxidative metabolism and inhibits reductive metabolism. The overall hypothesis is that the distribution of glucose depends on AMP and NAD^+ generated during energetic stress.

The results suggest that glucose metabolism is highly sensitive to ATP homeostasis via AMPK activity. NADH oxidation alone is not sufficient to influence glucose oxidation, but require co-activation of AMPK. AMP and NAD^+ signaling work independently in metabolic gene expression. The overall conclusion is that glucose metabolism depends on AMP signaling, but NAD signaling is unable to alter glucose disposal. AMP and NAD independently induced metabolic and differentiation adaptation. These findings suggest that other molecule may represent an additional gauge of aerobic and anaerobic metabolism.

1 CHAPTER

INTRODUCTION

1.1 Contractile activity imposes great metabolic load

Muscle contractile function requires the coordinated activity of membrane excitation, excitation-contraction coupling, contraction, and energy supply. Transmission of the signal from motor neuron into muscle fiber initiates contraction. Ca^{2+} is released from sarcoplasmic reticulum (SR), the intracellular storage site, to trigger the contractile response and sequestered by the sarcoplasmic/endoplasmic reticulum Ca^{2+}-ATPase (SERCA) pumps to permit relaxation (Maclntosh et al., 2005).

During exercise, intramuscular oxygen consumption and local blood flow increases. Glucose delivery, transport and metabolism are up-regulated in response to increasing ATP turnover. ATP consumption during muscle contraction dominantly comes from myofibrillar ATPase for cross-bridge cycling, and from Na^{+}-K^{+} exchange and SERCA for ionic transport (Schiaffino and Reggiani, 2011). The intracellular store of ATP is small, around 1-10 mM (Beis and Newsholme, 1975), but ATP concentration rarely declines below 50% of rest values (Hochachka and Matheson, 1992). During muscle contraction, the rate of ATP turnover can increase 500-fold or more. For example, ATP turnover rate in human muscle at rest is between 0.004 and 0.008 mM/s in hand and leg muscles (Amara et al., 2007). ATP turnover rate in human anterior tibialis and vastus lateralis muscle increased to 2.45mM/s (Jones et al., 2009) and 6-9 mM/s (Jacobs et al.,

1982) during muscle contraction. To facilitate such huge variations in ATP consumption, fast and efficient mechanisms of ATP resynthesis are needed.

1.1.1 Metabolic pathways

Energy for contraction comes from phosphocreatine (PCr)-creatine kinase (CK) system, glycolysis, and mitochondrial respiration (Lanza et al., 2005). For relatively brief periods of activity, skeletal muscle is able to renew it supply of ATP from PCr. The PCr-CK system dominates the total ATP regeneration during 5 to 6 seconds duration of maximal exercise and it is localized close to the sites of ATP consumption (Greenhaff et al., 1994). PCr exists in the resting muscle at four times the concentration of ATP and serves as a high-energy phosphate reservoir for the rapid regeneration of ATP. (McMahon and Jenkins, 2002).

Glycolysis is the stepwise degradation of glucose and is the major source of metabolic energy for exercise longer than a few seconds. Glycolysis can be separated into two phases. Phase I involves hexose phosphates and ATP consumption in each of the hexokinase (HK) and phosphofrucktokinase (PFK) reactions. In phase II, fructose 1,6-biphosphate is broken to yield dihydroxyacetone phosphate and glyceraldehydes 3-phosphate. The dihydroxyacetone phosphate is rapidly converted to glyceraldehyde 3-phosphate by triosephosphate isomerase. Two molecules of glyceraldehyde 3-phosphate then follow the same pathway in the second phase of glycolysis. The net reaction for the overall process generates two molecules of pyruvate, two molecules of NADH, and two ATP (Ortenblad and Nielsen, 2015). The equilibrium constants for HK, PFK and pyruvate kinase (PK) in skeletal muscle are much larger than the mass action ratios

suggesting that HK, PFK and PK are the rate limiting steps in the glycolysis (Beatty et al., 1976). Furthermore, these three kinases are all subject to allosteric regulation that controls the flow of carbon through the pathway and maintains constant levels of metabolic intermediates (Beatty et al., 1976).

In the presence of sufficient oxygen, pyruvate from glycolysis provides acetyl CoA for mitochondrial oxidative phosphorylation (Dashty, 2013). Each acetyl CoA from glycolysis or β-oxidation can generate 18 ATP with a consumption of oxygen in a ATP/O_2 ratio of 2.6 (Schiaffino and Reggiani, 2011). Mitochondria oxidize acetyl CoA to carbon dioxide during TCA cycle and generate reducing equivalents in the form of NADH and $FADH_2$. The electrons produced from the oxidation of NADH and $FADH_2$ flow through the electron transport chain (ETC), which contains four distinct protein complexes in the mitochondrial inner membrane and two mobile electron carriers-coenzyme Q and cytochrome c. The ETC reoxidizes NADH and $FADH_2$ from the TCA cycle and the liberated electrons move from a negative to a positive reduction potential along the complex until molecular oxygen is reduced to water. Oxygen molecules undergo one-or two-electron reduction reaction to form O_2. or H_2O_2 during aerobic respiration. A previous study has shown that mitochondrial complex I and III are the primary source of ROS production (St-Pierre et al., 2002). The ETC transports protons from the matrix to the cytosolic side of the inner membrane, and the ATP synthase utilizes the resulting proton gradient to produce ATP from inorganic phosphate (Pi) and ADP (Dashty, 2013). The capacity of oxidative respiration is largely limited by mitochondrial content and oxygen delivery (Jackman and Willis, 1996; Katz and Sahlin, 1987). Due to the long-range of electron transfer within mitochondria, the migration and

redox state of cytochrome c may also limit ETC activity (Mathai et al., 1993; Volkov and van Nuland, 2012).

1.1.2 Redox state

The redox state of muscle is critically dependent on the oxidation of glucose to CO_2. NAD is a ubiquitous cellular coenzyme acting as a carrier of electrons and transferring it from one molecular to another. NAD^+/NADH redox pair regulates flux through glycolysis, TCA cycle, and mitochondrial ETC. In glycolysis, NADH is generated via glyceraldehydes 3-phosphate dehydrogenase (GAPDH) by the conversion of glyceraldehyde 3-phosphate to glycerate 1,3-bisphosphate. NADH is reoxidized via lactate dehydrogenase (LDH) during the reduction of pyruvate to lactate. The coordinated flux through GAPDH and LDH continually regenerates NAD^+, thereby ensuring glycolytic flux (Ussher et al., 2012; Ying, 2008). Under oxidizing conditions, pyruvate is further metabolized by the mitochondria. Pyruvate dehydrogenase complex (PDH) catalyzes the conversion of pyruvate to acetyl CoA. Because NADH cannot freely cross the inner mitochondrial membrane, malate dehydrogenase and glycerol 3-phosphate shuttles are necessary for transporting NADH produced during glycolysis into mitochondria and subsequently regenerating cytosolic NAD^+ (McKenna et al., 2006). In the TCA cycle, acetyl CoA is oxidized by several NAD^+/NADH enzymes to generate NADH. These enzymes include isocitrate dehydrogenase, α-ketoglutarate dehydrogenase, and malate dehydrogenase coupling the oxidation of isocitrate, α-ketoglutarate, and malate, respectively, to the generation of NADH (Ussher et al., 2012). In mitochondrial ETC, the oxidation of NADH occurs at complex I and is coupled to the reduction of lipid

soluble ubiquinone, and the translocation of four protons per pair of electrons is transferred. The proton gradient across the inner mitochondrial membrane provides the potential energy to drive the synthesis of ATP via ATP synthase (Dashty, 2013). Numerous processes in glucose metabolism are influenced either directly or indirectly by the NAD^+/NADH. Therefore, disturbances or dysregulation of the redox state are likely to affect energy homeostasis and plasticity in the muscle and the decrease in the ratio of NAD^+/NADH is associated with diabetes-related alternations (Ido, 2007).

1.1.3 Phenotypic specialization

Skeletal muscle is a dynamic tissue with considerable specialization depending on use. There are three major muscle types (one slow and two fast) in human body. Type 1 (slow twitch), type 2A, and type 2X (fast witch) fibers are known to contain different myosin heavy chain (MyHC) composition, which are responsible for their different myosin ATPase activity (Han et al., 2003; He et al., 2000), and speed of shortening (Weiss et al., 2001).

ATPase activity in slow fibers was considerably low (0.045 mM/s) (Bottinelli et al., 1994). The amount of ATP consumed per unit tension is lower in slow (0.66 mM/N/s) than in fast myosin (2X: 1.89 and 2A: 1.52 ATP $mN^{-1}mm^{-1}s^{-1}$), thus making slow fibers suitable for maintaining tension in postural activity (Bottinelli et al., 1994). Slow fibers rely predominantly on the oxidative pathway, but fast fibers are specialized for rapid, anaerobic ATP synthesis. ATP generation based on glycolysis has been calculated to be 2.5mM/s in fast and 1.2 mM/s in slow fibers (Greenhaff et al., 1993). Fast muscle fibers (2A, 2X) depend mainly on glucose oxidation and anaerobic glycolysis, respectively

(Schiaffino and Reggiani, 2011). ATPase activity was significantly higher in 2X and 2A fibers (0.178 and 0.168 mM/s, respectively). In addition, the level of fructose-2,-6-biphosphate, a potent activator of PFK, is higher in fast fiber (Hers, 1984). Furthermore, higher LDH activity (9-10 times) in fast fibers allows the rapid accumulation of pyruvate with concomitant degradation of NADH (Lowry et al., 1978).

ATP generation through TCA cycle is more effective in slow than in fast fibers due to greater mitochondrial density and greater TCA cycle fueling due to β-oxidation. In human muscle, the mitochondrial volume is higher in slow fibers than in fast fibers (type 1:6%, type 2A: 4.5%, type 2X:2.3%) (Howald et al., 1985). The maximum oxygen consumption rate in rat soleus versus gastrocnemius is 48μM/s versus 22μM/s (Kuznetsov et al., 1996). Such values are in proportion to their mitochondrial volume, citric enzyme activity and electron transport chain capacity which are two fold higher in slow fiber (Jackman and Willis, 1996). Pyruvate dehydrogenase kinase (PDK) activity is three times lower in slow fiber than in fast fiber (Peters et al., 2001). These observations suggest that slow and fast muscles differ in the relative role of glycolysis and oxidative phosphorylation and this metabolic diversity of muscle fibers contributes to their ability to maintain contractile activity. In this project, my interest is primarily in the regulation of glucose metabolism, that this is better studied in faster muscles and systems, such as C2C12 myotubes.

1.2 Response to contractile activity

1.2.1 Immediate metabolic perturbation

Under physiological conditions, ATP concentration changes little because ATP production is immediately accelerated to cover the ATP consuming processes. Following a 30-second sprint, PCr and ATP concentration in vastus lateralis muscle reduced from resting values of 83.9 and 23.9 mmole/kg dry muscle (dm) to 34.8 and 18.7 mmole/kg dm and a further decline was reported to 24.2 and 17.3 mmole/kg dm after the second sprint (Casey et al., 1996). Although PCr had fallen by 71% of resting values, ATP fell by only 28% after second sprint. The relative changes in AMP are much greater than those occur in ATP. For example, after high intensity exercise, ATP only drops 37% (Cheetham et al., 1986), but AMP can increase from nanomole to micromole (Crowther et al., 2002).

Glycogen and glucose metabolism provide a second source of ATP with lower power but greater capacity (glycogen 300-900 mmole/kg dry muscle) compared with PCr-CK system (Ortenblad and Nielsen, 2015). Both PCr-CK and glycolysis system provide 15mM/s ATP over the first 6 seconds of exercise. Glycolysis rate does not achieve its maximum until 5 seconds, but PCr starts to decline at 1.6 seconds (Gastin, 2001). After high intensity exercise, glycolytic ATP production contributes to PCr resynthesis during the initial stage of recovery. If PCr is not fully restored during the recovery phase, the performance in subsequent exercise bout may decline. Over a period of 30-second of exercise the contribution from glycolysis to ATP turnover is nearly double that of PCr.

Glucose uptake, glycogenolysis, glycolysis, and mitochondrial respiration are increased as a consequence of muscle contraction. The glycolytic metabolites, glucose-6-phosphate, glucose-1-phosphate and Fructose 6-phosphate increase 13, 10 and 11 fold, respectively. Pyruvate and lactate concentrations in muscle increase 19 and 29 fold during sprint running (Cheetham et al., 1986). In the cascade from glycogen to CO_2, this represents a depletion of the input and substantial accumulation of intermediates. This suggests that glycolytic flux outpaces mitochondrial flux increasing ATP synthesis beyond the mitochondrial capacity.

Immediately starting exercise, an initial burst of ROS occurs, followed by increased scavenging. During exercise, muscle produces ROS steadily, and ROS is gradually accumulated (Powers et al., 2011). Oxygen delivery and mitochondrial activity increase during exercise. An increase of electron leak in ETC is the consequence of increasing ATP turnover (Ji, 2015). Another source of physiological ROS in the form of either H_2O_2 or $O_2^{\cdot}$ is NADPH oxidases (NOX). Although NOX has been shown to produce ROS during muscle contraction (Prosser et al., 2011), NOX produced ROS are most described in the context of neutrophils for the phagocytic killing of pathogens during the immune response (Lassegue et al., 2012). Mitochondria and the NOX family are the best characterized intracellular source of ROS, but other enzymes, such as xanthine oxidase, cyclooxygenases and lipoxygenases can all produce ROS during muscle contraction (Holmstrom and Finkel, 2014).

1.2.2 Functional accommodation

1.2.2.1 Glucose uptake

The increase in glucose uptake parallels the increase in exercise intensity and duration. After 35 min cycling at 30%, 55%, and 75% VO_{2max}, glucose uptake in quardricep femoris muscle increased 5 fold, 11fold ,and 15fold, respectively (Kemppainen et al., 2002). During 40min cycling at 50% VO_{2max}, leg glucose uptake increased 5.5 fold at 15min and 11.1 fold at 40min (Hargreaves et al., 1992), but muscle glycogen decreased 21% at 15min and 37% at 40min. These results suggest that glucose uptake increases in the proportion of exercise intensity and glycogen depletion.

Because glucose cannot freely cross plasma membrane, carrier mediated transporters are required to facilitate entry of glucose into muscle cell. Previous studies have suggested that glucose uptake initiated by insulin or energetic stress involves the translocation of glucose transporters from intracellular reserves and their subsequent insertion into the plasma membrane (Michelle Furtado et al., 2003). To date, 14 different isoforms of glucose transporter have been identified, and GLUT1 and GLUT4 are expressed most abundantly in skeletal muscle (Mitsumoto et al., 1991; Thorens and Mueckler, 2010). Insulin and muscle contraction increase glucose uptake by translocation of GLUT4. Insulin signaling involves rapid phosphorylation of the insulin receptor and the activation of the phosphatidylinositol 3-kinase and Akt. Insulin-induced Akt activation promotes GLUT4 exocytosis by phosphorylating the Akt substrate of TBC1D4 and TBC1D1 (Kramer et al., 2006; Middelbeek et al., 2013). Exercise enhances muscle glucose uptake through an insulin-independent mechanism that involves the increasing of

metabolic activity (Hayashi et al., 1998). Contraction-stimulated GLUT4 is independent of insulin receptor substrate-1 (IRS1) and Akt (Kramer et al., 2006; Wojtaszewski et al., 1999). It has been suggested that insulin- and contraction-stimulated glucose uptake may converge signaling in TBC1D4, TBC1D1 as well as GLUT4 translocation (An et al., 2010; Kramer et al., 2006). These observations suggest that one mechanism to increase glucose uptake is by Akt/AMPK transport of GLUT4. It is not clear whether GLUT4 translocation is the sole mechanism for the increase in glucose transport during exercise. Clone 9 cells only express GLUT1, but not GLUT4. SB203580, a p38 inhibitor, blocks AICAR-induced glucose uptake in clone 9 cells (Xi et al., 2001). Aim 1 is based on the possibility that p38 might be important for glucose uptake.

1.2.2.2 Glycolytic adaptation

In resting cells, glucose uptake appears to be limited by the availability of glucose transporters, but stimulation by contraction may shift the rate-limiting process downstream (Fueger et al., 2004; Fueger et al., 2005). This means that peak glucose uptake will be strongly influenced by glucose disposal. HK, PFK, and pyruvate kinase are all subject to allosteric regulation that controls the flow of carbon through the pathway. For example, muscle contraction causes ATP depletion, and ADP, AMP accumulation which significantly enhances PFK activity through allosteric regulation (Kemp and Gunasekera, 2002; Krause and Wegener, 1996; Schmitz et al., 2013). A computer model of glycolysis in skeletal muscle estimates that PFK activity increases 91fold with 5 fold increase in ADP during rest-to-intensive work transition (Liguzinski and Korzeniewski, 2006). At 250% $VO_{2\ max}$ cycling for 30 sec, PFK activity is 50-70 fold higher than 35%

$VO_{2\ max}$ (Spriet et al., 2000).These observations suggest that accumulation of ADP facilitates glycolysis by allosteric regulation. The accumulation of AMP increases glucose uptake through AMPK activation, but the extent to which AMPK-mediated increase in glucose uptake reflects mass action or post-translational modification is not clear.

1.2.2.3 Pyruvate disposal

Pyruvate stands at a metabolic crossroad between aerobic and anaerobic metabolism. The ability of muscle cells to switch between pyruvate reduction and oxidation may be determined by the ratio of NAD^+/NADH. NADH content and lactate production depend on exercise intensity (fig. 1-1 below). After an initial decrease to 60% of resting NADH at 40%$VO_{2\ max}$, NADH increases with intensity, eventually reaching 160% of control at 100%$VO_{2\ max}$ (Sahlin et al., 1987). It is possible that at low intensity (40% $VO_{2\ max}$), enzymatic activity within the mitochondria increases, depleting high-energy NADH, resulting in no change in lactate production. At high intensity (100% $VO_{2\ max}$), the resulting NADH production from glycolysis is accumulated and lactate production increases by 11 fold via LDH (Sahlin et al., 1990; Spriet et al., 2000). This suggests that the oxidation state of mitochondrial NAD reflects the balance of glycolytic production of pyruvate and the delivery of O_2, being more oxidized (NAD^+) when oxygen is delivered in excess and more reduced (NADH) when oxygen is limited.

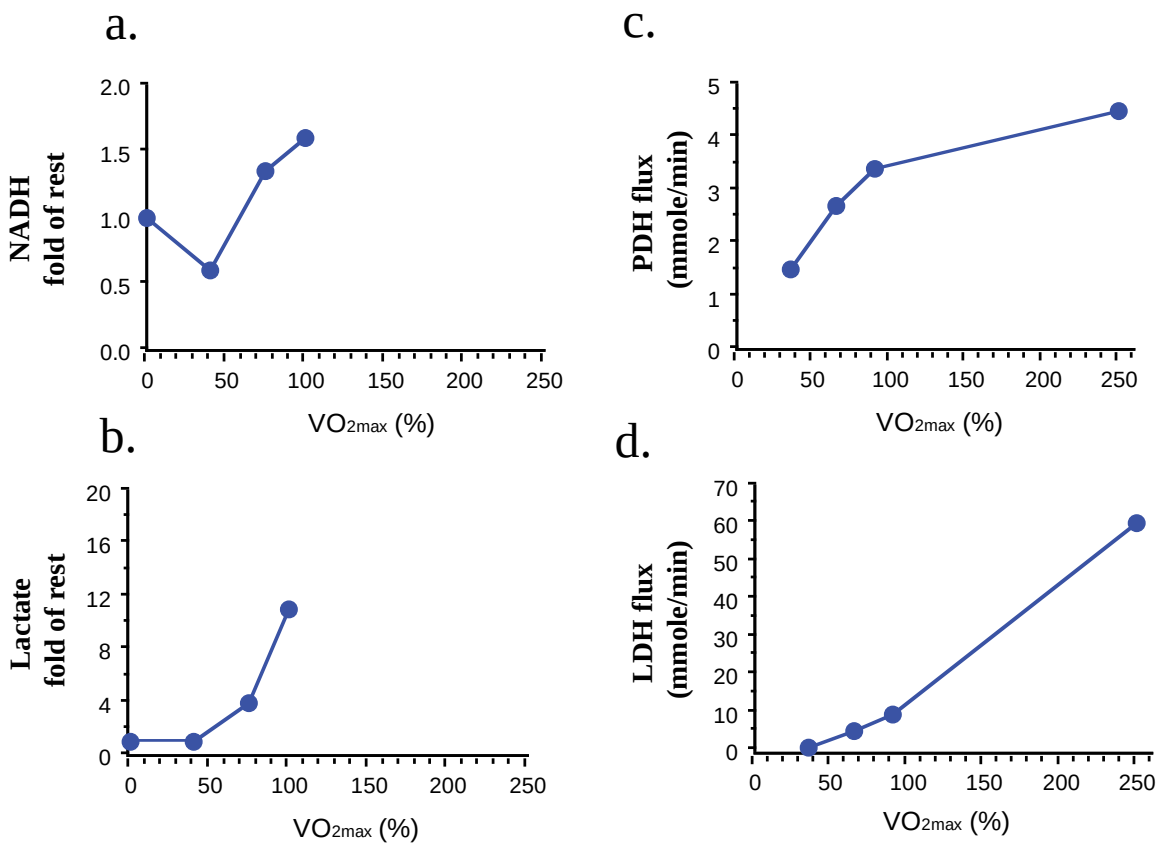

Figure 1-1 Glucose metabolites and PDH, LDH flux after exercise
Muscle content of a) NADH b) lactate, c) PDH flux, and d) LDH flux at rest and immediately after exercise at work loads corresponding to different VO_{2max}. Replotted from (Sahlin et al., 1987; Spriet et al., 2000).

During exercise, the flux of PDH and LDH changed to different extents (fig. 1-1 above) (Spriet et al., 2000). PDH flux increases from 1.5 to 2.7 mmole/min during the transition from 35% VO_{2max} to 65% VO_{2max}. LDH flux is estimated around 0.75 mmole/min at 40% VO_{2max}. At 65% VO_{2max}, LDH flux is increased to 5.2 mmole/min, which is about two fold higher than PDH. From 90% to 250% VO_{2max}, PHD flux slowly increases from 3.4 to 4.5mmole/min, but LDH flux rapidly increases from 9.6 to 60 mmole/min (Spriet et al., 2000).

1.2.3 Long-term metabolic adaptation

Endurance training causes a two-fold increase in the capacity of pyruvate oxidation in skeletal muscle. In addition, the activity of the enzymes of the mitochondrial electron transport chains doubles (Egan et al., 2011; Holloszy, 1967). Low intensity exercise stimulates mitochondrial biogenesis resulting in increased oxidative capacity and increased fatigue resistance (Little et al., 2010; Pilegaard et al., 2003). By contrast, high intensity training results in an decrease of the proportion of type 1 fibers from 57% to 48% and an increase of type 2A fibers from 32% to 38% (Jansson et al., 1990). CK, PFK, glycogen phosphorylase, LDH activity have been shown to increase after sprint training (Linossier et al., 1997; Thorstensson et al., 1975). Exercise changes intracellular metabolic profile rapidly and drastically suggesting that some key metabolite-protein interactions may mediate long term adaptation. The energy status (AMP) and oxidative status (NAD^+) may provide a stimulus for coherent conversion between glycolytic and oxidative phenotypes. For example, low intensity exercise is characterized by mitochondrial compensation for ATP turnover and net oxidation of NADH to NAD^+.

High intensity exercise is associated with workloads in excess of 60-70% VO_{2max}, anaerobic conditions, and net reduction of NAD^+ to NADH.

1.3 Metabolic signaling

Exercise-induced metabolic activity results in the perturbation of intracellular O_2, ROS, Ca^{2+}, AMP and NAD. These energetic stresses can serve as a mechanism for cells to reprogram their metabolism. These intracellular changes can in turn be detected by mitogen activated protein kinase (MAPK), AMP kinase (AMPK), and sirtuin. These signaling factors alter the activity of a number of transcription factors with the final result being a switch in protein distribution towards different phenotypes (Egan et al., 2010; Hoppeler et al., 2011).

1.3.1 AMP signaling

Dephosphorylated forms of ATP, especially, AMP, is a potent allosteric activator of enzymes influential to glucose metabolism, such as PFK (Schmitz et al., 2013), PDH and PDK (Lazo and Sols, 1980; Sugden and Holness, 2006). AMP activates PFK thereby allowing increased flux of hexose phosphates through glycolysis (Bruser et al., 2012). PDH is inhibited by PDK via phosphorylation. PDK is allosterically stimulated by ATP and inhibited by ADP (Bao et al., 2004a; Bao et al., 2004b).

AMP binding to the γ-subunit can stimulate AMPK allosterically and further leads to increased AMPK phosphorylation which can dramatically enhance AMPK activity (Hardie and Ashford, 2014). AMPK is a heterotrimeric enzyme consisting a catalytic α-subunit (α1 or α2) in combination with a regulatory β- (β1 or β2) and γ-

subunit (γ 1,γ2, or γ3) (Hardie, 2014). Two upstream kinases, serine-threonine liver kinase B1 (LKB1) and calcium/calmodulin kinase kinase-β (CaMKKβ), activate AMPK by phosphorylating a threonine residue (Thr172) on its catalytic α-subunit. LKB1 catalyzes the phosphorylation in response to metabolic stress. CaMKKβ activates AMPK in response to increases in intracellular $Ca2^{+}$caused by various hormones and calcium ionophores (Hawley et al., 2005).

Excess amounts of ROS impair ATP synthesis leading to AMP accumulation and subsequent AMPK activation (Rocha et al., 2016). However, a previous study has shown Lkb1is required for H_2O_2-induced AMPK activation independent of an increase in AMP/ATP ratio (Emerling et al., 2009). ROS may also directly influence AMPK activity through oxidation of cysteine299 and cysteine304 residues (Zmijewski et al., 2010). These observations suggest that AMPK activation, in addition to being a response to alterations in intracellular metabolic pathways, is directly influenced by cellular redox status.

Contraction-stimulated GLUT4 translocation is dependent on AMPK, but is independent of IRS1 and Akt . Mice lacking AMPKα1/2 show significantly impaired contraction-stimulated glucose uptake (O'Neill, 2013; O'Neill et al., 2011). (O'Neill, 2013). The AMPK inhibitor compound C (Funai and Cartee, 2009) and AMPK β-subunit knockout (O'Neill et al., 2011) have been shown to inhibit TBC1D1 phosphorylation and glucose uptake. Phosphorylation of three different sites (Ser237; Ser660; Thr597) of TBC1D1 increases with muscle contraction in an AMPK-dependent manner (Frosig et al., 2010; Pehmoller et al., 2009; Vichaiwong et al., 2010). These observations suggest that AMPK is required for contraction-stimulated GLUT4 translocation.

p38 MAPK has been suggested to be a downstream effector of AMPK and to participate in GLUT4 activation (Michelle Furtado et al., 2003; Somwar et al., 2002; Sweeney et al., 1999). Under metabolic stress, AMPK appears to recruit p38 to a transforming growth factor-beta-activated protein kinase 1-binding protein (TAB1) macromolecular complex, where it undergoes autophosphorylation. Activation of p38 may be required for maximal glucose uptake in skeletal myocytes, potentially by activating the GLUT4 transporter after its insertion into the cell membrane (Somwar et al., 2001; Somwar et al., 2000). These observations suggest that AMPK-mediated glucose uptake may involve p38 activation. However, dissociation of signaling between AMPK and p38 has been reported by several studies (Chambers et al., 2009; Ho et al., 2007; Jacquet et al., 2007). For example, in L6 myoblasts, and myotubes and in rat EDL muscle, AICAR activates AMPK and increases glucose uptake without increasing p38 phosphorylation (Ho et al., 2007). Mice deficient in AMPKα2 do not phosphorylate p38 after muscle stretch, but p38 inhibitors SB203580 and A304000 block stretch-induced glucose uptake (Chambers et al., 2009). Although p38 becomes active during exercise, whether p38 contributes to glucose metabolism is not clear.

There are several AMPK targets in the regulation of skeletal muscle adaptation to exercise (Mounier et al., 2015). AMPK phosphorylates the transcription repressor histone deacetylase 5 (HDAC5) following exercise. GLUT4 gene expression induced by exercise depends on the HDAC5 phosphorylation (McGee and Hargreaves, 2011). HDAC5 phosphorylation prevents the formation of HDAC-MEF2 complex and activates PGC-1a (McKinsey et al., 2000). AMPK activation has been shown to stimulate muscle atrophy by phosphorylating the transcription factor forkhead box protein O3a (FoxO3a) (Gross et

al., 2008). Activation of FOXOs increases the expression of muscle atrophy genes in response to starvation (Gross et al., 2008). PDK4 mRNA and protein expression are enhanced by AMPK, and thus decreases glucose oxidation and increases fatty acid oxidation (Fritzen et al., 2015; Houten et al., 2009).

In short-term exercise, AMP-mediated allosteric regulation and AMPK activation increase glucose uptake and glycolysis. In long-term exercise, AMPK up-regulates glycolytic gene expression and inhibits the differentiation or growth of muscle.

1.3.2 NAD-dependent signaling

PDH is a multi-enzyme complex located on the inside of the inner mitochondrial membrane. The activity of PDH is regulated by a variety of mechanisms: it is regulated by allosteric regulation by end products including acetyl CoA and NADH. PDH is also inactivated by phosphorylation by PDK at three sites on the E1 alpha subunit of PDH (PDHE1α): Ser^{232}, Ser^{293}, and Ser^{300} (Rardin et al., 2009). PDK is activated by ATP, NADH and acetyl-CoA and is inhibited by ADP, NAD^+, CoA-SH and pyruvate (Sugden and Holness, 2006). Because LDH is an equilibrium enzyme, increased lactate production will be due to a mass-action effect exerted by increases in pyruvate and NADH concentrations (Heigenhauser and Parolin, 1999).

NAD not only is an essential electron carrier, but also is a substrate in protein deacetylation and ADP-ribosylation (Canto and Auwerx, 2012; Nikiforov et al., 2015). NAD^+-dependent deacetylation is performed by silent information regulator-2 (Sir2) like proteins (sirtuins). Sirtuins deacetylate a broad range of protein substrates including histone, PGC-1α (Canto et al., 2009; Canto et al., 2010), p53 (Aksoy et al., 2006; McGee and Hargreaves, 2011) and FOXO (Canto et al., 2010; Hori et al., 2013) and various

mitochondrial proteins. Changes in intracellular NAD^+ may fluctuate by as much as 2-fold (Canto et al., 2009; Fulco et al., 2008; Rodgers et al., 2005). The estimated intracellular concentration of NAD^+ is in the 0.2 mM to 0.5mM range, and the Km of the sirtuins for NAD^+ falls into this range (Sauve et al., 2006). These observations suggest that sirtuin activity may be dependent on physiologically relevant changes in NAD^+. SIRT1 is the most studied member of the sirtuin family. SIRT1 activity is enhanced in mammalian tissues in response to metabolic stress, such as exercise (Canto et al., 2009), fasting (Rodgers et al., 2005), or calorie restriction (Chen et al., 2008), all conditions under which NAD^+ is elevated. This suggests that SIRT1 activity is linked to glucose metabolism and may regulate the cellular response to the environmental signals.

SIRT1 signaling may have a powerful influence on skeletal muscle performance and adaptation. SIRT1 deacetylates and positively regulates the activity of PGC-1α, a master regulator of mitochondrial biogenesis to regulate mitochondrial function (Canto et al., 2010; Rodgers et al., 2005). Nicotinamide riboside (NR) supplementation significantly increased SIRT1 activity, up-regulated PGC-1α target gene expressions, and improved mitochondrial function in mice (Canto et al., 2012). Treatment with the natural polyphenolic compound resveratrol, a SIRT1 and AMPK activator, significantly increased SIRT1 activity and improved mitochondrial function (Lagouge et al., 2006). SIRT1 also regulates differentiation of cultured skeletal muscle cells via deacetylation of transcription factors such as FOXO (Hori et al., 2013; Nedachi et al., 2008) and p53 (Cheng et al., 2003; Hori et al., 2013). Mouse primary myoblasts from SIRT1 knockout mice were resistant to inhibition of differentiation by glucose restriction or AICAR (Fulco et al., 2008). This suggests that some effects attributed to AMP-induced signaling may be mediated by SIRT1.

Another mechanism of NAD^+-dependent signaling is ADP-ribosylation. This reaction is catalyzed by ADP- ribosyltransferases which transfer ADP-ribose moiety from NAD to specific amino acid residues on substrate proteins or to ADP-ribose itself (Hottiger et al., 2010). ADP-ribosylation has been shown to regulate many essential cellular processes including: DNA repair, apoptosis, and glycolysis (Andrabi et al., 2014; Hassa and Hottiger, 2008). For example, poly (ADP-ribose) polymerase-1 (PARP1) activation inhibited hexokinase activity by the formation of poly (ADP-ribose) in neurons. Overexpression of PARP1 inhibited glycolysis, while preventing PAR formation by PAR glycohydrolase restored the glycolysis (Fouquerel et al., 2014).

NADH increases in high intensity exercise and may play a central role in the regulation of pyruvate oxidation and reduction. NAD^+ is increased during low-intensity exercise or starvation, and acts through SIRT1-mediated deacetylation to increase mitochondrial biogenesis and inhibits the differentiation or growth of muscle.

1.3.3 Interaction of AMP and NAD signaling

AMPK and SIRT share multiple downstream substrates in ways that allow the cell to respond differently to modest and extreme energetic stress. AMPK induces the phosphorylation of many transcription factors and co-activators, including PGC-1α and hypoxia-Inducible Factor 1-α (HIF-1α). Both of these transcription factors are also regulated by SIRT1. SIRT1 represses HIF-1α target genes (Lim et al., 2010), but enhances PGC-1α activity (Canto et al., 2012). HIF-1α is the ‘‘master regulator’’ of cell hypoxic signaling. HIF-1α is stabilized during oxygen deprivation and directly involved in the upregulation of several glycolytic enzymes, such as glyceraldehyde-3-phosphate

dehydrogenase (GAPDH) and LDH (Dehne et al., 2007; Kim et al., 2006). PGC-1α is required for the induction of mitochondrial gene expression (Rohas et al., 2007). Recently, evidence suggests that AMPK can either directly phosphorylate PGC-1α or increase its expression, and hypoxia inhibits the PGC-1α pathway and the expression of mitochondrial components through HIF-1α (Slot et al., 2014). These observations suggest that AMPK and SIRT1 have some distinctions and similarities in their regulation on phenotypic adaptation. It is also conceivable that SIRT1 and AMPK may co-mediate signaling to regulate glucose metabolism.

There are two slightly antagonistic models for AMPK-SIRT1 interaction. One is that AMPK can function as a SIRT1 activator by the up-regulation of Nicotinamide phosphoribosyltransferase (nampt) gene expression and subsequent increase of NAD^+ (Canto et al., 2009; Fulco et al., 2008). Nampt is the rate-limiting enzyme in the salvage pathway of NAD biosynthesis (Revollo et al., 2004). This mechanism suggests that all of the signaling that seems to be AMPK mediated maybe actually dependent on SIRT1. Activation of AMPK by glucose restriction or AICAR treatment impaired the differentiation of C2C12 myoblasts (Fulco et al., 2008). The inhibition of differentiation was accompanied by the increase of nampt gene expression, which in turn increased the NAD^+/NADH ratio. Conversely, AMPK activation has no effect on muscle differentiation in SIRT1 knockdown mice suggesting that SIRT1 maybe an AMPK downstream effector (Fulco et al., 2008).

Other studies proposed that AMPK could alter the NAD^+/NADH ratio and activate SIRT1 independently of nampt (Canto et al., 2009; Canto et al., 2010). AICAR treatment for 4-12 hour increased the NAD^+/NADH ratio in C2C12 myotubes transfected

with PGC-1α and enhanced PGC-1α deacetylation. However, acute blockage of nampt activity with the specific inhibitor FK866 did not affect AICAR's capacity to modulate PGC-1α acetylation or NAD^+/NADH ratio (Canto et al., 2009). These observations suggest that AMPK may act as the primordial trigger for fasting- and exercise-induced adaptations in skeletal muscle, and phosphorylation by AMPK might be required for PGC-1α deacetylation by SIRT1 and its downstream signaling.

1.4 Proposed model

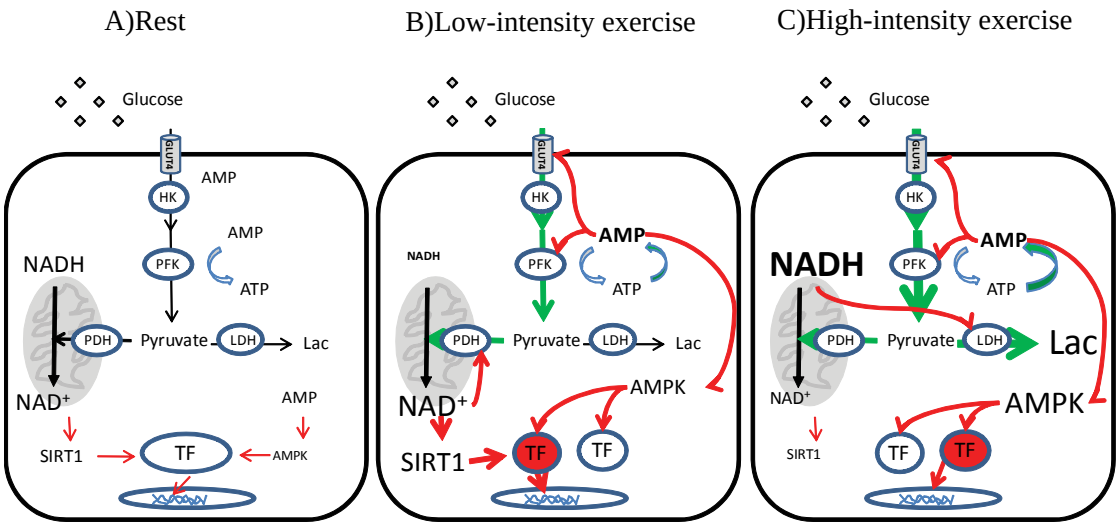

Figure 1-2 Proposed model
A model characterizing AMP and NAD(H) accumulation as a function of actual metabolic rates (Lac: lactate, TF: transcription factor, green arrow: glucose flux, red arrow: activation signaling). AMP contributes to glucose uptake and glycolysis. NAD(H) contributes to the weighting of PDH/LDH. At low intensity exercise, AMP and NAD^+ activate PGC-1α by AMPK-mediated phosphorylation and SIRT1-mediated deacetylation. Activation of PGC-1α contributes to mitochondrial adaptation. At high intensity exercise, accumulation of NADH and low SIRT1 activity limits PGC-1α activity, and AMP increases HIF-1α activity by AMPK-mediated phosphorylation. Activation of HIF-1α contributes to glycolytic adaptation.

This thesis is based on a conceptual model (fig. 1-2 above) in which AMP and NAD^+ accumulate as a function of actual metabolic rates. AMP/ATP ratio influences the activity of enzymatic processes in glycolysis to maintain ATP homeostasis. NAD^+/NADH ratio influences the balance of oxidative and anaerobic metabolism. The interactions of AMP and NAD^+ signaling contribute to glycolytic and mitochondrial adaptation. During exercise, the accumulation of AMP due to increased ATP turnover may increase glucose uptake and enzyme activity within glycolysis. At low intensity exercise, mitochondrial respiration is stimulated by increasing oxygen delivery and substrate availability. The net oxidation of NADH to NAD^+ increases. AMPK and SIRT1 activation increases mitochondrial biogenesis by activating PGC-1α. At high intensity exercise, glycolysis continues to increase, but mitochondria respiration is limited by O_2. NADH accumulates and encourages pyruvate reduction to lactate via LDH. AMPK activation is increased at low and high intensity exercise, but low SIRT1 activity at high intensity limits PGC-1α activity. Thus, the overall hypothesis is that distribution of glucose and mitochondrial remodeling depends on the AMP and NAD^+ generated during energetic stress. This model was tested in three specific applications.

1.5 Specific aims

Specific Aim 1: To evaluate the contribution of AMPK and p38 to AMP-dependent facilitation of glycolysis. Phosphorylation of p38 coincides with increased glucose uptake, but the role of p38 in glucose uptake is controversial. Evidence in the literature supports a role of p38 MAPK in glucose transport and it may be a downstream effector of AMPK. However, transgenic expression of dominant-negative p38α/β isoforms has little effect on insulin-stimulated glucose uptake, and AICAR activates AMPK without phosphorylation of p38. Both ATP depletion and AICAR stimulation increase AMPK activity and glucose uptake, but only ATP depletion increases glycolysis, suggesting that a metabolite of glycolysis indirectly stimulates p38 phosphorylation. Specific aim 1 examines the role of AMPK and p38 in glucose metabolism during ATP depletion and to determine whether p38 regulates glycolytic activity or is activated as a consequence of glycolysis. This aim is based on the specific hypothesis that p38 is activated by the accumulation of metabolites rather than controls glucose uptake during ATP depletion.

Specific Aim 2: To evaluate the contribution of cellular redox state in the balance of oxidative and anaerobic metabolism. Because LDH requires NADH and PDH requires NAD^+ to metabolize pyruvate, the balance of reductive and oxidative disposal of pyruvate depends on the redox state of NAD (within model description, fig. 1-2, above). However, whether oxidation of NADH is sufficient to increase pyruvate oxidation is not clear. Specific Aim 2 is designed to determine the weighting of AMP and NAD signaling in the balance of aerobic and anaerobic metabolism. This aim is based on the hypothesis that NADH oxidation increases glucose oxidation via both mass action and PDH phosphorylation.

Specific Aim 3: To evaluate models of AMP and NAD^+ signaling for transcriptional regulation of myogenic differentiation and metabolism. AMPK and SIRT1 share several

effector transcription factors. Controversy exists whether AMPK and SIRT1 activities are independent or sequential. Specific aim 3 is designed to manipulate the metabolites independently to test the independence of their signaling effectors. This aim is based on the hypothesis that AMP-dependent signaling is a necessary antecedent to deacetylation, but not sufficient to induce transcriptional activity.

1.6 Experimental methods

1.6.1 C2C12 myotubes

Although cell culture model does not exactly mimic human activity because of the absence of whole body response from different organs, it provides simplicity compared to the difficulties of studies using human or animal models. For example, cells are grown under controlled conditions, it allows us to study and interpret specific physiological intervention without other responses, such as nutrient availability. In this project the main focuses are the AMP and NAD signaling in glucose metabolism. C2C12 myotube is a well-defined model in glycolysis and mitochondrial respiration. It is a great model to study glucose and NADH oxidation because of the high glycolysis rate and low mitochondrial respiration. AICAR has been used to stimulate AMPK activation in C2C12 myotubes (Canto et al., 2009; Sasaki et al., 2014). NAD precursor supplementation has been used to boost NAD content in skeletal muscle, liver, and brown adipose tissue (Canto et al., 2012). Whether systemic application of AICAR or NAD has specific action on muscle is not clear. The limitations of C2C12 cell line include that only 60-80% myoblasts fuse into myotubes, and the culture medium is not well defined as its physiological environment, such as high glucose concentration (culture: 25mM, human:

5mM), high oxygen concentration and growth factors. Although cell line is easily manipulated and propagated, it escapes the in vivo condition. The prediction of the signaling pathways from this project might need to be tested in vivo in the future.

1.6.2 NAD supplementation

NAD is synthesized via de novo pathway and salvage pathway. The de novo pathway starts with the essential amino acid L-tryptophan, which is taken up from the diet. Tryptophan degradation generates quinolinic acid (QA), which is converted to nicotinic acid mononucleotide (NAMN), an intermediate of NAD metabolism. Although NAD can be synthesized de novo from tryptophan, it is assumed that the main source of NAD is from salvage pathways using NAM as precursor (Nikiforov et al., 2015). To date, several methods have been shown to increase NAD content. For example, changing nampt activity can influence NAD content in several mammalian cells and animals (Frederick et al., 2015; Pittelli et al., 2010; Revollo et al., 2004). Nampt gene expression has been observed to increase in C2C12 myotubes in response to glucose restriction, and changing the nampt activity was associated with changes in SIRT1 activity (Fulco et al., 2008). Another way to modulate NAD content resides in the modulation of the activity of non-sirtuin NAD consuming enzymes. Mice lacking CD38, as a main NAD consumer, displayed a 30-fold increase in NAD contents in the liver (Aksoy et al., 2006). Although this increase in NAD content is much higher than NAD precursor supplementation or caloric restriction, CD38 knockout mice display a severe impairment in beta-cell function (Antonelli and Ferrannini, 2004). Calorie restriction can boost NAD content, but this intervention may cause some off-target effects, such as muscle dystrophy. Studies have shown that supplementation with nicotinic acid (NA) (Canto et al., 2012), Nicotinamide mononucleotide (NMN) (Canto et al., 2012; Yamamoto et al., 2014; Yoshino et al., 2011) or nicotinamide riboside (NR) (Canto et al., 2012; Yang et al., 2007) increased NAD

content and that increase was associated with SIRT1 activation (Yamamoto et al., 2014; Yoshino et al., 2011). NMN was used to boost NAD content in this study.

1.6.3 Metabolic assay

ATP can be measured by HPLC, but it requires specialized instrumentation. ATP can be measured by utilizing the phosphorylation of glycerol to generate a product that can be quantified by colorimetric methods, or fluorometric methods. ATP can also be measured by bioluminescence methods after addition of luciferin-luciferase. In this project, ATP concentration was measured by bioluminescence assay because it is more sensitive than colorimetric and fluorometric assays. Fluorescent reporters are susceptible to photobleaching, and cellular components may have autofluorescent properties which increase the non-specific background. In contrast, photon emission from bioluminescence assay is located within the well-protected environment of the enzymatic active site, and cellular components have no inherent bioluminescence.

Lactate can react with specific enzymes to generate a product that is easily measured by colorimetric and fluorometric methods. Although fluorometric assay is much more sensitive than colorimetric assay, extracellular lactate concentration is around 300μM after 15min incubation. Colorimetric assay is sufficient to detect the lactate concentration. Therefore, colorimetric assay was used in this study.

NADH can be measured by colorimetric assay via monitoring of NADH absorption at 340nm or by fluorescence assay via monitoring of NADH auto fluorescence at 460nm. However, these methods suffer low sensitivity and high interference. Enzymatic cycling contains sample NAD and couples a cycling assay using the enzymes

aldehyde dehydrogenase (ADH) and diaphorase to provide an amplification of analytical sensitivity. Therefore, enzymatic cycling was used in this study.

2 CHAPTER

Activation of p38 in C2C12 myotubes following ATP depletion depends on extracellular glucose

2.1 Abstract

Muscle cells adjust their glucose metabolism in response to myriad stimuli, and particular attention has been paid to glucose metabolism after contraction, ATP depletion and insulin stimulation. Each of these requires translocation of GLUT4 to the cell membrane, and may require activation of glucose transporters by p38. In contrast, AICAR stimulates glucose transport without activation of p38, suggesting that p38 activation may be an indirect consequence of accelerated glucose transport or metabolism. This study was designed to investigate the contribution of AMPK and p38 to ATP homeostasis and glucose metabolism to test the hypothesis that p38 reflects glycolytic activity rather than controls glucose uptake. Treating mature myotubes with rotenone caused transient ATP depletion in 15 min with recovery by 120 min, associated with increased lactate production. Both ACC and p38 were rapidly phosphorylated, but ACC remained phosphorylated while p38 phosphorylation declined as ATP recovered. AMPK inhibition blocked ATP recovery, lactate production, and phosphorylation of p38 and ACC. Inhibition of p38 had little effect. AICAR-induced ACC phosphorylation, but not lactate production or p38 phosphorylation. Finally, removing extracellular glucose

potentiated rotenone-induced AMPK activation, but reduced lactate generation, ATP recovery and p38 activation. Thus, glucose metabolism is highly sensitive to ATP homeostasis via AMPK activity, but p38 activity is dispensable. Although p38 is strongly phosphorylated during ATP depletion, this appears to be an indirect consequence of accelerated glycolysis.

2.2 Introduction

Skeletal muscle has an exceptional capacity to alter its glucose metabolism in response to changes in energy demand and glucose availability. For example, glucose uptake can increase by 3-10-fold during contraction and insulin stimulation. Insulin-mediated glucose uptake is an important part of whole body glucose homeostasis, but can be disrupted, leading to type II diabetes. Insulin resistance does not affect glucose uptake stimulated by contraction or ATP depletion (Musi et al., 2001). These stimuli accelerate the metabolism of glucose by product depletion rather than substrate accumulation, and suggest a strategy to compensate for insulin resistance.

Elevated glucose uptake depends strongly on the translocation of glucose transporter protein 4 (GLUT4) to the cell membrane, but is also influenced by the subsequent disposal of glucose through glycolysis, glycogenesis, and the pentose phosphate pathway (PPP) (Richter and Hargreaves, 2013). Glucose disposal is subject to hormonal, allosteric and mass action effects separate from the regulation of GLUT4 activity, and stimuli that increase glucose uptake activate multiple signaling pathways linked to regulation of glycolysis and glycogenesis (Hunter et al., 2011). Among these, the p38 mitogen activated protein kinase (p38) has been suggested to participate in both

GLUT4 activation to control acute glucose transport (Furtado et al., 2002) and more complex processes dependent on stresses associated with hyperglycemia and disruption of metabolic homeostasis (Novellasdemunt et al., 2013; Susztak et al., 2006). This suggests two models describing the relationship between p38 and glucose transport. The first model proposes that concomitant activation of Akt or AMPK and p38 facilitates separate processes of GLUT4 translocation and transporter activation. This model is primarily derived from hypoxic or ischemic cardiac myocytes, insulin-stimulated cells, and cells not expressing GLUT4. Insulin directly activates both Akt and p38 (Furtado et al., 2002), while hypoxic conditions induce ATP depletion and AMPK activation, which subsequently activates p38 (Li et al., 2005; Pelletier et al., 2005). AMPK appears to recruit p38 to a transforming growth factor-beta-activated protein kinase 1-binding protein (TAB1) macromolecular complex, where it undergoes autophosphorylation (Li et al., 2005). In support of this, inhibiting AMPK suppresses p38 activation and glucose uptake following mitochondrial poisoning (Pelletier et al., 2005). Likewise, p38 inhibitors reduce insulin- and contraction-stimulated glucose uptake without changing the cell surface availability of GLUT4 (Somwar et al., 2001; Somwar et al., 2000). In heart muscle, p38 inhibitor SB203580 inhibits both 5-Aminoimidazole-4-carboxamide ribonucleotide (AICAR)- and hypoxia-stimulated glucose uptake (Pelletier et al., 2005). In cells expressing only glucose transporter protein 1 (GLUT1), inhibition of p38 blocks AICAR-stimulated glucose uptake, potentially by preventing p38-mediated activation of constitutively-resident GLUT1 transporters (Xi et al., 2001). In this model, energy depletion is signaled by an increase in AMP, which activates AMPK. AMPK then phosphorylates TBC1 domain family member 1 (TBC1D1) to initiate GLUT4 transport

(Kramer et al., 2006) and separately causes phosphorylation of p38 to activate glucose transporters.

The second model proposes that GLUT4 translocation is sufficient for maximal transport activity independent of p38 activity. This model is primarily derived from AICAR-stimulated skeletal myocytes and targeted genetic disruption of p38 isoforms. It is prompted by the recognition that the pyridinyl imidazole p38 inhibitors also reduce Akt phosphorylation and may directly interfere with glucose transport (Antonescu et al., 2005; Lali et al., 2000). For example, transgenic expression of dominant-negative p38α/β isoforms has little effect on insulin-stimulated glucose uptake, but SB203580 still reduces glucose transport, even in p38-defective cells (Antonescu et al., 2005), and disruption of p38β expression fails to alter insulin-stimulated glucose uptake in either adipose or muscle (Turban et al., 2005). AICAR treatment significantly increases AMPK phosphorylation without p38 phosphorylation in L6 myoblasts, myotubes and isolated rat extensor digitorum longus (EDL), so AICAR-induced glucose uptake occurs without p38 activation (Ho et al., 2007).

Activation of p38 may be related to processes parallel to GLUT4 activation during periods of energy stress. ATP depletion induces glucose uptake and activation of glycolytic pathway. The capacity of pyruvate dehydrogenase (PDH) to metabolize pyruvate and mitochondrial shuttle to regenerate NAD^+ may be saturated, resulting in accumulation of NADH (Locasale and Cantley, 2011). NAD^+/NADH ratio has been shown to decrease by more than tenfold in the presence of mitochondrial inhibitors compared with control (Fendt et al., 2013). Furthermore, pre-treating cardiomyocytes with resveratrol, a NAD^+ booster, caused a significant reduction in ischemia–reperfusion-

induced p38 phosphorylation (Becatti et al., 2012). This suggests an alternative model in which energy depletion is signaled by elevated AMP, activating AMPK. AMPK then phosphorylates TBC1D4 to initiate GLUT4 translocation, which is necessary and sufficient for maximum glucose uptake (Kramer et al., 2006). Subsequent metabolism of glucose disrupts the redox balance within the glucose network, resulting in phosphorylation of p38.

Mitochondrial inhibition is a well-established experimental strategy to challenge the energy status of cells and to study how cells cope with such a challenge (Bashan et al., 1993). Rotenone inhibits the transfer of electrons from iron-sulfur centers in complex I to ubiquinone, disrupting the oxidation of nicotinamide adenine dinucleotide (NADH) and mitochondrial synthesis of ATP (He et al., 2013). Limited ATP production causes a rise in the AMP: ATP ratio and activates AMPK. This study is designed to investigate the role of AMPK and p38 in ATP homeostasis and glucose metabolism during mitochondrial inhibition and to test the hypothesis that activation of p38 following ATP depletion depends on glycolysis. Our results show that ATP homeostasis is highly sensitive to AMPK activity, but that p38 activity is dispensable. Reducing AMPK activity blocks p38 activation, and this AMPK-induced increase p38 phosphorylation is dependent on extracellular glucose, but not on actual glucose uptake. These results are partially consistent with p38 being indirectly activated by glycolytic flux under energy depletion.

2.3 Materials and Methods

2.3.1 Materials

Antibodies for p38 T180/Y182, ACCS79 and Akt S473 were purchased from Cell Signaling Technology. C2C12 cells were obtained from the American Type Culture Collection (ATCC, Manassas, VA). Dublecco's Modified Eagle's Medium (DMEM) was purchased as a powdered mixture (Corning 50-003), supplemented with 3.7g/L NaHCO3 , and sterilized by 0.2 um filtration. Rotenone (Rot, 1 mM), FCCP (4 mM), dorsomorphin (Dors, 10 mM, also known as Compound C), cytochalasin B (20mM) and SB203580 (10 mM) were prepared as concentrates in DMSO and diluted to working strength in serum free DMEM prior to application to cells. AICAR was directly dissolved in serum free DMEM to give a final concentration of 0.1-10 mM.

2.3.2 Cell Culture

C2C12 myoblasts were maintained in growth medium (GM, DMEM supplemented with 10 % fetal bovine serum (FBS, Hyclone), 100 IU/ml penicillin, and 100 μg/ml streptomycin) in a humidified incubator under 10 % CO2 at 37 °C. Cells were seeded at 4.4x103 cells/cm2 on 12-well plates, and allowed to proliferate 1-2 days to 60-80% confluence, at which point they were switched to differentiation media (DM, DMEM supplemented with 2% horse serum (Hyclone) and antibiotics). Media was replenished every 48 h. Interventions were performed after 4-5 days in DM, with 44±7% of culture area covered by myotubes.

Mature myotubes were depleted of ATP by exposure to rotenone. Cultures were rinsed twice with serum and antibiotic free DMEM (SFM) and incubated 60min prior to application of rotenone. In most experiments, all wells were exposed to rotenone for 15 or 60 minutes, as indicated. For time-course studies, individual wells were exposed to drug for different times, but to minimize manipulation of each plate, the total pre-incubation and incubation time was 3 hours for all treatment groups. All cells were switched to SFM concurrently, treated with 250 nM rotenone or DMSO for the indicated time periods, and harvested concurrently. This resulted in varying length incubations in SFM equal to the difference between three hours and the duration of rotenone exposure. ATP recovery mechanisms were investigated by combining rotenone treatment with other treatments. Inhibitors of AMPK (dorsomorphin), glucose transporters (cytochalasin B) or p38 (SB203580) were included in both the pre-incubation media and the treatment media. Glucose restriction media was prepared from glucose, glutamine and pyruvate free DMEM (Corning 90-113), supplemented with 4mM glutamine, 0.5 mM glucose, and 24.5 mM mannitol. .

Culture media was collected immediately after treatment and boiled for 5 min to inactivate enzymatic activity. Samples were cleared by centrifugation at 16k xg for 2 min and stored at -20°C. Cultures were rinsed with ice cold PBS twice, and collected by scraping in detergent buffer (1% Triton-X100, 50 mM tris, 300 mM NaCl, 5 mM EDTA) supplemented with protease inhibitors (Sigma), 100 mM NaF, and 4 μg/ml $NaVO_3$. Because early experiments revealed that even a few minutes delay could substantially reduce ATP content, an aliquot of this suspension was immediately diluted 10x in water and heated for 2 min at 98°C to inactivate nucleotidases. The rest of the sample was

incubated on ice for 30 min. Insoluble material from both samples was cleared by centrifugation at 16k xg for 5 min. Soluble protein concentration was assayed by bicinchronic acid assay (Pierce).

2.3.3 Cell morphology

Micrographs of cultures were obtained immediately after treatment under phase contrast illumination using 20x objective (Leica). Two random fields were captured for each well, covering 13.5 mm2. Culture confluence and area density of myotubes were determined by point counting.

2.3.4 Metabolite assays

Cytoplasmic ATP was determined by the firefly luciferase method (33). ATP standards and samples were distributed in duplicate to 96 well plates, and assay buffer (1.5 mM MgCl2, 0.15 mM EDTA, 18 μM dithiothreitol (DTT), 0.25 mg/ml bovine serum albumin (BSA), and 6 mM HEPES, pH 7.8.) containing 30 μM luciferin and 0.75 μg/ml luciferase was rapidly added using a multi-channel pipettor. Luminescence was measured within 5 minutes (FLx800, BioTek). Luminescence values were calibrated to a standard curve and normalized to lysate protein content.

Lactate was measured by the lactate dehydrogenase method (Pesce et al., 1975). Samples were reacted in assay buffer (1 M glycine, 200 mM hydrazine, 2 mM NAD+, pH=9.5) containing 20 U/ml LDH at room temperature for 30 min. Absorbance at 340 nm was measured, and lactate concentration was calculated using 6.22 as the millimolar extinction coefficient for NADH. Values were normalized to lysate protein content.

2.3.5 Western-blot analysis

To assay phosphorylation of p38, Akt and ACC, 4 μg soluble protein was separated by SDS-PAGE through 10 % (p38 and Akt) or 7 %(ACC) acrylamide gels. Protein was transferred to nitrocellulose membranes, blocked with 5% nonfat dry milk in Tween-TBS (TTBS) and hybridized with phospho-specific antibody to p38 T180/Y182 (1:2000), Akt S473(1:2000) or ACC S79 (1:2000). Membranes were rinsed and incubated with horseradish peroxidase conjugated secondary antibody (Jackson, 1:80,000). Bands were detected by enhanced chemiluminescence (Amersham), visualized by exposure to radiographic film, and quantified by scanning densitometry. All samples from an experiment were run on the same gel, and normalized to the average of that experiment's DMSO-control samples.

2.3.6 Statistical analysis

Unless otherwise noted, experiments were repeated as three independent procedures, with duplicate or triplicate wells averaged prior to statistical analysis, giving a sample size of n=3 per group. This provides statistical resolution of 4 standard deviations with 91% power or two standard deviations with 25% power. Results are reported as means with S.D. to indicate population variability unless otherwise noted. The IC50 and EC50 were determined by fitting experimental data to the Hill equation using MatLab software version 2014a (fitnlm, MathWorks, Inc.), and are reported as mean ± S.E. to indicate confidence in the estimates. Time course data were fit to an exponential function for determination of time constant. Rotenone- dorsomorhpin and rotenone-glucose experiments were analyzed by two-way ANOVA. Dose and time

experiments were analyzed by 1-way ANOVA followed by post hoc T-tests using Bonferroni correction for multiple comparisons.

2.4 Results

Rotenone decreases ATP and increases phosphorylation of ACC and p38 with similar dose dependence (Fig. 2-1). Because rotenone can induce oxidative stress at high doses (Li et al., 2003), we first determined the minimum concentration to induce metabolic stress. Rotenone induced a dose-dependent reduction in ATP after 15 minutes (Fig. 2-1a), with IC_{50} of 40±20 nM (mean±s.e.m) and maximal depletion of 58±5% above 250nM. This was associated with a dose-dependent phosphorylation of p38 with EC_{50} 17±5 nM (Fig. 2-1b) and phosphorylation of ACC with EC_{50} 12±9 nM (Fig. 2-1c). The EC_{50} for neither p38 ($p=0.15$) nor ACC ($p=0.24$) was significantly different from ATP. Rotenone was used at 0.25 μM in all subsequent experiments to maximize ATP depletion.

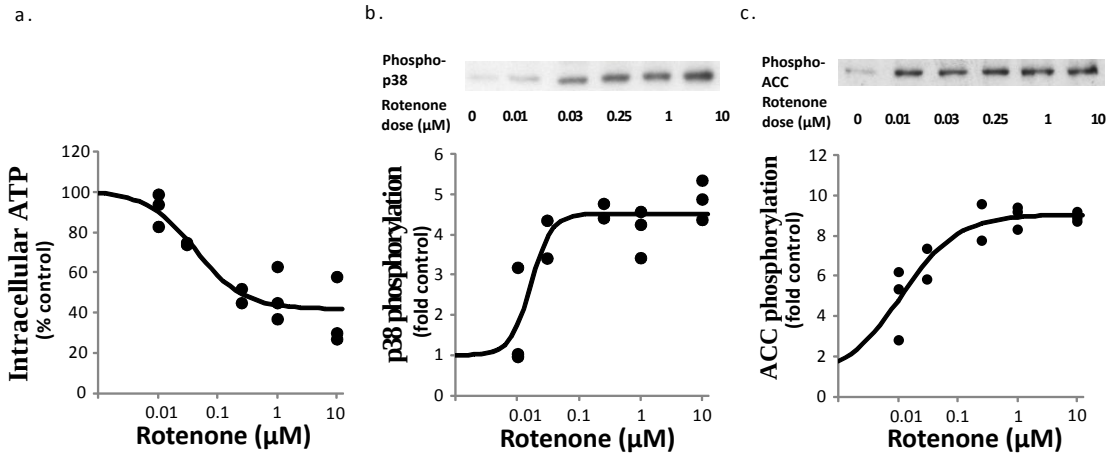

Figure 2-1 Effect of rotenone on ATP content and kinase activity
Effect of 15 minutes rotenone on a) cellular ATP content and the phosphorylation of b) p38 and c) ACC. Representative blots shown for p38 and ACC. All values are expressed relative to control. n=3 experiments with duplicate wells.

Rotenone poisoned myotubes recover ATP content within 2 hours, coincident with loss of p38 phosphorylation, but not ACC (Fig. 2-2). Compensation for mitochondrial poisoning was associated with an increase in lactate production rate from 19.0±4.7 µmole/g protein/min to 42.1±9.2 µmole/g/min ($p<0.0001$). Although lactate production appeared to increase further during recovery, this could not be statistically resolved ($p=0.12$; Fig. 2-2b). Likewise, phosphorylation of ACC, indicative of AMPK activity, increased to 6.4±1.2 fold of control by 15 minutes and remained elevated for the duration. ATP recovered from 63±11% of control at 15 minutes to 84±9.5% at 120 min ($p=0.0023$ Fig. 2-2a). The recovery of ATP was associated with a decline in phosphorylation of p38 from 3.6±0.5 fold to 0.9±0.5 fold ($p=0.02$; Fig. 2-2c) but not ACC (6.4±1.2 to 5.6±2.6; Fig. 2-2d). The half-time of ATP recovery was 46±41 min,

while the half-time of p38 dephosphorylation was 81±38 min, and these values could not be statistically distinguished ($p=0.48$) .

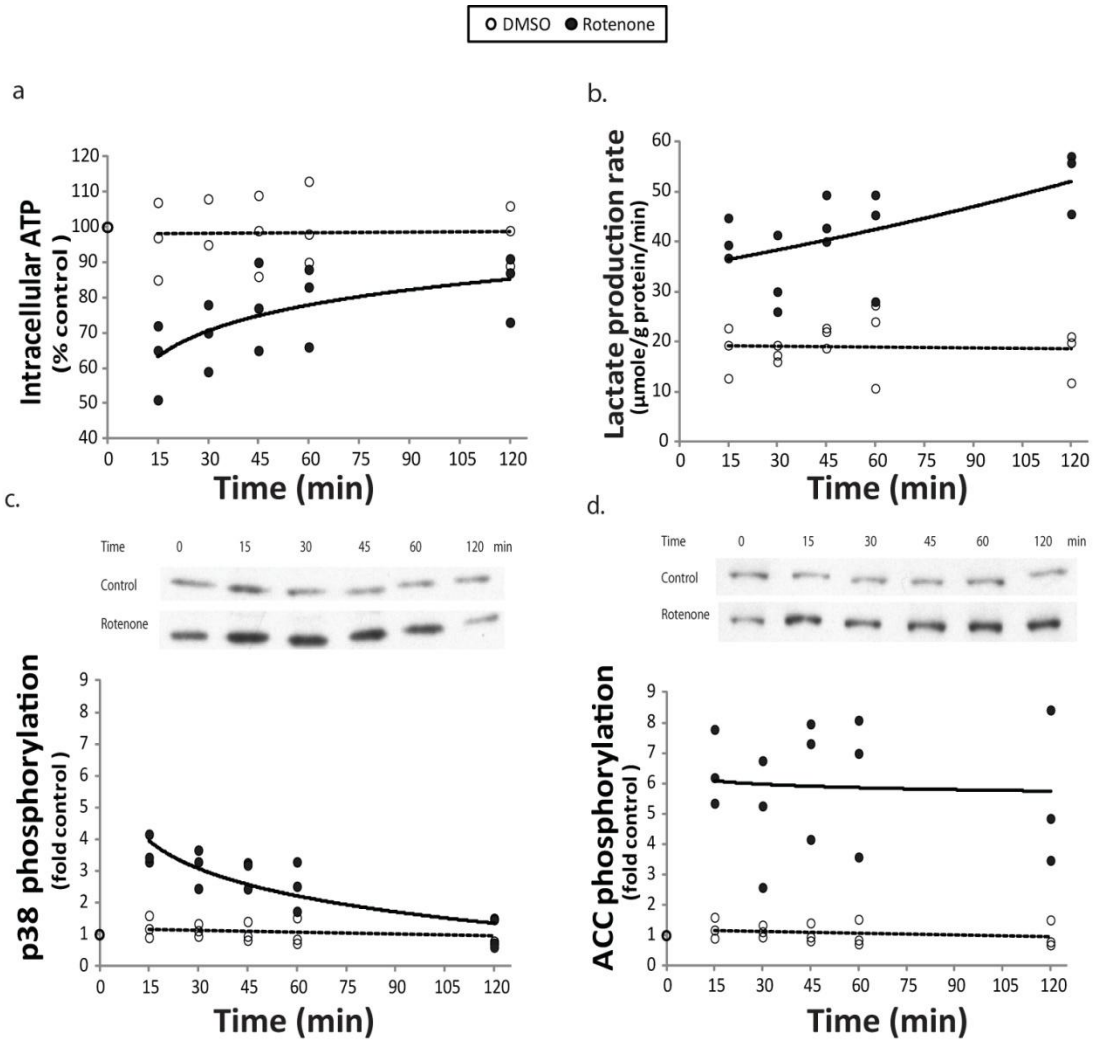

Figure 2-2 The time course of ATP content and kinase activity
The time course of a) ATP content b) rate of lactate release and phosphorylation of c) p38 and d) ACC during exposure to rotenone in the presence of complete media. Representative blots shown for p38 and ACC. DMSO: dashed line, open circles; rotenone: solid line, filled circles; Means ± SD.

Rotenone does not alter myotube density or morphology during our experimental window (Fig. 2-3). Although prolonged incubation with high doses of rotenone can induce apoptosis or necrosis, two hours with 250 nM rotenone did not reduce myotube number (Fig. 2-3c) nor induce visible changes in morphology, indicating little gross change in the composition of cultures during two hours of mitochondrial inhibition.

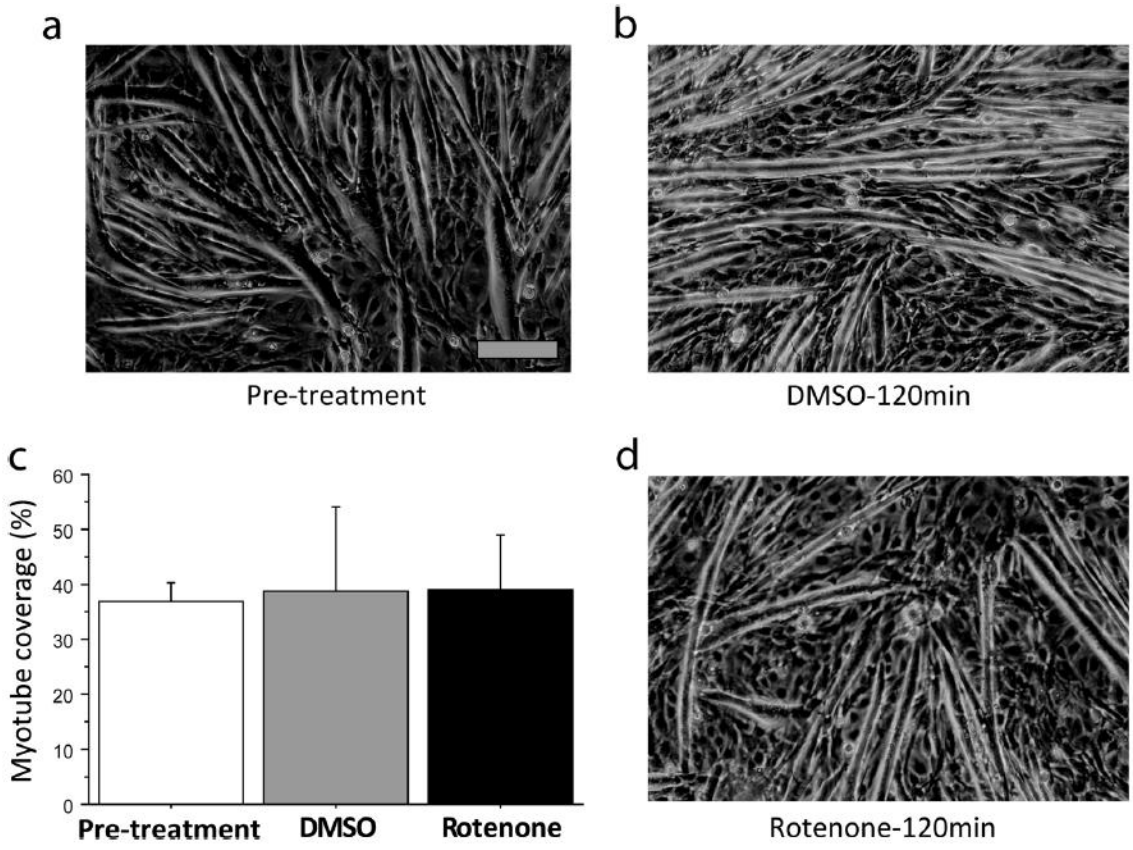

Figure 2-3 Morphology of C2C12 myotubes
Rotenone has no effect on myotube number. a) Pre-treatment b) DMSO and d) 250 nM rotenone (Scale bar 0.25mm). Quantification of myotube density (c) White bars, pre-treatment; Gray bars, DMSO; Black bars, rotenone. Mean ± SD, n=3 experiments.

Inhibition of AMPK with Dors (Compound C) prevents ATP recovery and p38 phosphorylation (Fig. 2-4). Dors is reported to inhibit AMPK activity at concentrations between 10-50 μM (17), and incubation with 40 μM reduced ACC phosphorylation at 60 minutes from 3.4±0.7 fold with rotenone alone to 1.7±0.2 fold (p=0.01; Fig. 2-4d). Dors alone induced only a small and not-significant reduction. At 15 minutes, Dors failed to produce a significant effect on ACC phosphorylation (data not shown), which may indicate that the Dors dose chosen is only marginally capable of countering AMPK activity. In the absence of Dors, ATP recovered from 27±4.1 μmole/g at 15 min to 35±0.1 μmole/g at 60 min (Fig. 2-4a), a gain of 7.6±1.1 μmole/g. In the presence of Dors, the initial ATP decline was greater (16±3.8 μmole/g), and recovered only to 18±5.5 μmole/g (Fig. 2-4a), representing recovery of only 1.1±0.4 μmole/g, significantly less than without Dors (p=.0004). Likewise, lactate production rate was reduced by Dors from 37±2.0 μmole/g/min to 26±3.1 μmole/g/min (rotenone X Dors p=0.0012, Fig. 2-4b). Rotenone-induced p38 phosphorylation at 15 min was reduced by Dors from 5.7±1.7 fold of control to 1.6±0.9 fold (p=0.02, Fig. 2-4c). There was a tendency for Dors alone to increase p38 phosphorylation, but this could not be statistically resolved.

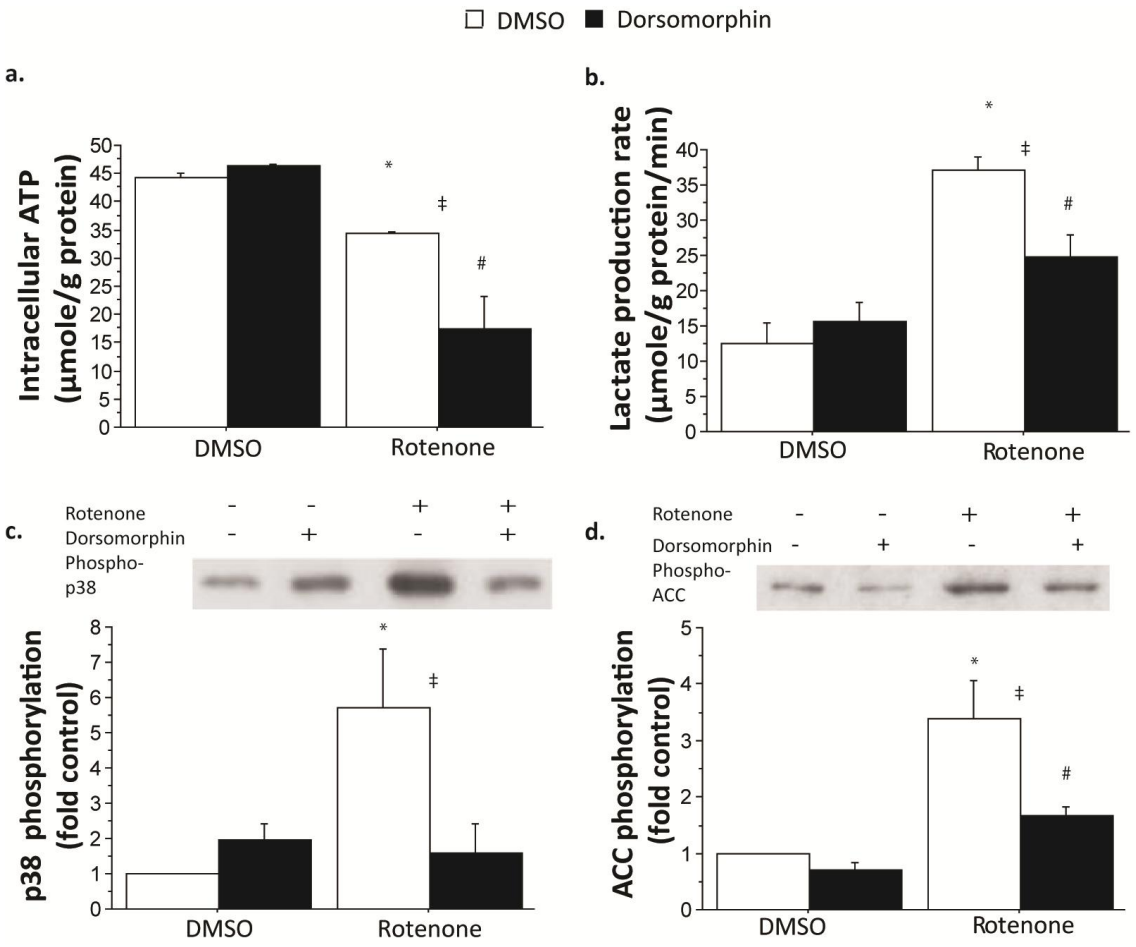

Figure 2-4 The effect of Dors on rotenone poisoning
The effect of Dors on rotenone-induced metabolite and kinase activity at recovery (60 min: a, b, d) and maximal ATP depletion (15 minutes: c). ATP content (a) and lactate production rate (b) in myotube cultures treated with rotenone with or without Dors. Phosphorylation of c) p38 at 15 minutes and d) ACC phosphorylation at 60min. Western blots are representative of 3 independent experiments, and bars represent Mean ± SD. ‡ interaction between rotenone and Dors $p < 0.05$; * main effect of rotenone $p < 0.05$; # main effect of Dors $p < 0.05$.

Direct activation of AMPK with AICAR does not change lactate production or p38 phosphorylation (Fig. 2-5). Because conflicting reports of the role of AMPK in p38 activation may be linked to energy depletion (Ho et al., 2007; Li et al., 2005), we examined the activation of p38 by the AMP-mimetic AICAR in the absence of ATP depletion. AICAR increased ACC phosphorylation, to a maximum of 6-fold with IC50 of 0.18±0.08μM (Fig. 2-5a.). However, AICAR did not increase p38 activation or lactate production (Fig. 2-5b & c), even at substantially higher concentrations, confirming that, although AMPK facilitates activation of p38 following rotenone treatment, AMPK itself is insufficient to activate p38 directly.

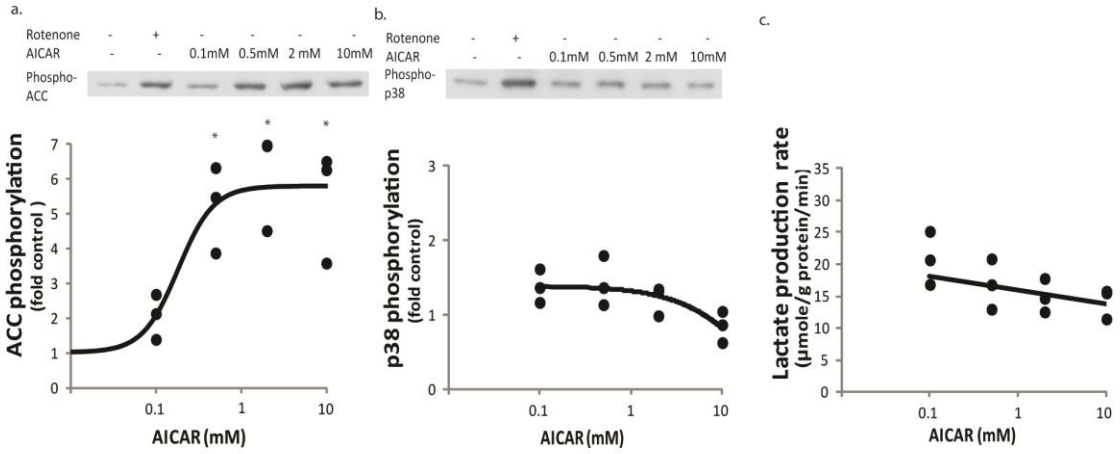

Figure 2-5 Effect of AICAR on phosphorylation of ACC and p38
Effect of AICAR on phosphorylation of ACC (a) and p38 (b) and lactate release (c). Representative Western blots also show concurrent treatment with 250 nM rotenone as positive control. Mean ± SD from 3 experiments; * $p<0.05$ *vs* vehicle.

Inhibition of p38α and p38β with SB203580 altered ATP recovery only at doses much higher than required to block kinase phosphorylation (Fig. 2-6). The pyridinyl imidazole SB203580 has been reported to inhibit p38α/β with IC50 0.3-0.5 μM, but is often applied at 10 μM, and may have off-target effects at concentrations above 3 μM (Lali et al., 2000). Rotenone-induced p38 phosphorylation at 15min was reduced from 3.7±0.5 fold of control to 2.2±0.3 in the presence of as little as 1 μM SB203580, and 1.3±0.7 fold with 20 μM SB203580 ($p=0.0029$, Fig. 2-6c). The dose range tested did not allow accurate determination of IC50, which appears to be less than 1 μM. ATP recovery was inhibited by SB203580, but only at doses of 10 μM and greater (Fig. 2-6a, $p=0.0006$). A slight reduction in lactate production rate was also noted only at the highest dose of 20 μM ($p= 0.0009$ Fig. 2-6b). SB203580 has been reported to directly inhibit Akt phosphorylation (16, 20). Rotenone alone reduced Akt S473 phosphorylation to 0.62±0.2 ($p=0.001$), and SB203580 resulted in a further reduction to 0.38±0.14 at 1 μM and 0.08±0.02 at 20 μM (Fig. 2-6d). Incubation with 1μM SB203580 and 0.1μM BIRB796 further decreased p38 phosphorylation, but had no effect on ATP recovery, similar to SB203580 treatment (Fig 2-6e, f). Inhibitor doses lactate production, indicating that p38 phosphorylation is not required for ATP recovery.

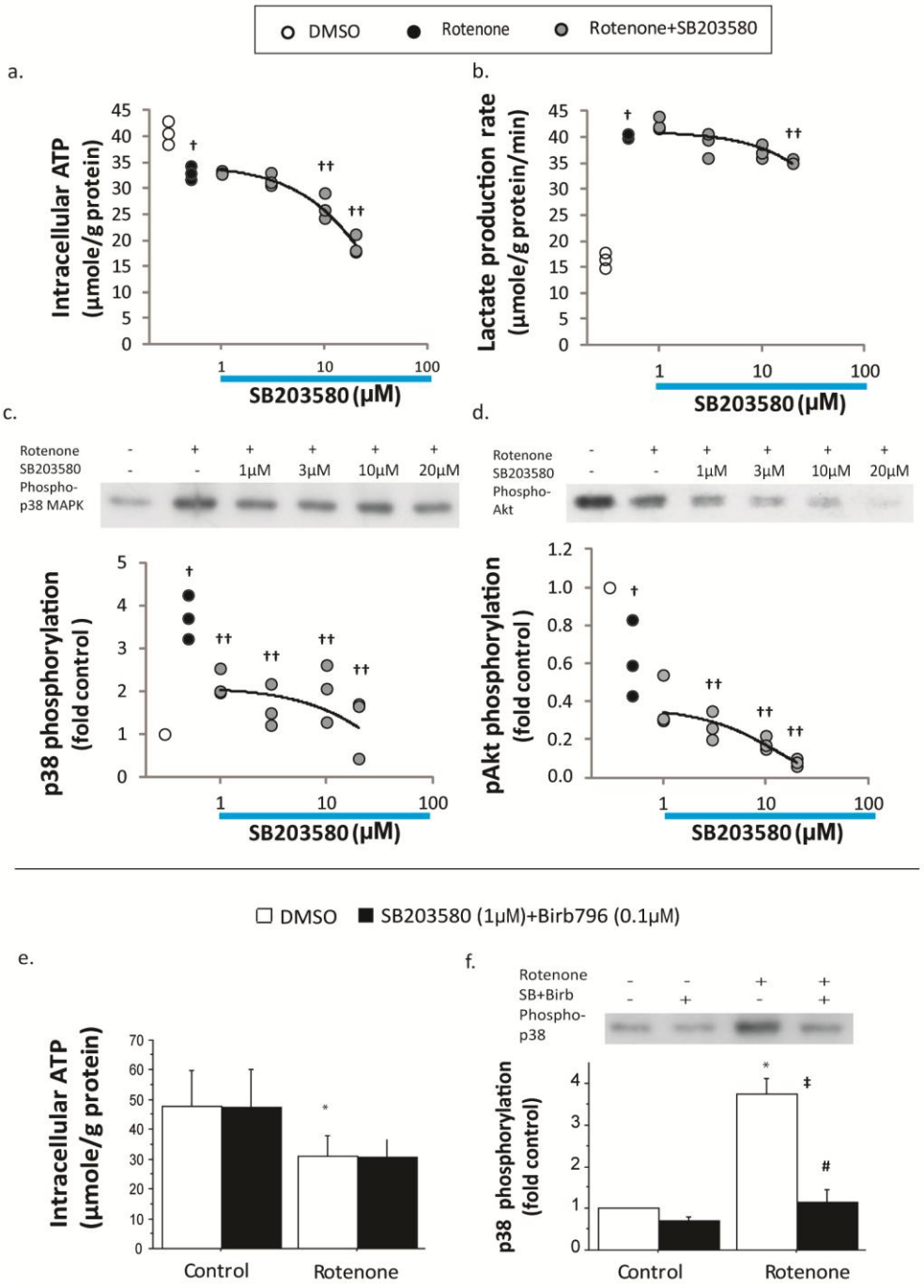

Figure 2-6 The influence of SB203580+ Birb on rotenone poisoning

The influence of SB203580 alone (a-d) or with Birb796 (e-f) on rotenone-induced metabolite and kinase activity at recovery (60 min) and maximal ATP depletion (15 min). ATP content (a: 60 minutes; e: 15 minutes) Lactate production rate (b, 60 minutes) p38 phosphorylation (c; f 15 minutes) and Akt phosphorylation (d, 15 minutes). (Mean ± SD; † significantly different from control, $p < 0.0033$; †† significantly different from rotenone alone, $p < 0.0033$. *main effect of rotenone $p < 0.05$; $^{\#}$ main effect of SB203580+Birb796 $p < 0.05$; ‡ interaction between rotenone and SB203580+Birb796 $p < 0.05$)

Inhibition of glucose uptake with cytochalasin B reduced lactate production without altering p38 phosphorylation. (Fig. 2-7). Because AMPK activity was required for both increased lactate production and p38 phosphorylation, but p38 activity was dispensable for ATP recovery, we tested whether the AMPK-facilitated lactate production was necessary for p38 phosphorylation. Incubation with 1μM cytochalasin B blocked the rotenone-induced increase in lactate production and exaggerated the decline in cytoplasmic ATP (Fig. 2-7a,b), which is consistent with inhibition of glucose transport. Cytochalasin B alone had no effect on ACC and p38 phosphorylation. In the presence of rotenone, there was a tendency for cytochalasin B to decrease p38 ($p=0.29$) and increase ACC phosphorylation ($p=0.12$), but these effects could not be statistically resolved (Fig. 2-7c, d). This suggests that uptake of extracellular glucose is not necessary for induction of p38 activity following ATP depletion, but that AMPK contributes to p38 phosphorylation more directly, although the statistical power is low.

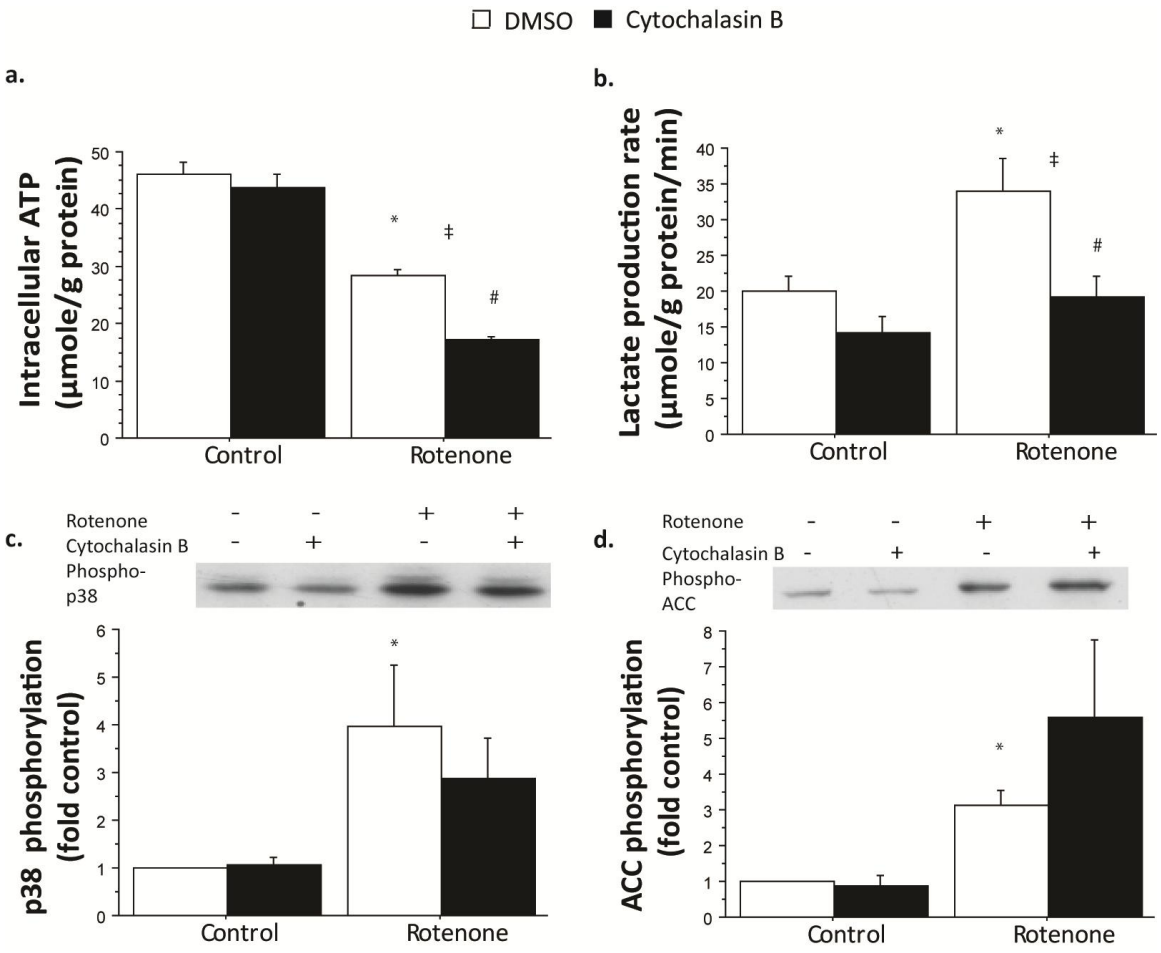

Figure 2-7 The effect of cytochalasin B on the rotenone poisoning
Effect of glucose transporter inhibition on the rapid response of myotubes to rotenone poisoning.(a) ATP content, (b) lactate production rate, (c) p38 phosphorylation, and (d) ACC phosphorylation with 250 nM rotenone at 15min. Western blots are representative of 3 independent experiments, and bars represent Mean ± SD. ‡ interaction between rotenone and cytochalasin B $p < 0.05$; * main effect of rotenone $p < 0.05$; # main effect of cytochalasin B $p < 0.05$.

Restricting extracellular glucose during the recovery phase eliminated lactate production and reduced p38 phosphorylation (Fig. 2-8). Because cytochalasin B disrupts actin filaments, including those of nascent sarcomeres (Manasek et al., 1972), and the cytochalasin B results were inconclusive, we further tested the involvement of glucose in roteneone-induced p38 phosphorylation by restricting extracellular glucose. In the absence of rotenone, restricting glucose to 0.5 mM reduced lactate production to 8.9±0.5 μmole/g/min, with a modest and unresolvable increase in ATP (Fig. 2-8a), suggesting that cells are easily able to accommodate this challenge by increasing oxidation of glucose. Combined with rotenone, glucose restriction resulted in a significant exaggeration of ATP depletion (Fig. 2-8a). Rotenone-treated cells in low glucose media were able to increase lactate production from 8.9±0.5 umole/g/min to 13.5±0.6 μmole/g/min ($p=0.0002$), but did not rise to control-25 mM glucose levels (Fig. 2-8b). Rotenone-induced ACC phosphorylation increased from 3.2±0.4 fold of control in 25 mM glucose media to 4.7±1.0 fold of control in 0.5 mM glucose with mannitol media ($p=0.0072$) (Fig. 2-8d.), consistent with the exaggerated decline in ATP. In contrast, glucose restriction reduced p38 phosphorylation from 4.2±0.6 fold to 2.7±0.3 fold of control ($p=0.0008$) (Fig. 2-8c). Because osmotic pressure can influence both glucose transport and p38 phosphorylation, these experiments were also performed in media containing 0.5 mM glucose without osmotic balance by mannitol. This reduction in extracellular osmotic pressure had no further effect on ATP depletion, lactate production, or ACC phosphorylation, but did result in a further reduction in p38 phosphorylation.

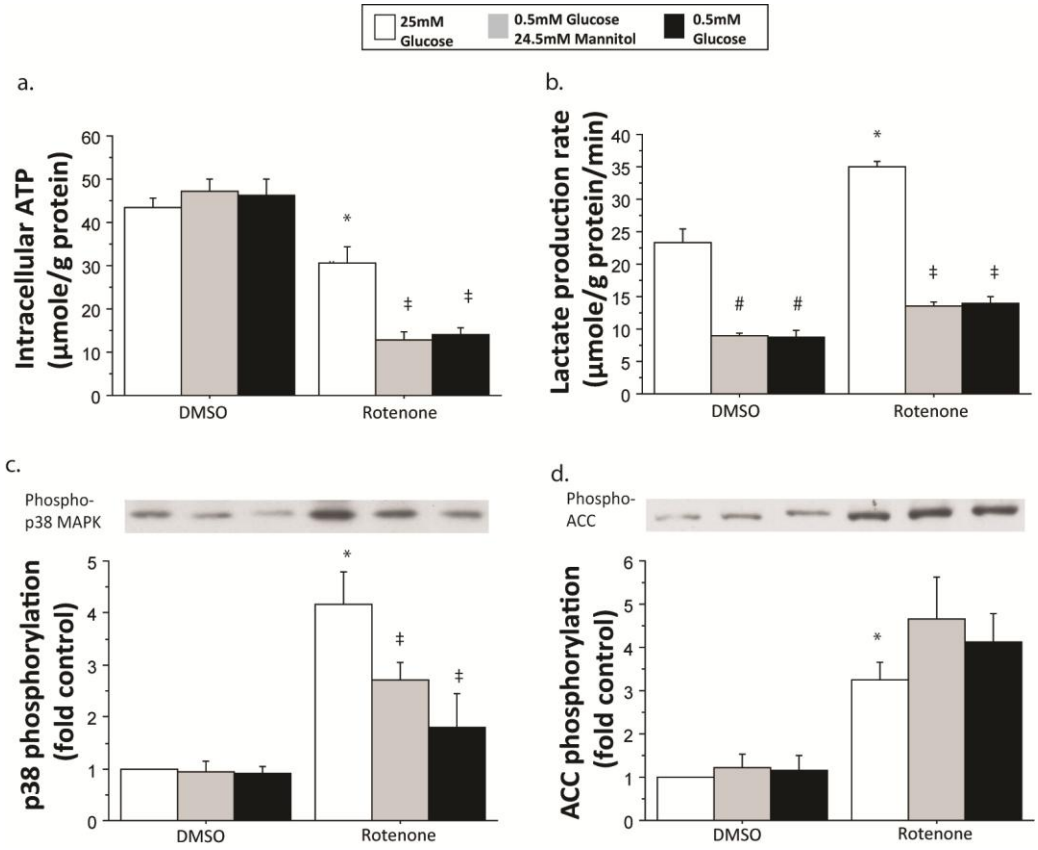

Figure 2-8 Effect of glucose restriction on rotenone poisoning

Effect of glucose restriction on the rapid response of myotubes to rotenone poisoning.(a) ATP content, (b) lactate production rate, (c) p38 phosphorylation, and (d) ACC phosphorylation with 250 nM rotenone at 15min. Western blots are representative of 3 independent experiments, and bars represent Mean ± SD. ‡ interaction between rotenone and glucose $p < 0.05$; * main effect of rotenone $p < 0.05$; # main effect of glucose $p < 0.05$

2.5 Discussion

Inhibiting mitochondrial respiration in myotubes with rotenone rapidly depletes cellular ATP with substantial recovery by two hours. Both ACC and p38 are rapidly phosphorylated, and the synchronous recovery of ATP and decline in p38 phosphorylation suggests that p38 may participate in a feedback control process. However, preventing glycolytic recovery by dorsomorphin or glucose restriction abolishes p38 activation, while inhibition of p38 with SB203580 or Birb 796 has no effect on ATP recovery or AMPK activity. We interpret these results as indication that phosphorylation of p38 in rotenone-stimulated muscle cells requires AMPK and extracellular glucose, but does not participate in control of glycolysis.

These observations are generally consistent with literature reports. Mitochondrial poisoning by DNP evokes a similar time-course of ATP depletion and recovery (Bashan et al., 1993). Reports of cytoplasmic ATP in cultured myotubes span a surprisingly wide range from 5-50 μmoles ATP per gram of protein (Bashan et al., 1993; Dehne et al., 2007; Wagenknecht and Lieberman, 1991). Some of this difference can be attributed to normalization by Triton-soluble, SDS-soluble, or other measures of protein. We found ATP content to be extremely labile, decaying at 4 μmole/g protein/hour, even at 4 °C (data not shown). Because of this, collection and nucleotidase inactivation of ATP samples was performed as rapidly as possible, generally less than 10 minutes between application of lysis buffer and boiling. GLUT4 translocation following insulin or mitochondrial poisoning is reported to complete within 5 minutes (Michelle Furtado et al., 2003), well before our first time point, so the relatively constant rate of lactate

production is reasonable. Finally, under similar conditions, reports of ACC phosphorylation and p38 phosphorylation are between 3 and 10 fold of control (Hao et al., 2010; Newhouse et al., 2004; Pelletier et al., 2005). Variability in ACC phosphorylation was somewhat high, reflecting the very low level of phosphorylation in vehicle-treated cultures and the limited dynamic range of film-based quantification.

AMPK is generally accepted to stimulate GLUT4 translocation, to inhibit energy consuming processes like lipogenesis, and to facilitate energy producing processes like glycolysis (Hardie and Ashford, 2014). In the present study, inhibition of AMPK effectively blocks lactate production and ATP recovery following rotenone treatment. Although Dors can also inhibit a number of receptor-mediated kinases (Bain et al., 2007; Boergermann et al., 2010; Yu et al., 2008), these pathways are unlikely to contribute to the acute response of isolated myotubes. With AMPK inhibited, metabolic compensation would be limited to a combination of substrate effects and allosteric action, which may be capable of doubling the rate of ATP synthesis (Ghorbaniaghdam et al., 2014), and the present results support that prediction. C2C12 myotubes have relatively low expression of GLUT4, but these results suggest that about half of the increase in glycolysis can be attributed to substrate effects and half to AMPK-dependent effects, including GLUT4 translocation and phosphofructokinase 2 (PFK2) activation. Inhibition of AMPK also blocked p38 phosphorylation, and AMPK has been reported to participate in activation of p38 through formation of a TAB1 complex (Li et al., 2005). Activation of AMPK appears not to be sufficient to nucleate this process, as AICAR treatment fails to induce p38 activation (Fig 2-5b) (Ho et al., 2007). Treatments where AMPK-TAB1 mediated activation of p38 is reported seem to include oxidative stress (Lanna et al., 2014; Li et al.,

2005), and this complex may help to refine the cellular response to excess AMP based on additional chemical states.

The p38 MAP kinase has been suggested to activate glucose transporters to facilitate glucose uptake (Somwar et al., 2000). Subsequent work from the same group seems to refute that role (Antonescu et al., 2005), and the present results (Fig.2-6) also support no role for p38 in glucose uptake. Although SB203580 and other pyridinyl imidazole compounds are frequently described as specific inhibitors of p38α and p38β, this specificity depends strongly on careful control of concentration. The present results indicate near maximal reduction of p38 phosphorylation with only 1μm SB203580, which has no effect on lactate production or glycolytic recovery of ATP. There is progressive reduction in lactate production and ATP recovery above 10 μM, which closely parallels reduction in Akt phosphorylation, and high concentrations of SB203580 compounds have been reported to inhibit Akt (Lali et al., 2000). Although SB203580 does not block p38γ, which is the major isoform in mature skeletal muscle, adding BIRB796, which is highly selective for p38 γ (Kuma et al., 2005) in combination with SB203580 further decreased p38 phosphorylation but had no effect on ATP recovery (Fig. 2-6e, f).

Although these experiments do not support a requirement for p38 in the acceleration of glycolysis, there are limitations in the experimental design that might obscure this effect. According to model 1, p38 acts by facilitating glucose uptake by activation of GLUT4 transporters, and glucose uptake was not directly measured. C2C12 myotubes express relatively little GLUT4 (Kotliar & Pilch, 1992), relying more on GLUT1 for glucose uptake. It is GLUT1 transporters in Clone 9 cells that seem to be

regulated by p38 (Xi et al., 2001), which suggests C2C12 myotubes might even be more sensitive to p38 than other muscle models. Our cells were maintained and treated in media containing superphysiological 25 mM glucose, which may provide enough driving force for transport to overcome permeability limitations in the baseline conditions. Pharmacological interventions were chosen in this study to minimize long-term compensatory processes associated with genetic manipulations.

The objective of this study was to determine whether p38 regulates glycolytic activity or is activated as a consequence of glycolysis. Results indicate that it does not control glycolysis, but the converse is less clear. Phosphorylation of p38 does require AMPK activity, but the interventions used to reduce glucose metabolism had mixed outcomes. Cytochalasin B disrupts actin filaments, upon which many cellular transport, motility, and adhesion processes depend, and prevents the increase in lactate production without blocking lactate production completely, but has no effect on p38. Glucose restriction, by simple mass action, also prevents the increase in lactate production, reduces basal lactate production, exaggerates the ATP-stress associated with rotenone even beyond cytochalasin B, and does reduce p38 phosphorylation. One way to reconcile these data is the possibility that p38 phosphorylation depends on extracellular glucose and allows the cell to select among extracellular nutrients for ATP recovery. There are glucose sensitive receptors and channels, but they do not seem particularly prominent in skeletal muscle (Diez-Sampedro et al., 2003; Ozcan et al., 1998). It is possible that the combination of rotenone and cytochalasin B activate p38 through a different mechanism than rotenone alone. That is, that cytochalasin B may effectively block glucose transport and glycolysis-induced p38 activation, but render the cell more sensitive to volume,

osmotic, or oxidative stresses. It seems likely that activation of p38 following rotenone treatment depends on a combination of cellular processes, of which AMPK is one.

3 CHAPTER

Modulation of glucose metabolism and AMPK activity through redox state and ROS in C2C12 myotubes

3.1 Abstract

From rest to exercise, the rate of glucose metabolism dramatically increases with ATP turnover. This increase is accompanied and mediated by changes in intermediate metabolite concentration. Muscle contraction causes a small drop of ATP and a significant increase in AMP. AMP/ATP ratio strongly influences the activity of glycoylsis enzymes. NAD^+/NADH ratio strongly influences the disposal of pyruvate by the oxidative or reductive pathways. The goal of this study was to evaluate the contribution of cellular redox state in the balance of oxidative and anaerobic metabolism to test the hypothesis that NADH oxidation and ATP depletion increase glucose oxidation via both mass action and PDH phosphorylation. Treating C2C12 myotubes with PMS completely oxidized NADH at 200μM, but oxygen consumption, ATP depletion, $DCFH_2$ oxidation and the phosphorylation of PDH were significantly induced by PMS only above 1μM. Thus, NADH oxidation is not sufficient to influence glucose oxidation, but ROS-AMPK signaling may play the role in stimulating oxygen consumption.

3.2 Introduction

The rate of glucose metabolism changes dramatically with activity. The control of that rate is mediated by several glucose metabolites, such as ADP, AMP, and NADH (Sahlin et al., 1987). Skeletal muscle catabolizes glucose to generate ATP via glycolysis and oxidative phosphorylation. Glycolytic flux is facilitated by glucose uptake and the regulation of several key enzymes along the glycolysis pathway. Phosphofructokinase (PFK) controls the conversion of fructose 6-phosphate into fructose 1,6-biphosphate and has been suggested to be a critical step in determining the rate of glycolysis during muscle contraction (Schmitz et al., 2013). In order to adapt to dramatic changes of condition, such as resting and sprinting, skeletal muscle has ability to reprogram glucose metabolism. During periods of low activity, muscular ATP demand is satisfied primarily by oxidative metabolism of fatty acids. As activity increases, much of the marginal energy derives from oxidative metabolism of glucose. As activity increases further, anaerobic metabolism of glucose into lactate increases dramatically.

Regulation and control of the scaling of ATP synthesis involves a large network of metabolites and metabolic sensors. The fluxes of glucose through glycolysis and mitochondrial respiration are regulated by mass action, allosteric regulation through ATP/AMP. During rest, the ratio of ATP/AMP is high. During exercise, the accumulation of AMP activates the energy sensor, 5' AMP-activated protein kinase (AMPK). Lowering the ratio of ATP/AMP increases PFK and PDH activity via allosteric regulation (Hardie and Ashford, 2014).

Muscle cells also possess several metabolic sensors which are regulated by the NAD^+/NADH ratio. Pyruvate stands at a metabolic crossroad between anaerobic and

aerobic metabolism. The ability of muscle cells to switch between lactate production and pyruvate oxidation may be determined by the ratio of NAD^+/NADH. Pyruvate dehydrogenase complex (PDH) catalyzes irreversible decarboxylation of pyruvate into acetyl-CoA (Sugden and Holness, 2006). The activity of PDH is highly regulated by pyruvate dehydrogenase kinases (PDKs) (Sugden and Holness, 2006). During high intensity exercise, the accumulation of NADH allosterically stimulates PDK activity which exerts an inhibitory effect on PDH through the phosphorylation of the E1-α subunit (Bowker-Kinley et al., 1998; Rardin et al., 2009). Lactate dehydrogenase (LDH) is a key enzyme in anaerobic metabolism converting pyruvate and NADH into lactate and NAD^+. LDH converting pyruvate to lactate is considered to be near equilibrium (Williamson et al., 1967). Accumulation of NADH and pyruvate increase lactate production by mass action.

Redox state and the accumulation of ADP or AMP may serve as molecular transducers driving a switch from oxidative phosphorylation to glycolysis. The goal of this study was to evaluate the contribution of cellular redox state in the balance of oxidative and anaerobic metabolism. We used phenazine methosulfate (PMS) to chemically alter cellular redox state to test the hypothesis that the oxidation of NADH to NAD^+ increases oxidative metabolism by both mass action and activation of PDK. We found that low dose PMS increases NAD^+/NADH ratio without any change on PDH phosphorylation or oxidative metabolism. PMS-induced oxygen consumption was correlated with ROS production, ATP depletion and ACC phosphorylation suggesting that ROS-AMPK signaling may contribute to the glucose oxidation.

3.3 Materials and Methods

3.3.1 Materials

Antibodies for ACC^{S79}, and PDHE1-A type I ^{S293} were purchased from Cell Signaling Technology and EMD Millipore, respectively. CM-H_2DCFDA was purchased from Invitrogen and was dissolved in DMSO to 10mM on the same day of experiment. C2C12 cells were obtained from the American Type Culture Collection (ATCC, Manassas, VA). Dulbecco's modified Eagle's medium (DMEM) was purchased as a powdered mixture (Corning 50–003), supplemented with 3.7 g/L NaHCO3, and sterilized by 0.2 um filtration. PMS (10mM) was prepared in dH2O as stock solution. FCCP (5mM), rotenone (10mM), antimycin a (10mM) were prepared in DMSO.

3.3.2 Cell culture

C2C12 myoblasts were maintained in growth medium (GM, DMEM supplemented with 10% fetal bovine serum (FBS, Hyclone), 100IU/ml penicillin, and 100 μg/ml streptomycin) in a humidified incubator under 10% CO2 at 37 °C. Cells were seeded at $1.6x10^4$ cells/well , $2x10^3$ cells/well, and $1.6x10^3$ cells/well on 12-well plates, XFp 8-well plates and 96-well plates, respectively and allowed to proliferate 1-2 days to 60-80% confluence, at which point they were switched to differentiation media (DM, DMEM supplemented with 2% horse serum (Hyclone) and antibiotics). Media was replenished every 48 h. Interventions were performed after 5-6 days in DM.

Mature myotubes were rinsed twice with serum and antibiotic-free DMEM (SFM) and incubated 60 min prior to application of PMS. Culture were rinsed with ice-cold PBS

twice. Cultures collected for metabolite analysis were harvested by scraping in cold carbonate buffer (100mM Na_2CO_3, 20 mM $NaHCO_3$, 20 mM NAM). Cultures collected for ACC phosphorylation and PDH phosphorylation were collected by scraping in detergent buffer (1%Triton-X100, 50mMtris, 300mM NaCl, 5mM EDTA) supplemented with protease inhibitors (Sigma), 100mM NaF, and 4ug/ml $NaVO_3$. Sample was incubated on ice for 30min. Insoluble material from both samples was cleared by centrifugation at 16K xg for 5min. Soluble protein concentration was assayed by bicinchronic acid assay (Pierce).

3.3.3 Metabolite assay

Lysate NAD and NADH contents were determined by alcohol dehydrogenase (ADH)-diaphorase enzymatic cycling using 40µl of sample and 200µl assay buffer (40µg/mL yeast ADH (Alfa Aesar, MA), 0.2% ethyl alcohol, 2mM $MgCl_2$, 0.2 U/ mL diaphorase (Innovative Research, MI), 1µM resazurin (Alfa Aesar, MA)). Resorufin formation was monitored with excitation at 540 nm and emission at 590 nm every 2 minutes for a total of 20 minutes. The standard curve is produced by measuring the rate of fluorescence increase by standards of known concentration of NAD^+. NAD and NADH content are normalized to lysate protein content. For measurement of NAD, 10µl samples were diluted in 90µl lysis buffer and were incubated on ice, For measurement of NADH, 100µl samples were incubated for 15min at 60°C to destroy NAD^+ (Wagner and Scott, 1994). NAD^+ was determined by subtracting NADH from NAD.

Cytoplasmic ATP was determined by the firefly luciferase method (Hsu and Burkholder, 2015). ATP standards and samples were distributed in duplicate to 96 well

plates, and assay buffer (1.5mM $MgCl_2$, 0.15mM EDTA, 18μM dithiothreitol (DTT), 0.25 mg/ml bovine serum albumin (BSA), and 6mM HEPES, pH 7.8) containing 30μM luciferin and 0.75 μg/ml luciferase was rapidly added using a multichannel pipettor. Luminescence was measured within 5min (FLx800, BioTek). Luminescence values were calibrated to a standard curve and normalized to lysate protein content.

3.3.4 Western blot

To assay phosphorylation of ACC and PDH, 4 μg soluble protein was separated by SDS-PAGE through 7 % (ACC) or 10% (PDH) acrylamide gels. Protein was transferred to nitrocellulose membranes, blocked with 5% nonfat dry milk in Tween-TBS (TTBS) and hybridized with phospho-specific antibody to ACC^{S79} (1:2000) or PDHE1-A type I^{S293} (1:1000). Membranes were rinsed and incubated with horseradish peroxidase conjugated secondary antibody (Jackson, 1:80,000). Bands were detected by enhanced chemiluminescence (Amersham), visualized by exposure to radiographic film, and quantified by scanning densitometry. All samples from an experiment were run on the same gel, and normalized to the average of that experiment's control samples.

3.3.5 Metabolic flux analysis

On the day of metabolic flux analysis, cells were changed to unbuffered DMEM (DMEM base medium (Seahorse Bioscience) supplemented with 25mM glucose, 1mM sodium pyruvate, 4mM glutamine, pH 7.4). Oxygen consumption rate (OCR) and extracellular acidification rate (ECAR) were determined in three measurement intervals (one measurement interval consists of a 3min mixing, 0min waiting ,and 3min measurement step) in live cells before and after sequential injection of PMS (final

concentration 0.01, 0.05, 0.1, 0.5, 1μM) , FCCP (final concentration 1μM) to uncouple respiration and rotenone and antimycin a (final concentration rot 0.5μM/aa 0.5μM) to inhibit Complex I/III. Protein concentration of each sample was determined by bicinchronic acid assay (Pierce) and was used to normalize OCR and ECAR.

3.3.6 Cellular ROS analysis

Mature myotubes were rinsed once and incubated 30 min with SFM. Cells were incubated with 10μM CM-H_2DCFDA in SFM for another 30min in the dark prior to the treatment. Cultures were rinsed twice with DMEM (no $NaHCO_3$) and exposed to PMS (0, 0.05, 0.2, 1 μM) for 30min. Fluorescence was monitored with excitation at 485 nm and emission at 528 nm every 3 minutes for a total of 30 minutes.

3.3.7 Statistical analysis

Experiments were repeated as three independent procedures, with duplicate or quadruplicate wells (ROS) averaged prior to statistical analysis, giving a sample size of n=3 per group. Results are reported as means with SD to indicate population variability. The EC50 were determined by fitting experimental data to the Hill equation using MatLab software version 2014a (fitnlm, MathWorks, Inc.). Dose experiments were analyzed by one-way ANOVA followed by post hoc T tests using Bonferroni correction for multiple comparisons

3.4 Results

PMS and other phenazine analogs can directly oxidize NADH. To determine the efficacy of this reaction in our culture model, we measured the content of NAD and

NADH. We found a dose dependent decrease in NADH (minimum of 0.167±0.035 control; 10μM PMS) with EC_{50} of 33.6±109.7nM (fig. 3-1a) and a reduction of the total NAD pool (p=0.0012, fig. 3-1b) with EC_{50} above 10μM (fig. 3-1c). The NAD^+/NADH ratio, a common measure of redox state increased in a dose dependent manner with EC_{50}=3645.2±1.1e^{+8}nM. We investigated the production of reactive oxygen species in the presence of PMS. Incubation of PMS for 10min increased $DCFH_2$ oxidation with EC_{50} > 200nM (fig. 3-1d).

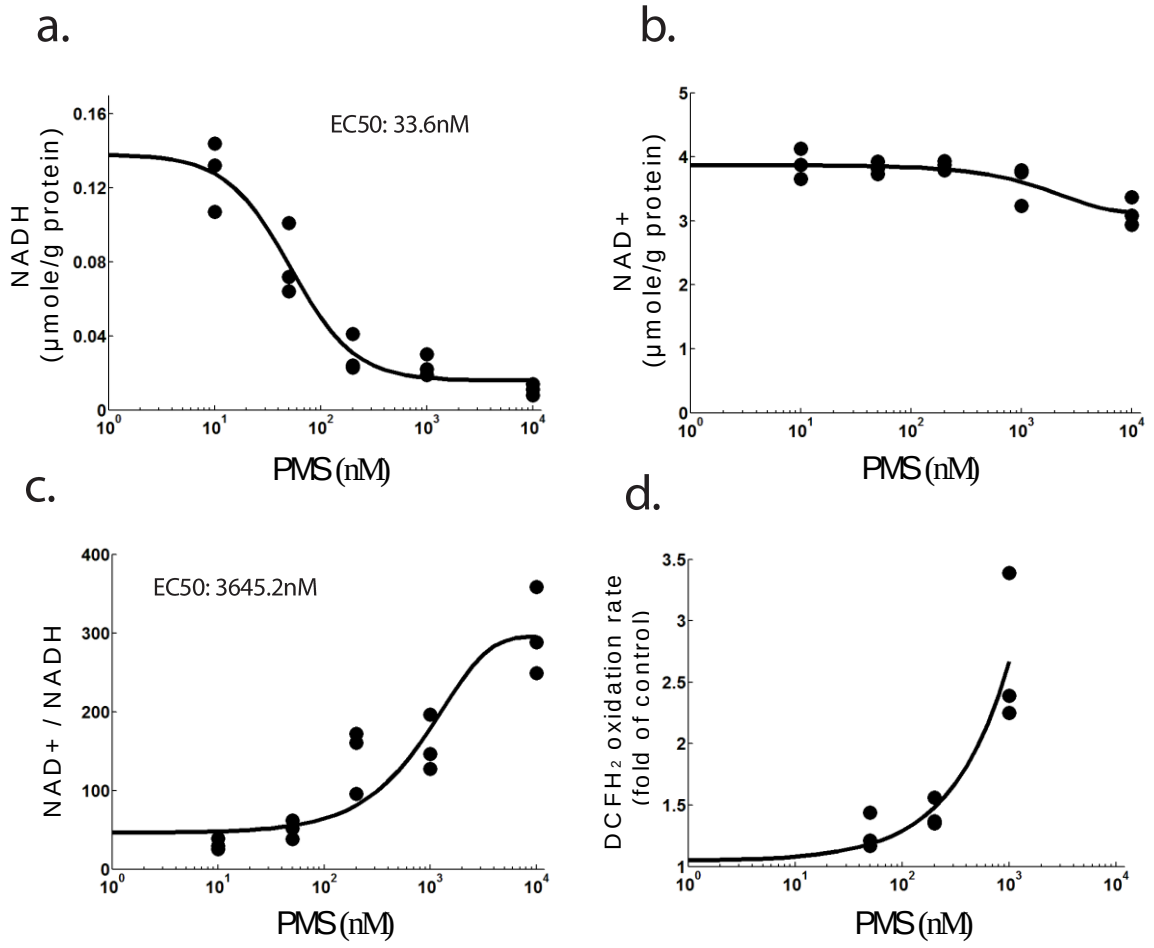

Figure 3-1 Effect of PMS on cellular NAD and ROS production
Effect of 15min PMS on cellular (a) NADH (b) NAD^+, (c) NAD^+/NADH ratio, and (d) $DCFH_2$ oxidation rate. N=3 experiments with duplicate or quadruplicate wells ($DCFH_2$).

Because the redox state of NAD may influence glucose metabolism and the efficiency of ATP production, we measured the effect of PMS on cellular ATP. PMS induced a dose-dependent reduction in ATP after15min with $EC_{50} > 3\mu M$ (fig. 3-2a). This was associated with phosphorylation of ACC with $EC_{50} > 2\mu M$ (fig. 3-2b). PDK is allosterically activated by NADH and ATP and inhibited by NAD^+ and AMP (Bowker-Kinley et al., 1998).To test whether oxidation of NAD or reduction of ATP would inhibit PDK, we measured PDH phosphorylation. PMS reduces the phosphorylation of PDH with $EC_{50} > 3\ \mu M$ (fig. 3-2c). This is consistent with inhibition of PDK only with decreasing ATP.

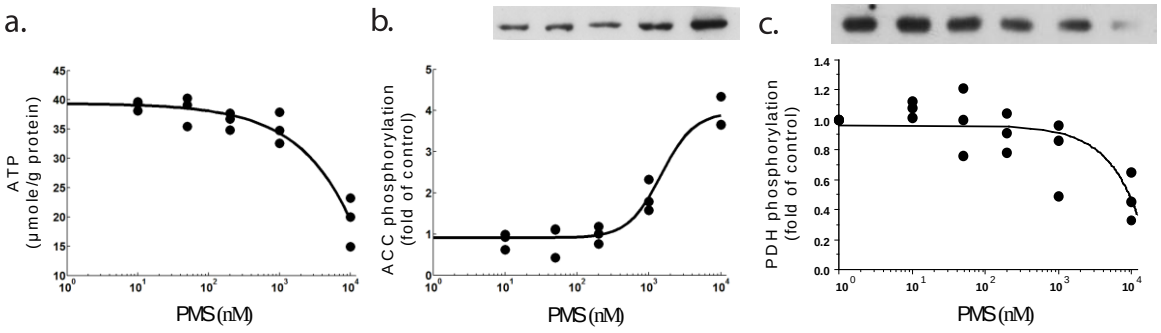

Figure 3-2 Effect of PMS on ATP and the phosphorylation of ACC and PDH
Effect of 15min PMS on cellular (a) ATP, (b) ACC phosphorylation, and (c) PDH phosphorylation (to be revised). N=3 experiments with duplicate wells.

To evaluate effect of redox state on aerobic metabolism, we measured oxygen consumption of PMS-treated cells (fig. 3-3). Oxygen consumption rate (OCR) was increased by PMS with EC_{50}>1 µM, much higher than the dose required to deplete NADH. OCR does increase at PMS doses similar to those that deplete ATP and activate AMPK, consistent with a regulated response to ATP depletion. Extracellular acidification (ECAR), representative of lactate production and glycolytic metabolism does appear to decrease at low PMS concentrations. C2C12 cells, grown in high glucose conditions perform aerobic glycolysis, and the decreased ECAR may represent anaerobic compensation for elevated oxidative metabolism.

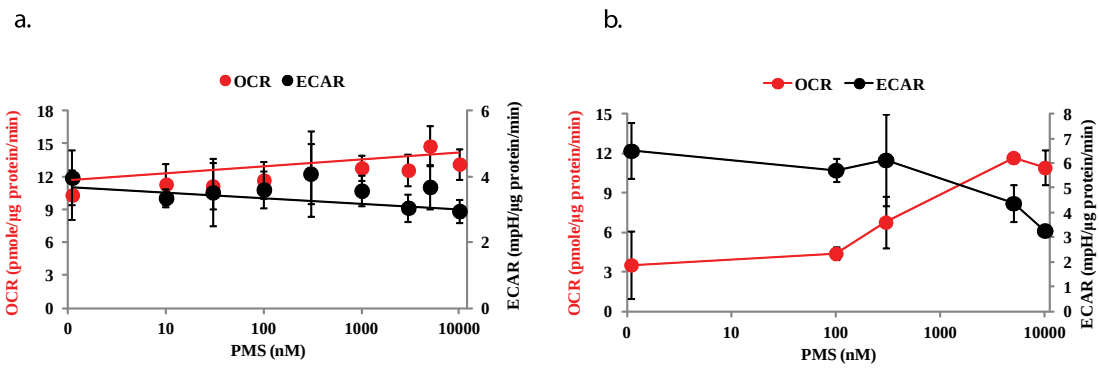

Figure 3-3 Effect of PMS on OCR and ECAR
Effect of PMS on cellular (a) OCR and ECAR (b) OCR and ECAR with injection of 0.5µM rotenone. N= 3 experiments with duplicate wells. Red: OCR ; Black: ECAR

3.5 Discussion

In this study, PMS completely oxidized NADH at 200μM in 15min, but OCR, ATP depletion, $DCFH_2$ oxidation and the phosphorylation of PDH were significantly altered by PMS only above 1μM. We interpret these results as indication that NADH oxidation alone is not sufficient to influence PDK activity or oxygen consumption, but that ROS production may induce ATP depletion and oxygen consumption at high concentrations.

The study was based on a model of metabolic control where adenosine phosphorylation state strongly influences the activity of glycoylsis enzymes and NAD oxidation state strongly influences the disposal of pyruvate by the oxidative or reductive pathways. According to this model, conversion of ATP to ADP or AMP would be expected to increase glucose transport, PFK activity, and the rate of pyruvate production. Reduction in ATP may also increase oxidative disposal of pyruvate by inhibiting phosphorylation of PDH. According to this model, it was expected that oxidation of NADH would increase the oxidative disposal of pyruvate by inhibiting phosphorylation of PDH. Increased oxidation of pyruvate would be expected to increase oxygen consumption and decrease lactate production.

The O_2 consumption could come from inhibition of PDK. Previous in vitro study has shown that increasing NAD^+/NADH ratio reduced PDK4 activity which may increase PDH activity and glucose oxidation (Sugden and Holness, 2006). However, we found that NADH was depleted at much lower PMS concentration than influences PDH phosphorylation.

PMS can increase mitochondrial complex I (COXI), complex III (COXIII) activity, which would also increase OCR. PMS derivative, methylene blue, has been used effectively as an antidote for neurodegenerative disease caused by rotenone (Zhang et al., 2006). NADH can reduce PMS to $PMSH_2$ (reduced form), whereas cytochrome C reoxidizes $PMSH_2$ to PMS (oxidized form). PMS-mediated bypass might reduce ROS production by COXI/III, which would be expected near PMS concentration of 40nM. However, we found that NADH was depleted at much lower PMS concentrations than influence O_2 consumption. This suggests that direct shuttling of electrons from NADH to cytochrome C, bypassing proton transport by COXI and COXIII, and reducing the efficacy of NADH : ATP conversion, does not substantially alter mitochondrial respiration in C2C12 cells.

PMS might also directly transfer electrons from NADH to molecular oxygen to produce superoxide (Van Noorden and Butcher, 1989), and the DCF fluorescence was consistent with this mechanism. ROS may inhibit mitochondrial ATP synthesis and subsequently activate AMPK (Irrcher et al., 2009). We did find that ATP depletion and AMPK activation were induced by PMS in the same concentration range as generated ROS.

AMPK activation increases glucose uptake, glycolysis and mitochondrial respiration in skeletal muscle (Hardie and Ashford, 2014). ROS generated by muscle contraction has been shown to facilitate glucose uptake (Chambers et al., 2009), to induce mitochondrial biogenesis (Irrcher et al., 2009), and to activate AMPK through liver kinase B1 (LKB1) and Calcium/Calmodulin-dependent kinase kinase (CaMMK) (Morales-Alamo and Calbet, 2016; Xie et al., 2006). Exercise-induced metabolic

challenge is coupled with oxidative challenge resulting in a wide range of adaptive responses, but excessive exercise training leading to overproduction of ROS which can have detrimental effects on cellular function. To understand redox –sensitive pathway may help to design optimal training strategies and to maximize muscular adaptation.

4 CHAPTER

Independent AMP and NAD signaling regulate C2C12 differentiation and metabolic adaptation

4.1 Abstract

The balance of ATP production and consumption is reflected in AMP and NAD content and has been associated with phenotypic plasticity in striated muscle. Some studies have suggested that AMPK-dependent plasticity may be an indirect consequence of increased NAD synthesis and SIRT1 activity. The primary goal of this study was to assess the interaction of AMP and NAD dependent signaling in adaptation of C2C12 myotubes. Changes in myotube developmental and metabolic gene expression were compared following incubation with AICAR and nicotinamide mononucleotide (NMN) to activate AMPK and SIRT1. AICAR showed no effect on NAD pool and nampt expression, but significantly reduced histone H3 acetylation, GLUT1, COX2 and MYH3 expression and reduced myotube density. In contrast, NMN supplementation for 24 hours increased NAD pool by 45% but did not reduce histone H3 acetylation nor promote mitochondrial gene expression. The combination of AMP and NAD signaling did not induce further metabolic adaptation, but NMN ameliorated AICAR-induced myotube reduction. We interpret these results as indication that AMP and NAD contribute to C2C12 differentiation and metabolic adaptation independently.

4.2 Introduction

Cellular energy status impacts almost all cellular functions. In skeletal muscle cells, the rate of ATP turnover increases 100-fold or more during contraction (Schmitz et al., 2013), and the cells must accommodate long periods of low metabolic activity interspersed with discrete bouts of very high activity. The pattern of this activity seems to be very important to the establishment and maintenance of muscle size and phenotype, although the mechanism by which activity is transduced to growth remains unclear. Two molecules have gained wide recognition as likely transducers of energy metabolism: AMP and NAD^+. Cytoplasmic AMP may rise from nanomolar concentrations at rest to micromolar during exercise, while ATP undergoes only fractional declines (Cheetham et al., 1986), which makes AMP a very sensitive indicator of ATP balance and AMPK a ubiquitous effector of energetic stress. Nicotinamide adenine dinucleotide (NAD) is one of the major electron carriers in both oxidative and glycolytic metabolism, and the ratio of oxidized NAD^+ to reduced NADH can be used as a dynamic indicator of metabolite balance. In skeletal muscle, this ratio is dominated by the activity of lactate dehydrogenase, and the pyruvate / lactate ratio is often used as a proxy for NAD^+ / NADH. In cell culture, NAD^+ / NADH declines as media glucose is converted to lactate, and is elevated in glucose-restricted media (Fulco et al., 2008). Because NAD^+ is a required substrate for SIRT1, SIRT1 activity might be modulated by the relative production of ATP through the oxidative and anaerobic pathways.

AMPK and SIRT1 are especially interesting because of their apparent interactions. Although they share several common transcriptional targets, including PGC-1α, p53, and FOXO, the cellular consequences of AMPK and/or SIRT1 activation

are highly dependent on cell type and phase. In quiescent satellite cells, SIRT1 reduces expression of apoptosis markers (Ryall et al., 2015). In differentiating myoblasts, activation of AMPK or SIRT1 represses differentiation and facilitates proliferation (Fulco et al., 2008). In mature muscle and fully differentiated myotubes, AMPK and SIRT1 contribute to mitochondrial biogenesis and expression of a "slow-like" phenotype (Gerhart-Hines et al., 2007; Zong et al., 2002). Some evidence suggests that the above-mentioned transcriptional modifiers or SIRT1 itself may require priming phosphorylation by AMPK prior to deacetylation (Canto et al., 2010; McGee and Hargreaves, 2011). A number of studies have shown that activation of AMPK increases transcription of nampt, the rate-limiting enzyme in the NAD salvage pathway, suggesting that activation of AMPK necessarily leads to activation of SIRT1 via increased NAD^+ or reduced nicotinamide (NAM) (Canto et al., 2009; Fulco et al., 2008).

These interactions suggest three models for transcriptional regulation by cytoplasmic metabolites: an independent model, a nampt model and an AMPK priming model. The AMPK-dependent phosphorylation and SIRT1-dependent deacetylation may be independent, which would allow additive transcriptional effects from the two enzymes. The nampt model suggests that ultimate control of transcription lies in the activity of SIRT1 and the availability of NAD^+ (or depletion of NAM). In this model, AMPK participates only as a precursor to elevation of NAD^+. Finally, if AMPK-dependent phosphorylation is a necessary antecedent to deacetylation, but not sufficient to induce transcriptional activity, then AMPK or SIRT1 activation alone should have limited effect, but their co-activation should have strong synergy.

The goal of this study was to evaluate these models in the context of myogenic differentiation and energy metabolism. We found that wild type C2C12s do not demonstrate the AICAR-induced increase of NAD^+ observed in PGC-1α-transgenic cells, allowing independent manipulation of AMPK activation and NAD^+ availability to test the independence, priority, or synergy of AMP and NAD signaling. Results suggest that no single model captures the behavior of all phenotypic markers, but generally support independent signaling through the two mechanisms, providing myocytes flexibility to respond to diverse metabolic conditions.

4.3 Materials and Methods

4.3.1 Materials

Antibody for Acetyl-CoA carboxylase (ACC^{S79}) and Acetyl-Histone H3 (Lys9)was purchased from Cell Signaling Technology. C2C12 cells were obtained from the American Type Culture Collection (ATCC, Manassas, VA). Dublecco's Modified Eagle's Medium (DMEM) was purchased as a powdered mixture (Corning 50-003), supplemented with 3.7g/L $NaHCO_3$, and sterilized by 0.2 um filtration. AICAR (Enzo, NY, 50mM) and NMN (Sigma-Aldrich, MO, 100mM) were prepared as concentrates in ultra-pure water and diluted to working strength in serum free DMEM prior to application to cells.

4.3.2 Cell Culture

C2C12 myoblasts were maintained in growth medium (GM, DMEM supplemented with 10 % fetal bovine serum (Hyclone), 100 IU/ml penicillin, and 100

μg/ml streptomycin) in a humidified incubator under 10 % CO_2 at 37 °C. Cells were seeded at $4.4x10^3$ cells/cm^2 on 12-well plates, and allowed to proliferate 2 days to 60-80% confluence, at which point they were switched to differentiation media (DM, DMEM supplemented with 2% horse serum (Hyclone) and antibiotics). Media was replenished every 48 h. Cultures generally fused into myotubes within 4 days in DM. For treatment, cultures were rinsed twice with serum and antibiotic free DMEM (SFM) and incubated 60min prior to application of treatment media. In dose experiments, all wells were exposed to NMN for 24 hours. For time-course studies, individual wells were exposed to drug for different times, but to minimize manipulation of each plate, the total pre-incubation and incubation time was 24 hours for all treatment groups. All cells were switched to SFM concurrently, treated with NMN for the indicated time periods, and harvested concurrently. This resulted in varying length incubations in SFM equal to the difference between 24 hours and the duration of NMN exposure.

Following treatment, culture media was collected and boiled for 5 min to inactivate enzymatic activity. Media samples were cleared by centrifugation at 16k xg for 2 min and stored at -20°C. Cultures were rinsed twice with ice cold PBS. Cultures collected for metabolite analysis were harvested by scraping in cold lysis buffer (100mM Na_2CO_3, 20 mM $NaHCO_3$, 20 mM NAM). Cultures collected for ACC phosphorylation and citrate synthase activity were harvested in non-denaturing lysis buffer (1% Triton-X100, 50 mM tris, 300 mM NaCl, 5 mM EDTA) supplemented with protease inhibitors (Sigma), 100 mM NaF, and 4 μg/ml $NaVO_3$. Cells were dissociated by trituration and sonication for 1 min at room temperature. Lysates were incubated on ice for 10 min and cleared by centrifugation at 16k xg for 5 min. Soluble protein concentration was assayed

by bicinchronic acid assay (Pierce). Cultures collected for analysis of gene expression were harvested in Trizol (Life Technologies) according to the manufacturer's protocol, and RNA quantified by UV spectroscopy.

4.3.3 Cell morphology

Micrographs of cultures were obtained at the end of the treatment period under phase contrast illumination using 20x objective (Leica). Two random fields were captured for each well, covering 13.5 mm^2. Culture confluence and area density of myotubes were determined by point counting.

4.3.4 Metabolite assays

Media lactate was measured by the lactate dehydrogenase method (Pesce et al., 1975). Samples were reacted in assay buffer (1 M glycine, 200 mM hydrazine, 2 mM NAD^+, pH 9.5) containing 20 U/ml LDH at room temperature for 30 min. Absorbance at 340 nm was measured, and lactate concentration was calculated using 6.22 as the millimolar extinction coefficient for NADH. Values were normalized to lysate protein content.

Lysate NAD and NADH contents were determined by alcohol dehydrogenase (ADH)-diaphorase enzymatic cycling using 10µl of sample and 200ul assay buffer (40µg/mL yeast ADH (Alfa Aesar, MA), 0.2% ethyl alcohol, 2mM $MgCl_2$, 0.2 U/ mL diaphorase (Innovative Research, MI), 1µM resazurin (Alfa Aesar, MA)). Resorufin formation was monitored with excitation at 540 nm and emission at 590 nm every 2 minutes for a total of 20 minutes. The fluorescence slope was calibrated to standard curve and normalized to lysate protein content. For measurement of NADH, 80µl aliquot

samples were incubated for 15min at 60°C to destroy NAD^+ (Wagner and Scott, 1994). NAD^+ was determined by subtracting NADH from NAD.

4.3.5 Citrate synthase

Citrate synthase (CS) activity was measured in whole cell lysates using an assay mixture containing 10mM KCl, 100 mM acetyl-CoA, 100 mM 5,5'-dithiobis(2-nitrobenzoic acid) and 1M oxaloacetate (Sigma-Aldrich, MO) at 22 °C. Enzyme activity was monitored by recording the changes in absorbance at 412 nm every 1min over 5 min and normalized to protein content.

4.3.6 Western blot

To assay phosphorylation of ACC and acetylation of histone 3, 4 μg soluble protein was separated by SDS-PAGE through 7 % acrylamide gels. Protein was transferred to nitrocellulose membranes, blocked with 5% nonfat dry milk in Tween-TBS (TTBS) and hybridized with phospho-specific antibody. Membranes were rinsed and incubated with horseradish peroxidase conjugated secondary antibody (Jackson, 1:80,000). Bands were detected by enhanced chemiluminescence (Amersham), visualized by exposure to radiographic film, and quantified by scanning densitometry. All samples from an experiment were run on the same gel, and normalized to the average of that experiment's control samples.

4.3.7 Gene expression

Complimentary DNA was synthesized from 2 μg RNA by reverse transcription (Multiscribe) using random hexamers. Amplification reactions contained a target-specific

fraction of the reverse transcription product and 250 nM forward and reverse primers in Platinum Sybr Green QPCR Supermix (Invitrogen). All samples were run in duplicate. Fluorescence was monitored and analyzed in a StepOnePlus real time PCR system (Applied Biosystems). Gene expression was normalized by the average of three housekeeping genes (GAPDH, RPLP0 and CSNK2A2) and an independent reference sample using the relative quantification method. Amplification of specific transcripts was initially confirmed by gel and melting curve analysis and routinely validated by melting curve profiles at the end of each PCR experiment. Amplification targets were chosen to represent differentiation (MYH3, β-actin), oxidative metabolism (COX2, TFAM) and glycolytic metabolism (GLUT1, HK1), using primers shown in (Table 4-1 below)

Table 4-1 List of targets and primers used in quantitative PCR

Target	Forward Primer	Reverse Primer
β-actin	TTCAACACCCCAGCCATGT	GTAGATGGGCACAGTGTGGGT
COX2	CAAGACGCCACATCCCCT	ACGGGGTTGTTGATTTCGTC
CSNK2A2	CCCGAGCTGGGGTAATCA	TCTTTTTCTTCACTGGCTTG
GAPDH	AACATCAAATGGGGTGAG	GTTGTCATGGATGACCTTG
GLUT1	GAGGCTTGCTTGTAGAGT	GAACTCCTCAATAACCTTCT
HK1	CACTGCTCACCAGGGCTA	ATCCCCCTTTTCTGAGCCGT
MYH3	CTTGAGCACTGAGCTCTTC	TCAGCTGCTCGATCTCTTCA
nampt	AGCACAGTACCATAACGG	TCCACGCCATCTCCTTGAAT
RPLP0	AGATTCGGGATATGCTGTT	AAAGCCTGGAAGAAGGAG
Tfam	GAGTTCCCACGCTGGTAG	CTGAAAGTTTTGCATCTGG

4.3.8 Statistics

All values are expressed as means ± S.D. unless otherwise stated. All experiments were performed on multiwell tissue culture plates with at least two replicates per condition and at least three independent plates, giving sample size (n) of at least 6. Dose-response experiments were analyzed by two-way, mixed-mode ANOVA in StatView (Abacus Software). AICAR * NMN experiments were analyzed by two-way ANOVA in R (Team, 2015) using repeated measures blocked by plate. Sample size of 6 with repeated measures provides statistical resolution within main effects of 1 S.D. with 87% power. The Bonferroni-Dunn correction was used for post hoc T-tests.

The independent model predicts that AICAR and NMN may each have independent effects, but there should be no interaction. The nampt model predicts that AICAR should have no effect, but all signaling should be dependent on NMN. The AMPK priming model predicts that there should be strong interaction between AICAR and NMN, but that neither will have an effect alone.

4.4 Results

AICAR treatment failed to induce nampt expression or alter the NAD pool, but did reduce histone H3 acetylation (fig. 4-1). We have previously found 0.5 mM AICAR sufficient to induce maximal ACC phosphorylation within 15 minutes (Hsu and Burkholder, 2015), and show here that incubation with 0.5 mM AICAR increased ACC phosphorylation to 3.3±0.77 fold of control for 24 hours ($p=0.0015$). In contrast to differentiating myoblasts (Fulco et al., 2008), we did not find induction of nampt

expression by AICAR in mature myotubes (p=0.49). Consistent with the absence of nampt induction, AICAR did not alter NAD or NADH contents after 24 hour treatment. However, AICAR significantly reduced histone H3 acetylation.

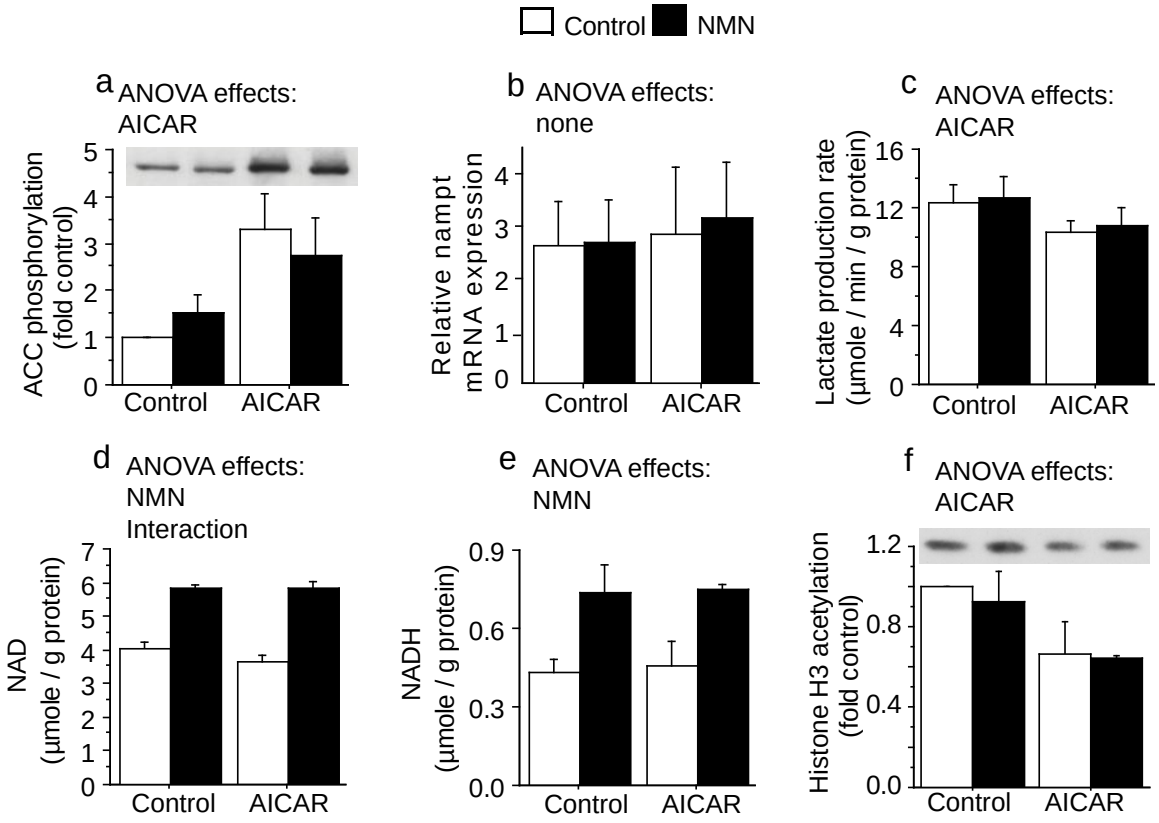

Figure 4-1 Effect of AICAR and NMN on AMP and NAD signaling
Effect of AICAR and NMN on (a) ACC phosphorylation (b) nampt mRNA expression (c) lactate production rate (d) NAD (e) NADH content and (f) Histone H3 acetylation. N=3 experiments with triplicate wells. Bars represent mean ± S.D. Main effect of AICAR $p<0.05$; Main effect of NMN $p<0.05$; Interaction between AICAR and NMN $p<0.05$)

Because SIRT1 activity depends on NAD^+, we determined the concentration of NMN to achieve a maximum increase in total NAD. In untreated cells, the NAD pool was constant around 4.4±0.3 µmole/g protein over time, with a small accumulation of NADH, from 0.08±0.02 µmole/g protein to 0.28±0.07 µmole/g protein ($p<0.0001$), primarily driven by lactate accretion (fig. 4-2). NMN supplementation resulted in a dose- and time- dependent increase in total NAD, with maximal increase of 45±4% at 200 µM and 8 hours. Similar dose-dependent increases were seen in NAD^+ and NADH with EC50 of 15.6 µM and 27.4 µM respectively (Fig -4-2b,c), and the increase in NAD^+ could be resolved as early as 2 hours (Fig. 4-2e). Because NAD and NADH increased similarly, the NAD^+/NADH ratio, a common measure of redox state, was unaffected. NMN was used at 200µM in all subsequent experiments.

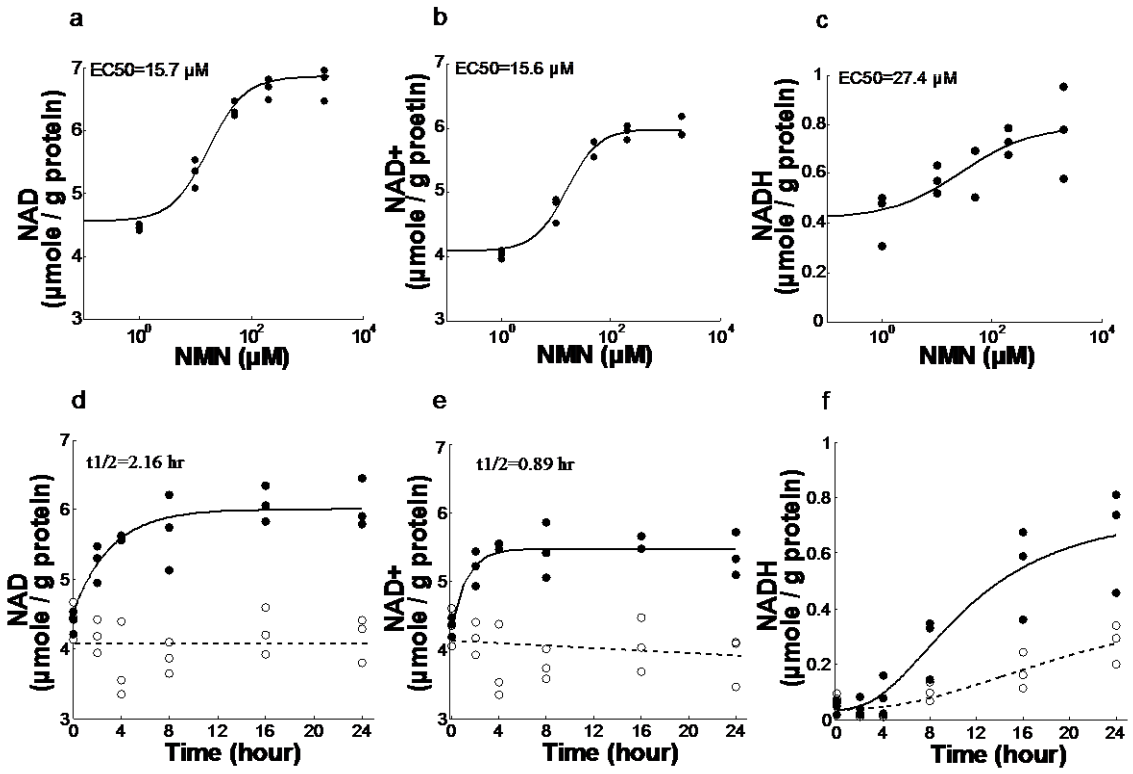

Figure 4-2 Effect of NMN supplementation on NAD content
Effect of 24 hour NMN on cellular (a) NAD (b) NAD+ and (c) NADH content. The time course of cellular (d) NAD (e) NAD+ and (f) NADH content during exposure to MNM in SFM. N=3 experiments with duplicate wells. control: dashed line, open circles; NMN: solid line, filled circles.

The combination of AICAR and NMN altered cellular metabolites independently. AICAR treatment decreased lactate production (fig. 4-3c, p=0.014) with no effect on NAD, while NMN treatment increased both total and reduced NAD by 40%, with no effect on lactate production (fig. 4-1c) or . Examining the signaling expected from these changes, AICAR increased ACC phosphorylation to 3.3±0.77 fold of control, while NMN had no effect (fig. 4-1b). The increase in NAD^+ did not alter H3 acetylation (fig. 4-1f, p=0.49). Unexpectedly, AICAR treatment did reduce H3 acetylation (p=0.001), and no interaction effect could be resolved (p=0.67).

One of the major effects ascribed to AMP/NAD signaling is a PGC-1α mediated increase in oxidative metabolism. In our hands, expression of PGC-1α-dependent Tfam was unaffected by either AICAR or NMN (fig. 4-3a). Consistent with this, CS activity was unaffected by AICAR or NMN (fig. 4-3e). However, two-way ANOVA revealed a significant interaction between AICAR and NMN on the expression of mitochondrial cytochrome oxidase 2 (COX2, p=0.026,). COX2 expression was reduced by treatment with either AICAR or NMN, but the combination was no more effective than either substance alone (fig. 4-3b). Changes in oxidative metabolism are often mirrored by reciprocal changes in glycolytic metabolism. Although AICAR reduced expression of the constitutive glucose transporter, GLUT1, by 19% (fig. 4-3c, p<0.001), we found no effect or interaction with NMN. Conversely, NMN, but not AICAR reduced expression of HK1 (fig. 4-3d, NMN p=0.014, AICAR p=0.14).

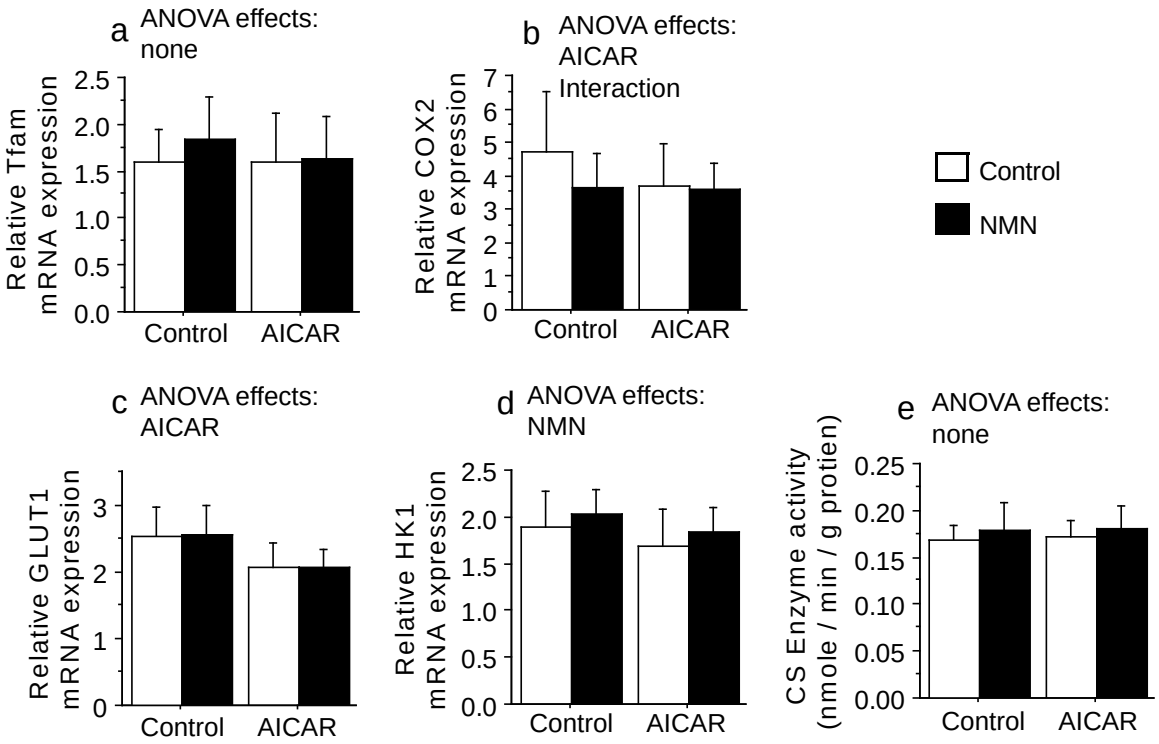

Figure 4-3 Effect of AICAR and NMN on metabolic gene expression
Effect of AICAR and NMN on (a) Tfam (b) COX2 (c) GLUT1 (d) HK1 mRNA expression (e) citrate synthase activity. N=6 experiments with duplicate wells for gene expression and N=3 with triplicate wells for enzyme activity. Results are shown as mean ± S.D. Main effect of AICAR $p<0.05$; Main effect of NMN $p<0.05$; Interaction between AICAR and NMN $p<0.05$)

AMP and NAD may also influence FOXO and p53 mediated cell survival and differentiation (Jones et al., 2005; Motta et al., 2004). Two way ANOVA did reveal an interaction between AICAR and NMN on the area fraction of myotube coverage (fig. 4-4b, $p=0.005$). Treatment with either AICAR alone or NMN alone resulted in a reduction in myotube coverage (44±8% Control; 35±10% AICAR, $p=0.006$; 37±10% NMN, $p=0.003$), but this was substantially attenuated by the combination of AICAR and NMN (41±7%, $p=0.16$ vs. control). In contrast, AICAR reduced expression of MYH3, the earliest of the sarcomeric myosins (fig. 4-4a, $p=0.023$), while NMN had no effect ($p=0.75$), with no interaction. Treatment with AICAR alone resulted in a significant ($P<0.0001$) reduction on the expression of β-actin, a structural gene that decreases during myogenic differentiation (Shimokawa et al., 1998), and this was further enhanced by the combination with NMN (fig. 4-4c, $p=0.03$).

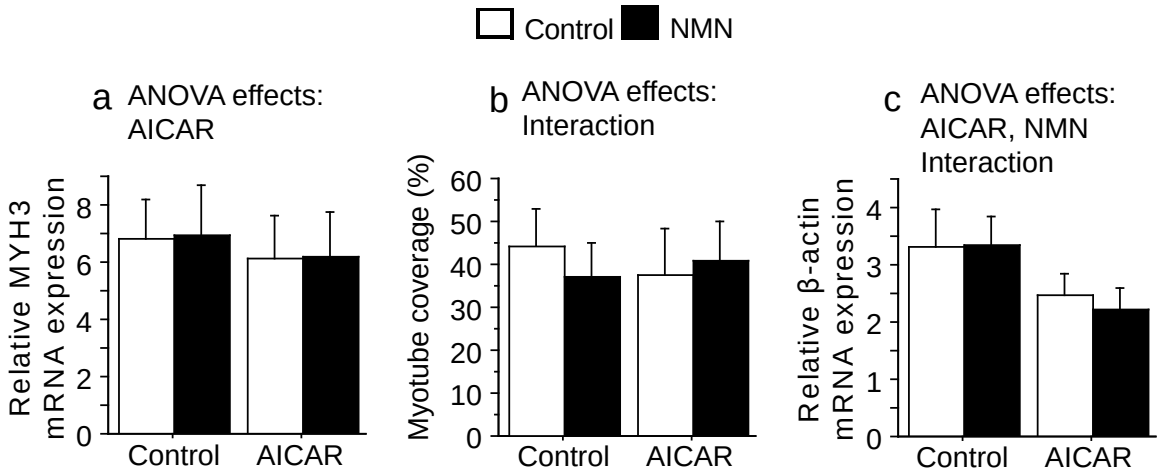

Figure 4-4 Effect of AICAR and NMN on differentiation gene expression
Effect of AICAR and NMN on (a) MYH3 mRNA expression (b) myotube coverage (c) β-actin mRNA expression. N=6 experiments with duplicate wells for gene expression and triplicate wells for myotube coverage. Results are shown as mean ± S.D. Main effect of AICAR $p<0.05$; Main effect of NMN $p<0.05$; Interaction between AICAR and NMN $p<0.05$)

4.5 Discussion

The goal of this study was to evaluate potential models for transcriptional regulation by cytoplasmic metabolites in the context of myogenic differentiation and energy metabolism. To examine combinatorial signaling by AMP and NAD, we treated C2C12 myotubes with AICAR to activate AMPK and NMN to increase SIRT1 substrate availability. NMN did substantially increase NAD^+ content, but AICAR had no effect on either NAD content or oxidation state. AICAR increased ACC phosphorylation and reduced H3K9 acetylation, but NMN had no apparent effect on AMPK or SIRT1 activity. AICAR reduced expression of COX2, GLUT1, MYH3, and β-actin and reduced myotube area coverage. NMN also reduced COX2 expression and myotube area, while increasing HK1 expression. Although we did find statistical interaction between AICAR and NMN on myotube area fraction and COX2 expression, these interactions resulted from less-than-additive effect of the two compounds. These results are most consistent with the independent signaling model.

Cooperative signaling between AMPK and SIRT1 was suggested by their common dependence on metabolites associated with ATP metabolism and their shared substrates. AMPK is a key energy-sensing kinase, and its activity can be increased by energy depletion secondary to many stimuli. NAD^+ is converted to NADH by GAPDH and by the citric acid cycle and back to NAD^+ by LDH and oxidative phosphorylation. NADH rises dramatically during exercise (Sahlin, 1985) and NAD^+ rises during fasting or glucose restriction (Canto and Auwerx, 2009; Fulco et al., 2008), so potentially provides distinction between accelerated ATP consumption and limited ATP synthesis.

Results of the present study suggest that metabolite accumulation alone is insufficient to induce coherent control of either metabolic phenotype or myoblast differentiation. Signaling seems to be dominated by AMPK, both at the intermediate level, where it increased ACC phosphorylation and decreased H3 acteylation, and at the transcriptional level, where it reduced expression of multiple targets.

AICAR reduced H3K9 acetylation independent of nampt expression or changes in NAD content. We examined H3K9 acetylation because it is a substrate of the NAD-dependent sirtuins and the canonical substrate, PGC1a, is expressed at very low levels in C2C12. Some investigators have suggested that the responses to low glucose, fasting, or AICAR may result from AMPK-mediated upregulation of nampt and increase cellular NAD^+, providing substrate for SIRT1 (Canto et al., 2010; Fulco et al., 2008), but this seems to be strongly dependent on cell phenotype. Fulco and colleagues (2008) found that the inhibition of differentiation in C2C12s depends on the upregulation of nampt, and Costford and colleagues (2010) report that AICAR treatment induces nampt in C2C12s only during differentiation and not when applied to mature myotubes (Costford et al., 2010). Canto and colleagues (2010) find AMPK-mediated upregulation of nampt in C2C12s only with transgenic PGC-1α. Systemic AICAR increases muscle nampt mRNA and protein, but the increase in mRNA is independent of AMPKα2 kinase activity (Brandauer et al., 2013). Further, AICAR-induced NAD^+ accumulation and PGC-1α deacetylation were not blocked by inhibition of nampt even in C2C12s overexpressing PGC-1α (Canto et al., 2009). The present results are consistent with a minimal role for NAD^+ availability in the deacetylase activity of C2C12 myotubes with only endogenous

PGC1α. Systems with greater PGC1α, such as mature muscle or transfected cells, may become more sensitive to NAD^+ homeostasis.

Energy status, via AMPK, is an important regulator of nutrient uptake and cell differentiation (Fulco et al., 2008). AMPK has been shown to induce muscle atrophy and protein degradation through FOXO transcriptional activation (Nakashima and Yakabe, 2007; Romanello et al., 2010). C2C12s retain a sizable population of mononucleated cells, and AICAR-induced loss of MYH3 gene expression and reduced myotube area fraction (fig. 4-4) are consistent with retarded differentiation of those cells. The onset of muscle differentiation is accompanied by the activation of mitochondrial biogenesis. The reduction of mitochondrial COX2 gene expression may reflect inhibition of differentiation rather than a specific metabolic adaptation.

NAD is a coenzyme in energy production and a substrate modulating cellular signaling through the PARP1and SIRT1 pathways. In our study, NMN treatment increased NAD content and HK1 expression, but differences in NAD account for only 7% of total HK1 variability. NAD content also affected myotube area and COX2 expression, similar to the effect of AMPK. Although NMN supplementation raised NAD similar to previous studies (Canto et al., 2012), NMN failed to alter CS activity and the expression of Tfam, a key factor which governs mitochondrial DNA transcription and replication. These results suggest that surplus NAD is not able to enhance mitochondrial adaptation, and previous results suggest that C2C12 cells require PGC-1α overexpression to unmask substantial SIRT1-dependent mitochondrial plasticity (Gerhart-Hines et al., 2007). Although dietary NMN or nicotinamide riboside (NR) supplementation improves glucose tolerance in high fat diet-induced obesity (Yoshino et al., 2011) and enhances

oxidative metabolism in mice with mitochondrial disorder (Khan et al., 2014), it has no effect in normal mice (Canto et al., 2012). Interestingly, nampt gene expression and NAD^+ are significantly lower in the liver and white adipose tissue, but not in skeletal muscle after high fat diet-induced obesity (Yoshino et al., 2011). Overexpression of nampt in muscle increases NAD^+ by 50% but fails to increase mitochondrial enzyme activity, protein content or gene expression or to protect against metabolic consequences of high fat diet (Frederick et al., 2015). These results suggest that NAD pool in skeletal muscle is not sufficient to induce metabolic remodeling, but requires an additional stressor.

The present results are most consistent with the independent signaling model. In our hands, nampt was not upregulated, and NAD was not increased by AICAR treatment. With the exception of Tfam, all markers were affected by either AICAR or NMN treatment. The limited interactions, seen only in COX2 expression and myotube area fraction, are consistent with saturation, that is: either AICAR or NMN treatment alone induces a maximal effect. In some models, the response to AICAR or metabolic stress depends on AMPK-mediated upregulation of nampt and can be mimicked by pharmacological increase in NAD (Canto et al., 2009; Canto et al., 2010; Fulco et al., 2008). These models suggest that NAD^+-dependent signaling is necessary, and possibly sufficient for adaptation. However, the most dramatic effects of NAD^+ are observed during differentiation of myoblasts (Fulco et al., 2008), in myotubes overexpressing PGC-1α (Canto et al., 2009) , or in mature muscle interacting with other tissues. The effect of SIRT1 disruption, in C2C12s with only endogenous PGC-1α, is quite modest

(Gerhart-Hines et al., 2007), consistent with the small effects we have seen on metabolic gene expression.

5 CHAPTER

CONCLUSION

5.1 Summary

Although the rate of ATP turnover during high intensity exercise is more than 100 times higher than that at rest, the level of ATP in skeletal muscle is relatively stable (Cheetham et al., 1986). This is because skeletal muscle not only possesses fast and efficient mechanisms of ATP resynthesis, but also has ability to switch rapidly from an aerobic to an anaerobic energy system during high intensity exercise. The activation of glycolysis and mitochondrial respiration are related to the elevation of glucose metabolite concentrations (Brown, 1992; Sahlin et al., 1990). Substantial control is exerted by allosteric feedback, particularly of ATP and NAD. Substrate-level inhibition, in which the build-up of reaction products slows the reaction rate by mass action, contributes strongly to balance among the steps of glycolysis and mitochondrial respiration. This project is based on the conceptual model that ATP depletion causes the accumulation of AMP and NADH, in which AMP regulates glycolysis, NADH determines the aerobic and anaerobic glucose distribution and the AMP/NAD interaction signaling serves as a mechanism for metabolic adaptation. The overall hypothesis in this study is that the distribution of glucose depends on the AMP and NAD generated during energetic stress, and the AMPK-SIRT1 interactions contribute to the adaptation.

The objective of the first study was to investigate the role of AMPK and p38 in glucose metabolism during ATP depletion and to determine whether AMP-mediated activation of AMPK is sufficient to induce p38 activation and maximize glucose transport. We found rotenone poison causes transient ATP depletion and p38 phosphorylation with increased lactate production, but p38 inhibition had no effect on ATP recovery. Glucose restriction and dors blocked rotenone-induced p38 phosphorylation following rotenone treatment, but AICAR failed to activate p38. The conclusion from this study is that metabolic stress activates both AMPK and p38, but p38 required extracellular glucose, in addition to AMPK. This illustrates that simple AMP signaling is not sufficient to completely define the cellular response.

The objective of the second study was to investigate the role of NADH in glucose distribution and to determine whether NADH oxidation increases mitochondrial respiration through PDH phosphorylation. We found that PMS completely oxidized NADH at low dose, but oxygen consumption, ATP depletion, ROS production and the phosphorylation of PDH were significantly induced by PMS only at high dose. The conclusion from this study is that NADH oxidation alone is not sufficient to define the balance of reductive and oxidative metabolism of pyruvate, but ROS-AMPK signaling may be involved in stimulating oxygen consumption.

The objective of the third study was to investigate the role of AMP and NAD signaling for transcriptional regulation in the context of myogenic differentiation and metabolism. We found AICAR reduced H3K9 acetylation, COX2 and MYH3 mRNA expression, but failed to increase NAMPT mRNA expression, or NAD content. In contrast, NMN increased NAD content similar to previous studies (Canto et al., 2012),

but failed to alter H3K9 acetylation, CS activity and the expression of Tfam. The conclusion from this study is that energetic stress-induced metabolic adaptation may depend on AMP signaling, but NAD is dispensable.

The overall conclusion of this project is that C2C12 myotubes, with few mitochondria and with only endogenous PGC-1α, are not sensitive to NAD signaling. In these cells, the metabolism and distribution of glucose depend on AMP signaling. Furthermore, AMP mediated AMPK activation contributes to metabolic adaptation, but NAD mediated SIRT1 signaling is dispensable. This contrasts with studies in whole muscle or in myotubes overexpressing PGC-1α, which showed that NAD signaling is able to influence metabolic adaptation via SIRT1 signaling. These findings suggest that glucose metabolism is not controlled by single molecule. Other molecules may represent an additional gauge of aerobic and anaerobic metabolism.

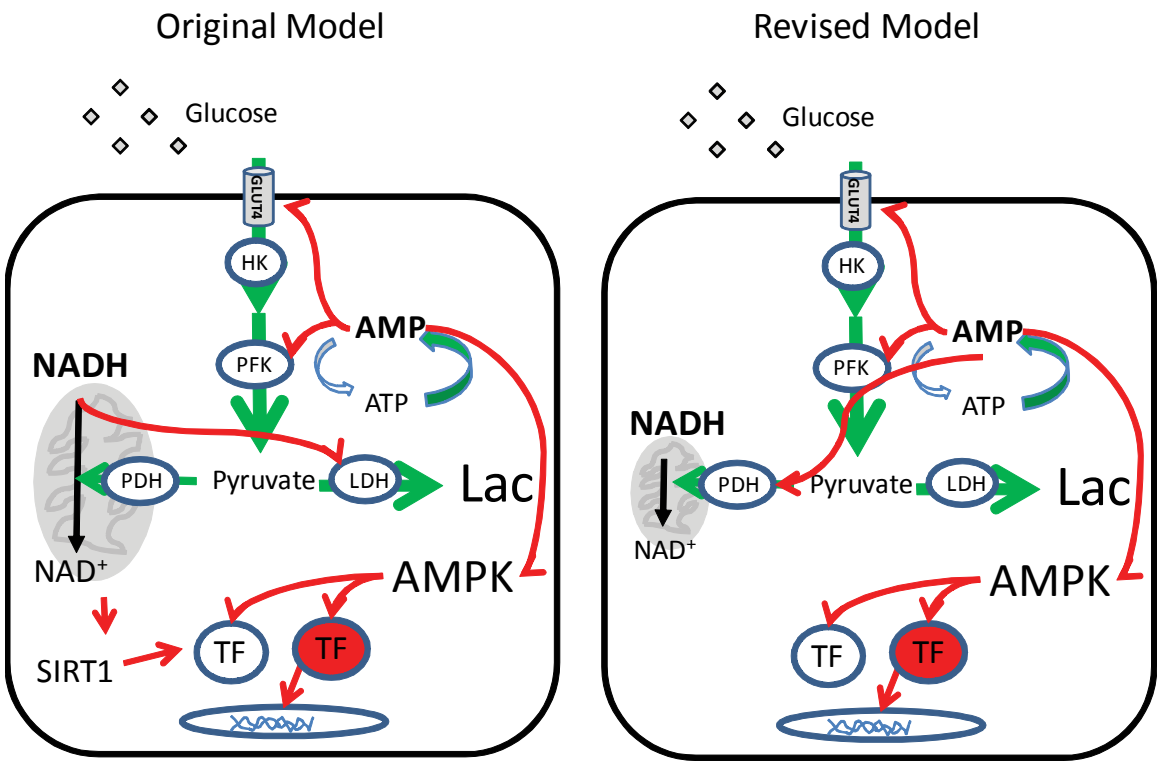

Figure 5-1 Revised model in C2C12 myotubes
In C2C12 myotubes, low mitochondrial content minimizes the influence of NAD-mediated signaling, both in the control of pyruvate disposal and long-term plasticity. High glucose availability and low expression of SIRT1 and PGC1α minimize the cellular ability to switch between aerobic and anaerobic adaptation.

5.2 Implications

Mitochondrial complex dysfunction in skeletal muscle has been implicated in type 2 diabetes (Kelley et al., 2002). NADH supplied from glucose and fatty acid is the main substrate for ETC. Mitochondrial complex I dysfunction inhibits the oxidation of lipid and glucose and causes the accumulation of NADH. Low dose of PMS is able to oxidize NADH and acts as an electron carrier that replaces the damaged mitochondrial complex. Phenothiazine compounds, such as methylene blue, may provide a useful treatment for mitochondrial dysfunction in diabetes. However, in this project high dose of PMS inhibits ATP synthesis which may cause muscle fatigue and stimulate ROS production. The phenothiazine compounds have been used for the treatment of malaria, cyanide and carbon monoxide poisoning. Careful dosing and post-treatment monitoring are highly recommended.

Exercise is a powerful intervention for the treatment of many different diseases (Pedersen and Saltin, 2015). Caloric restriction and endurance exercise activate AMPK and SIRT1 which are thought to increase mitochondrial biogenesis. In contrast to this idea, the combination of AICAR and NMN to directly activate AMPK and SIRT1 had no effect on Tfam mRNA expression. Instead, AICAR significantly reduced COX2 and MYH3 gene expression suggesting that AMPK activation may inhibit differentiation and myotube formation. It is consistent with the report that AMPK inhibits protein synthesis by inactivating the mammalian target of rapamycin (mTOR) signaling pathway. Given the potentially negative effects of AMPK on muscle growth, those who want to increase muscle mass and muscle strength should avoid high volume and long duration training. In

contrast, low nutrient state may enhance exercise-induced AMP and NAD signaling which may amplify metabolic adaptation. This is supported by the recent studies that repeated endurance training with low muscle glycogen availability results in greater endurance adaptation (Bartlett et al., 2015; Hawley and Morton, 2014).

Previous studies have shown that low intensity muscle contraction with blood flow restriction training enhances muscle strength and muscle mass without increasing the incidence of muscle damage (Loenneke et al., 2014; Slysz et al., 2015). However, the cellular mechanisms underlying the muscle hypertrophy induced by blood flow restriction are unknown. Muscle hypoxia resulting from impaired blood flow could evaluate HIF-1α, the major transcription factor triggered by hypoxia (Semenza, 2000). Blood flow restriction limits NADH oxidation and lowers NAD^+ due to the decrease of oxygen delivery. The inactivation of SIRT1 and SIRT2 increases HIF-1α transcriptional activity by preventing the hydroxylation of HIf-1α (Seo et al., 2015) or increasing the recruitment of p300 (Lim et al., 2010). Muscle contraction also increases HIF-1α activity through AMPK-mediated phosphorylation (Lee et al., 2003). It is possible that the activation of AMPK and inactivation of SIRT1 in muscle contraction with blood flow restriction augment muscle hypertrophy.

5.3 Future Directions

The first study found that p38 activation by rotenone required extracellular glucose. Growth factor, UV light, inflammatory cytokine or oxidative stress activates p38 through MKK3/6 canonical pathway (Cuadrado and Nebreda, 2010), but the mechanism in which hyperglycemia activates p38 is less clear. The activation of p38 in hyperglycemia may results in many pathological conditions (Igarashi et al., 1999). To characterize the mechanisms by which elevation of glucose levels activates p38 signaling may provide useful therapies to prevent complications in diabetes.

In this project, we are able to boost NAD content through NMN supplementation, but there is no change in H3K9 acetylation. NAD can be synthesized in nucleus, cytosol, and mitochondria via salvaging pathway, but the regulation of NAD biosynthesis by NAD^+-consuming signaling is still not clear. Sirtuins act in different compartments and NAD concentrations differ among these cellular compartments. It is possible that NAD-consuming signaling selectively depends on the compartmentalization of NAD. Mitochondrial NAD concentration is usually higher than that in the cytosol (Alano et al., 2007). To understand how NAD is shuttled among these organelles and how NAD pool is maintained in the individual compartments may elucidate the NAD-sirtuin signaling in glucose metabolism.

In this project, AMPK is clearly an important signaling mediator in glycolysis and metabolic adaptation. This is supported by the fact that World Anti-Doping Agency has included AICAR in the prohibited list since 2009 (WADA, 2016). Since SIRT1 may improve mitochondrial biogenesis in skeletal muscle whether NAD precursors can

enhance endurance training and should be added to prohibited list are not clear (Thevis and Schanzer, 2016). Further human research is warranted to see the effect of NMN or NR supplementation in exercise performance.

REFERENCES

Aksoy P, Escande C, White TA, Thompson M, Soares S, Benech JC, Chini EN. 2006. Regulation of SIRT 1 mediated NAD dependent deacetylation: a novel role for the multifunctional enzyme CD38. Biochem Biophys Res Commun 349(1):353-359.

Alano CC, Tran A, Tao R, Ying W, Karliner JS, Swanson RA. 2007. Differences among cell types in NAD(+) compartmentalization: a comparison of neurons, astrocytes, and cardiac myocytes. J Neurosci Res 85(15):3378-3385.

Amara CE, Shankland EG, Jubrias SA, Marcinek DJ, Kushmerick MJ, Conley KE. 2007. Mild mitochondrial uncoupling impacts cellular aging in human muscles in vivo. Proc Natl Acad Sci U S A 104(3):1057-1062.

An D, Toyoda T, Taylor EB, Yu H, Fujii N, Hirshman MF, Goodyear LJ. 2010. TBC1D1 regulates insulin- and contraction-induced glucose transport in mouse skeletal muscle. Diabetes 59(6):1358-1365.

Andrabi SA, Umanah GK, Chang C, Stevens DA, Karuppagounder SS, Gagne JP, Poirier GG, Dawson VL, Dawson TM. 2014. Poly(ADP-ribose) polymerase-dependent energy depletion occurs through inhibition of glycolysis. Proc Natl Acad Sci U S A 111(28):10209-10214.

Antonelli A, Ferrannini E. 2004. CD38 autoimmunity: recent advances and relevance to human diabetes. J Endocrinol Invest 27(7):695-707.

Antonescu CN, Huang C, Niu W, Liu Z, Eyers PA, Heidenreich KA, Bilan PJ, Klip A. 2005. Reduction of insulin-stimulated glucose uptake in L6 myotubes by the protein kinase inhibitor SB203580 is independent of p38MAPK activity. Endocrinology 146(9):3773-3781.

Bain J, Plater L, Elliott M, Shpiro N, Hastie CJ, McLauchlan H, Klevernic I, Arthur JS, Alessi DR, Cohen P. 2007. The selectivity of protein kinase inhibitors: a further update. Biochem J 408(3):297-315.

Bao H, Kasten SA, Yan X, Hiromasa Y, Roche TE. 2004a. Pyruvate dehydrogenase kinase isoform 2 activity stimulated by speeding up the rate of dissociation of ADP. Biochemistry 43(42):13442-13451.

Bao H, Kasten SA, Yan X, Roche TE. 2004b. Pyruvate dehydrogenase kinase isoform 2 activity limited and further inhibited by slowing down the rate of dissociation of ADP. Biochemistry 43(42):13432-13441.

Bartlett JD, Hawley JA, Morton JP. 2015. Carbohydrate availability and exercise training adaptation: too much of a good thing? Eur J Sport Sci 15(1):3-12.

Bashan N, Burdett E, Guma A, Sargeant R, Tumiati L, Liu Z, Klip A. 1993. Mechanisms of adaptation of glucose transporters to changes in the oxidative chain of muscle and fat cells. Am J Physiol 264(2 Pt 1):C430-440.

Beatty CH, Young MK, Bocek RM. 1976. Control of glycolysis in skeletal muscle from fetal rhesus monkeys. Pediatr Res 10(3):149-153.

Becatti M, Taddei N, Cecchi C, Nassi N, Nassi PA, Fiorillo C. 2012. SIRT1 modulates MAPK pathways in ischemic-reperfused cardiomyocytes. Cell Mol Life Sci 69(13):2245-2260.

Beis I, Newsholme EA. 1975. The contents of adenine nucleotides, phosphagens and some glycolytic intermediates in resting muscles from vertebrates and invertebrates. Biochem J 152(1):23-32.

Boergermann JH, Kopf J, Yu PB, Knaus P. 2010. Dorsomorphin and LDN-193189 inhibit BMP-mediated Smad, p38 and Akt signalling in C2C12 cells. Int J Biochem Cell Biol 42(11):1802-1807.

Bottinelli R, Canepari M, Reggiani C, Stienen GJ. 1994. Myofibrillar ATPase activity during isometric contraction and isomyosin composition in rat single skinned muscle fibres. J Physiol 481 (Pt 3):663-675.

Bowker-Kinley MM, Davis WI, Wu P, Harris RA, Popov KM. 1998. Evidence for existence of tissue-specific regulation of the mammalian pyruvate dehydrogenase complex. Biochem J 329 (Pt 1):191-196.

Brandauer J, Vienberg SG, Andersen MA, Ringholm S, Risis S, Larsen PS, Kristensen JM, Frosig C, Leick L, Fentz J, Jorgensen S, Kiens B, Wojtaszewski JF, Richter EA, Zierath JR, Goodyear LJ, Pilegaard H, Treebak JT. 2013. AMP-activated protein kinase regulates nicotinamide phosphoribosyl transferase expression in skeletal muscle. J Physiol 591(Pt 20):5207-5220.

Brown GC. 1992. Control of respiration and ATP synthesis in mammalian mitochondria and cells. Biochem J 284 (Pt 1):1-13.

Bruser A, Kirchberger J, Kloos M, Strater N, Schoneberg T. 2012. Functional linkage of adenine nucleotide binding sites in mammalian muscle 6-phosphofructokinase. J Biol Chem 287(21):17546-17553.

Canto C, Auwerx J. 2009. PGC-1alpha, SIRT1 and AMPK, an energy sensing network that controls energy expenditure. Curr Opin Lipidol 20(2):98-105.

Canto C, Auwerx J. 2012. Targeting sirtuin 1 to improve metabolism: all you need is NAD(+)? Pharmacol Rev 64(1):166-187.

Canto C, Gerhart-Hines Z, Feige JN, Lagouge M, Noriega L, Milne JC, Elliott PJ, Puigserver P, Auwerx J. 2009. AMPK regulates energy expenditure by modulating NAD+ metabolism and SIRT1 activity. Nature 458(7241):1056-1060.

Canto C, Houtkooper RH, Pirinen E, Youn DY, Oosterveer MH, Cen Y, Fernandez-Marcos PJ, Yamamoto H, Andreux PA, Cettour-Rose P, Gademann K, Rinsch C, Schoonjans K, Sauve AA, Auwerx J. 2012. The NAD(+) precursor nicotinamide riboside enhances oxidative metabolism and protects against high-fat diet-induced obesity. Cell Metab 15(6):838-847.

Canto C, Jiang LQ, Deshmukh AS, Mataki C, Coste A, Lagouge M, Zierath JR, Auwerx J. 2010. Interdependence of AMPK and SIRT1 for metabolic adaptation to fasting and exercise in skeletal muscle. Cell Metab 11(3):213-219.

Casey A, Constantin-Teodosiu D, Howell S, Hultman E, Greenhaff PL. 1996. Metabolic response of type I and II muscle fibers during repeated bouts of maximal exercise in humans. Am J Physiol 271(1 Pt 1):E38-43.

Chambers MA, Moylan JS, Smith JD, Goodyear LJ, Reid MB. 2009. Stretch-stimulated glucose uptake in skeletal muscle is mediated by reactive oxygen species and p38 MAP-kinase. J Physiol 587(Pt 13):3363-3373.

Cheetham ME, Boobis LH, Brooks S, Williams C. 1986. Human muscle metabolism during sprint running. J Appl Physiol (1985) 61(1):54-60.

Chen D, Bruno J, Easlon E, Lin SJ, Cheng HL, Alt FW, Guarente L. 2008. Tissue-specific regulation of SIRT1 by calorie restriction. Genes Dev 22(13):1753-1757.

Cheng HL, Mostoslavsky R, Saito S, Manis JP, Gu Y, Patel P, Bronson R, Appella E, Alt FW, Chua KF. 2003. Developmental defects and p53 hyperacetylation in Sir2 homolog (SIRT1)-deficient mice. Proc Natl Acad Sci U S A 100(19):10794-10799.

Costford SR, Bajpeyi S, Pasarica M, Albarado DC, Thomas SC, Xie H, Church TS, Jubrias SA, Conley KE, Smith SR. 2010. Skeletal muscle NAMPT is induced by exercise in humans. Am J Physiol Endocrinol Metab 298(1):E117-126.

Crowther GJ, Carey MF, Kemper WF, Conley KE. 2002. Control of glycolysis in contracting skeletal muscle. I. Turning it on. Am J Physiol Endocrinol Metab 282(1):E67-73.

Cuadrado A, Nebreda AR. 2010. Mechanisms and functions of p38 MAPK signalling. Biochem J 429(3):403-417.

Dashty M. 2013. A quick look at biochemistry: carbohydrate metabolism. Clin Biochem 46(15):1339-1352.

Dehne N, Kerkweg U, Otto T, Fandrey J. 2007. The HIF-1 response to simulated ischemia in mouse skeletal muscle cells neither enhances glycolysis nor prevents myotube cell death. Am J Physiol Regul Integr Comp Physiol 293(4):R1693-1701.

Diez-Sampedro A, Hirayama BA, Osswald C, Gorboulev V, Baumgarten K, Volk C, Wright EM, Koepsell H. 2003. A glucose sensor hiding in a family of transporters. Proc Natl Acad Sci U S A 100(20):11753-11758.

Egan B, Carson BP, Garcia-Roves PM, Chibalin AV, Sarsfield FM, Barron N, McCaffrey N, Moyna NM, Zierath JR, O'Gorman DJ. 2010. Exercise intensity-dependent regulation of peroxisome proliferator-activated receptor coactivator-1 mRNA abundance is associated with differential activation of upstream signalling kinases in human skeletal muscle. J Physiol 588(Pt 10):1779-1790.

Egan B, Dowling P, O'Connor PL, Henry M, Meleady P, Zierath JR, O'Gorman DJ. 2011. 2-D DIGE analysis of the mitochondrial proteome from human skeletal muscle reveals time course-dependent remodelling in response to 14 consecutive days of endurance exercise training. Proteomics 11(8):1413-1428.

Emerling BM, Weinberg F, Snyder C, Burgess Z, Mutlu GM, Viollet B, Budinger GR, Chandel NS. 2009. Hypoxic activation of AMPK is dependent on mitochondrial ROS but independent of an increase in AMP/ATP ratio. Free Radic Biol Med 46(10):1386-1391.

Fendt SM, Bell EL, Keibler MA, Olenchock BA, Mayers JR, Wasylenko TM, Vokes NI, Guarente L, Vander Heiden MG, Stephanopoulos G. 2013. Reductive glutamine metabolism is a function of the alpha-ketoglutarate to citrate ratio in cells. Nat Commun 4:2236.

Fouquerel E, Goellner EM, Yu Z, Gagne JP, Barbi de Moura M, Feinstein T, Wheeler D, Redpath P, Li J, Romero G, Migaud M, Van Houten B, Poirier GG, Sobol RW. 2014. ARTD1/PARP1 negatively regulates glycolysis by inhibiting hexokinase 1 independent of NAD+ depletion. Cell Rep 8(6):1819-1831.

Frederick DW, Davis JG, Davila A, Jr., Agarwal B, Michan S, Puchowicz MA, Nakamaru-Ogiso E, Baur JA. 2015. Increasing NAD Synthesis in Muscle via Nicotinamide Phosphoribosyltransferase Is Not Sufficient to Promote Oxidative Metabolism. J Biol Chem 290(3):1546-1558.

Fritzen AM, Lundsgaard AM, Jeppesen J, Christiansen ML, Bienso R, Dyck JR, Pilegaard H, Kiens B. 2015. 5'-AMP activated protein kinase alpha2 controls

substrate metabolism during post-exercise recovery via regulation of pyruvate dehydrogenase kinase 4. J Physiol 593(21):4765-4780.

Frosig C, Pehmoller C, Birk JB, Richter EA, Wojtaszewski JF. 2010. Exercise-induced TBC1D1 Ser237 phosphorylation and 14-3-3 protein binding capacity in human skeletal muscle. J Physiol 588(Pt 22):4539-4548.

Fueger PT, Hess HS, Posey KA, Bracy DP, Pencek RR, Charron MJ, Wasserman DH. 2004. Control of exercise-stimulated muscle glucose uptake by GLUT4 is dependent on glucose phosphorylation capacity in the conscious mouse. J Biol Chem 279(49):50956-50961.

Fueger PT, Shearer J, Bracy DP, Posey KA, Pencek RR, McGuinness OP, Wasserman DH. 2005. Control of muscle glucose uptake: test of the rate-limiting step paradigm in conscious, unrestrained mice. J Physiol 562(Pt 3):925-935.

Fulco M, Cen Y, Zhao P, Hoffman EP, McBurney MW, Sauve AA, Sartorelli V. 2008. Glucose restriction inhibits skeletal myoblast differentiation by activating SIRT1 through AMPK-mediated regulation of Nampt. Dev Cell 14(5):661-673.

Funai K, Cartee GD. 2009. Inhibition of contraction-stimulated AMP-activated protein kinase inhibits contraction-stimulated increases in PAS-TBC1D1 and glucose transport without altering PAS-AS160 in rat skeletal muscle. Diabetes 58(5):1096-1104.

Furtado LM, Somwar R, Sweeney G, Niu W, Klip A. 2002. Activation of the glucose transporter GLUT4 by insulin. Biochem Cell Biol 80(5):569-578.

Gastin PB. 2001. Energy system interaction and relative contribution during maximal exercise. Sports Med 31(10):725-741.

Gerhart-Hines Z, Rodgers JT, Bare O, Lerin C, Kim SH, Mostoslavsky R, Alt FW, Wu Z, Puigserver P. 2007. Metabolic control of muscle mitochondrial function and fatty acid oxidation through SIRT1/PGC-1alpha. EMBO J 26(7):1913-1923.

Ghorbaniaghdam A, Henry O, Jolicoeur M. 2014. An in-silico study of the regulation of CHO cells glycolysis. J Theor Biol 357:112-122.

Greenhaff PL, Nevill ME, Soderlund K, Bodin K, Boobis LH, Williams C, Hultman E. 1994. The metabolic responses of human type I and II muscle fibres during maximal treadmill sprinting. J Physiol 478 (Pt 1):149-155.

Greenhaff PL, Soderlund K, Ren JM, Hultman E. 1993. Energy metabolism in single human muscle fibres during intermittent contraction with occluded circulation. J Physiol 460:443-453.

Gross DN, van den Heuvel AP, Birnbaum MJ. 2008. The role of FoxO in the regulation of metabolism. Oncogene 27(16):2320-2336.

Han YS, Geiger PC, Cody MJ, Macken RL, Sieck GC. 2003. ATP consumption rate per cross bridge depends on myosin heavy chain isoform. J Appl Physiol (1985) 94(6):2188-2196.

Hao W, Chang CP, Tsao CC, Xu J. 2010. Oligomycin-induced bioenergetic adaptation in cancer cells with heterogeneous bioenergetic organization. J Biol Chem 285(17):12647-12654.

Hardie DG. 2014. AMP-activated protein kinase: a key regulator of energy balance with many roles in human disease. J Intern Med.

Hardie DG, Ashford ML. 2014. AMPK: Regulating Energy Balance at the Cellular and Whole Body Levels. Physiology (Bethesda) 29(2):99-107.

Hargreaves M, Meredith I, Jennings GL. 1992. Muscle glycogen and glucose uptake during exercise in humans. Exp Physiol 77(4):641-644.

Hassa PO, Hottiger MO. 2008. The diverse biological roles of mammalian PARPS, a small but powerful family of poly-ADP-ribose polymerases. Front Biosci 13:3046-3082.

Hawley JA, Morton JP. 2014. Ramping up the signal: promoting endurance training adaptation in skeletal muscle by nutritional manipulation. Clin Exp Pharmacol Physiol 41(8):608-613.

Hawley SA, Pan DA, Mustard KJ, Ross L, Bain J, Edelman AM, Frenguelli BG, Hardie DG. 2005. Calmodulin-dependent protein kinase kinase-beta is an alternative upstream kinase for AMP-activated protein kinase. Cell Metab 2(1):9-19.

Hayashi T, Hirshman MF, Kurth EJ, Winder WW, Goodyear LJ. 1998. Evidence for 5' AMP-activated protein kinase mediation of the effect of muscle contraction on glucose transport. Diabetes 47(8):1369-1373.

He Q, Wang M, Petucci C, Gardell SJ, Han X. 2013. Rotenone induces reductive stress and triacylglycerol deposition in C2C12 cells. Int J Biochem Cell Biol 45(12):2749-2755.

He ZH, Bottinelli R, Pellegrino MA, Ferenczi MA, Reggiani C. 2000. ATP consumption and efficiency of human single muscle fibers with different myosin isoform composition. Biophys J 79(2):945-961.

Heigenhauser GJ, Parolin ML. 1999. Role of pyruvate dehydrogenase in lactate production in exercising human skeletal muscle. Adv Exp Med Biol 474:205-218.

Hers HG. 1984. The discovery and the biological role of fructose 2,6-bisphosphate. Biochem Soc Trans 12(5):729-735.

Ho RC, Fujii N, Witters LA, Hirshman MF, Goodyear LJ. 2007. Dissociation of AMP-activated protein kinase and p38 mitogen-activated protein kinase signaling in skeletal muscle. Biochem Biophys Res Commun 362(2):354-359.

Hochachka PW, Matheson GO. 1992. Regulating ATP turnover rates over broad dynamic work ranges in skeletal muscles. J Appl Physiol (1985) 73(5):1697-1703.

Holloszy JO. 1967. Biochemical adaptations in muscle. Effects of exercise on mitochondrial oxygen uptake and respiratory enzyme activity in skeletal muscle. J Biol Chem 242(9):2278-2282.

Holmstrom KM, Finkel T. 2014. Cellular mechanisms and physiological consequences of redox-dependent signalling. Nat Rev Mol Cell Biol 15(6):411-421.

Hoppeler H, Baum O, Lurman G, Mueller M. 2011. Molecular mechanisms of muscle plasticity with exercise. Compr Physiol 1(3):1383-1412.

Hori YS, Kuno A, Hosoda R, Horio Y. 2013. Regulation of FOXOs and p53 by SIRT1 modulators under oxidative stress. PLoS One 8(9):e73875.

Hottiger MO, Hassa PO, Luscher B, Schuler H, Koch-Nolte F. 2010. Toward a unified nomenclature for mammalian ADP-ribosyltransferases. Trends Biochem Sci 35(4):208-219.

Houten SM, Chegary M, Te Brinke H, Wijnen WJ, Glatz JF, Luiken JJ, Wijburg FA, Wanders RJ. 2009. Pyruvate dehydrogenase kinase 4 expression is synergistically induced by AMP-activated protein kinase and fatty acids. Cell Mol Life Sci 66(7):1283-1294.

Howald H, Hoppeler H, Claassen H, Mathieu O, Straub R. 1985. Influences of endurance training on the ultrastructural composition of the different muscle fiber types in humans. Pflugers Arch 403(4):369-376.

Hsu CG, Burkholder TJ. 2015. Activation of p38 in C2C12 myotubes following ATP depletion depends on extracellular glucose. J Physiol Biochem 71(2):253-265.

Hunter RW, Treebak JT, Wojtaszewski JF, Sakamoto K. 2011. Molecular mechanism by which AMP-activated protein kinase activation promotes glycogen accumulation in muscle. Diabetes 60(3):766-774.

Ido Y. 2007. Pyridine nucleotide redox abnormalities in diabetes. Antioxid Redox Signal 9(7):931-942.

Igarashi M, Wakasaki H, Takahara N, Ishii H, Jiang ZY, Yamauchi T, Kuboki K, Meier M, Rhodes CJ, King GL. 1999. Glucose or diabetes activates p38 mitogen-activated protein kinase via different pathways. J Clin Invest 103(2):185-195.

Irrcher I, Ljubicic V, Hood DA. 2009. Interactions between ROS and AMP kinase activity in the regulation of PGC-1alpha transcription in skeletal muscle cells. Am J Physiol Cell Physiol 296(1):C116-123.

Jackman MR, Willis WT. 1996. Characteristics of mitochondria isolated from type I and type IIb skeletal muscle. Am J Physiol 270(2 Pt 1):C673-678.

Jacobs I, Bar-Or O, Karlsson J, Dotan R, Tesch P, Kaiser P, Inbar O. 1982. Changes in muscle metabolites in females with 30-s exhaustive exercise. Med Sci Sports Exerc 14(6):457-460.

Jacquet S, Zarrinpashneh E, Chavey A, Ginion A, Leclerc I, Viollet B, Rutter GA, Bertrand L, Marber MS. 2007. The relationship between p38 mitogen-activated protein kinase and AMP-activated protein kinase during myocardial ischemia. Cardiovasc Res 76(3):465-472.

Jansson E, Esbjornsson M, Holm I, Jacobs I. 1990. Increase in the proportion of fast-twitch muscle fibres by sprint training in males. Acta Physiol Scand 140(3):359-363.

Ji LL. 2015. Redox signaling in skeletal muscle: role of aging and exercise. Adv Physiol Educ 39(4):352-359.

Jones DA, Turner DL, McIntyre DB, Newham DJ. 2009. Energy turnover in relation to slowing of contractile properties during fatiguing contractions of the human anterior tibialis muscle. J Physiol 587(Pt 17):4329-4338.

Jones RG, Plas DR, Kubek S, Buzzai M, Mu J, Xu Y, Birnbaum MJ, Thompson CB. 2005. AMP-activated protein kinase induces a p53-dependent metabolic checkpoint. Mol Cell 18(3):283-293.

Katz A, Sahlin K. 1987. Effect of decreased oxygen availability on NADH and lactate contents in human skeletal muscle during exercise. Acta Physiol Scand 131(1):119-127.

Kelley DE, He J, Menshikova EV, Ritov VB. 2002. Dysfunction of mitochondria in human skeletal muscle in type 2 diabetes. Diabetes 51(10):2944-2950.

Kemp RG, Gunasekera D. 2002. Evolution of the allosteric ligand sites of mammalian phosphofructo-1-kinase. Biochemistry 41(30):9426-9430.

Kemppainen J, Fujimoto T, Kalliokoski KK, Viljanen T, Nuutila P, Knuuti J. 2002. Myocardial and skeletal muscle glucose uptake during exercise in humans. J Physiol 542(Pt 2):403-412.

Khan NA, Auranen M, Paetau I, Pirinen E, Euro L, Forsstrom S, Pasila L, Velagapudi V, Carroll CJ, Auwerx J, Suomalainen A. 2014. Effective treatment of mitochondrial myopathy by nicotinamide riboside, a vitamin B3. EMBO Mol Med 6(6):721-731.

Kim JW, Tchernyshyov I, Semenza GL, Dang CV. 2006. HIF-1-mediated expression of pyruvate dehydrogenase kinase: a metabolic switch required for cellular adaptation to hypoxia. Cell Metab 3(3):177-185.

Kramer HF, Witczak CA, Fujii N, Jessen N, Taylor EB, Arnolds DE, Sakamoto K, Hirshman MF, Goodyear LJ. 2006. Distinct signals regulate AS160 phosphorylation in response to insulin, AICAR, and contraction in mouse skeletal muscle. Diabetes 55(7):2067-2076.

Krause U, Wegener G. 1996. Control of adenine nucleotide metabolism and glycolysis in vertebrate skeletal muscle during exercise. Experientia 52(5):396-403.

Kuma Y, Sabio G, Bain J, Shpiro N, Marquez R, Cuenda A. 2005. BIRB796 inhibits all p38 MAPK isoforms in vitro and in vivo. J Biol Chem 280(20):19472-19479.

Kuznetsov AV, Tiivel T, Sikk P, Kaambre T, Kay L, Daneshrad Z, Rossi A, Kadaja L, Peet N, Seppet E, Saks VA. 1996. Striking differences between the kinetics of regulation of respiration by ADP in slow-twitch and fast-twitch muscles in vivo. Eur J Biochem 241(3):909-915.

Lagouge M, Argmann C, Gerhart-Hines Z, Meziane H, Lerin C, Daussin F, Messadeq N, Milne J, Lambert P, Elliott P, Geny B, Laakso M, Puigserver P, Auwerx J. 2006. Resveratrol improves mitochondrial function and protects against metabolic disease by activating SIRT1 and PGC-1alpha. Cell 127(6):1109-1122.

Lali FV, Hunt AE, Turner SJ, Foxwell BM. 2000. The pyridinyl imidazole inhibitor SB203580 blocks phosphoinositide-dependent protein kinase activity, protein kinase B phosphorylation, and retinoblastoma hyperphosphorylation in interleukin-2-stimulated T cells independently of p38 mitogen-activated protein kinase. J Biol Chem 275(10):7395-7402.

Lanna A, Henson SM, Escors D, Akbar AN. 2014. The kinase p38 activated by the metabolic regulator AMPK and scaffold TAB1 drives the senescence of human T cells. Nat Immunol.

Lanza IR, Befroy DE, Kent-Braun JA. 2005. Age-related changes in ATP-producing pathways in human skeletal muscle in vivo. J Appl Physiol (1985) 99(5):1736-1744.

Lassegue B, San Martin A, Griendling KK. 2012. Biochemistry, physiology, and pathophysiology of NADPH oxidases in the cardiovascular system. Circ Res 110(10):1364-1390.

Lazo PA, Sols A. 1980. Pyruvate dehydrogenase complex of ascites tumour. Activation by AMP and other properties of potential significance in metabolic regulation. Biochem J 190(3):705-710.

Lee M, Hwang JT, Lee HJ, Jung SN, Kang I, Chi SG, Kim SS, Ha J. 2003. AMP-activated protein kinase activity is critical for hypoxia-inducible factor-1 transcriptional activity and its target gene expression under hypoxic conditions in DU145 cells. J Biol Chem 278(41):39653-39661.

Li J, Miller EJ, Ninomiya-Tsuji J, Russell RR, 3rd, Young LH. 2005. AMP-activated protein kinase activates p38 mitogen-activated protein kinase by increasing recruitment of p38 MAPK to TAB1 in the ischemic heart. Circ Res 97(9):872-879.

Li N, Ragheb K, Lawler G, Sturgis J, Rajwa B, Melendez JA, Robinson JP. 2003. Mitochondrial complex I inhibitor rotenone induces apoptosis through enhancing mitochondrial reactive oxygen species production. J Biol Chem 278(10):8516-8525.

Liguzinski P, Korzeniewski B. 2006. How to keep glycolytic metabolite concentrations constant when ATP/ADP and NADH/NAD+ change. Syst Biol (Stevenage) 153(5):332-334.

Lim JH, Lee YM, Chun YS, Chen J, Kim JE, Park JW. 2010. Sirtuin 1 modulates cellular responses to hypoxia by deacetylating hypoxia-inducible factor 1alpha. Mol Cell 38(6):864-878.

Linossier MT, Dormois D, Perier C, Frey J, Geyssant A, Denis C. 1997. Enzyme adaptations of human skeletal muscle during bicycle short-sprint training and detraining. Acta Physiol Scand 161(4):439-445.

Little JP, Safdar A, Cermak N, Tarnopolsky MA, Gibala MJ. 2010. Acute endurance exercise increases the nuclear abundance of PGC-1alpha in trained human skeletal muscle. Am J Physiol Regul Integr Comp Physiol 298(4):R912-917.

Locasale JW, Cantley LC. 2011. Metabolic flux and the regulation of mammalian cell growth. Cell Metab 14(4):443-451.

Loenneke JP, Thiebaud RS, Abe T. 2014. Does blood flow restriction result in skeletal muscle damage? A critical review of available evidence. Scand J Med Sci Sports 24(6):e415-422.

Lowry CV, Kimmey JS, Felder S, Chi MM, Kaiser KK, Passonneau PN, Kirk KA, Lowry OH. 1978. Enzyme patterns in single human muscle fibers. J Biol Chem 253(22):8269-8277.

Maclntosh B, Gardiner P, McComas A. 2005. Skeletal muscle form and function.

Manasek FJ, Burnside B, Stroman J. 1972. The sensitivity of developing cardiac myofibrils to cytochalasin-B (electron microscopy-polarized light-Z-bands-heartbeat). Proc Natl Acad Sci U S A 69(2):308-312.

Mathai JC, Sauna ZE, John O, Sitaramam V. 1993. Rate-limiting step in electron transport. Osmotically sensitive diffusion of quinones through voids in the bilayer. J Biol Chem 268(21):15442-15454.

McGee SL, Hargreaves M. 2011. Histone modifications and exercise adaptations. J Appl Physiol (1985) 110(1):258-263.

McKenna MC, Waagepetersen HS, Schousboe A, Sonnewald U. 2006. Neuronal and astrocytic shuttle mechanisms for cytosolic-mitochondrial transfer of reducing equivalents: current evidence and pharmacological tools. Biochem Pharmacol 71(4):399-407.

McKinsey TA, Zhang CL, Lu J, Olson EN. 2000. Signal-dependent nuclear export of a histone deacetylase regulates muscle differentiation. Nature 408(6808):106-111.

McMahon S, Jenkins D. 2002. Factors affecting the rate of phosphocreatine resynthesis following intense exercise. Sports Med 32(12):761-784.

Michelle Furtado L, Poon V, Klip A. 2003. GLUT4 activation: thoughts on possible mechanisms. Acta Physiol Scand 178(4):287-296.

Middelbeek RJ, Chambers MA, Tantiwong P, Treebak JT, An D, Hirshman MF, Musi N, Goodyear LJ. 2013. Insulin stimulation regulates AS160 and TBC1D1 phosphorylation sites in human skeletal muscle. Nutr Diabetes 3:e74.

Mitsumoto Y, Burdett E, Grant A, Klip A. 1991. Differential expression of the GLUT1 and GLUT4 glucose transporters during differentiation of L6 muscle cells. Biochem Biophys Res Commun 175(2):652-659.

Morales-Alamo D, Calbet JA. 2016. AMPK signaling in skeletal muscle during exercise: Role of reactive oxygen and nitrogen species. Free Radic Biol Med.

Motta MC, Divecha N, Lemieux M, Kamel C, Chen D, Gu W, Bultsma Y, McBurney M, Guarente L. 2004. Mammalian SIRT1 represses forkhead transcription factors. Cell 116(4):551-563.

Mounier R, Theret M, Lantier L, Foretz M, Viollet B. 2015. Expanding roles for AMPK in skeletal muscle plasticity. Trends Endocrinol Metab 26(6):275-286.

Musi N, Fujii N, Hirshman MF, Ekberg I, Froberg S, Ljungqvist O, Thorell A, Goodyear LJ. 2001. AMP-activated protein kinase (AMPK) is activated in muscle of subjects with type 2 diabetes during exercise. Diabetes 50(5):921-927.

Nakashima K, Yakabe Y. 2007. AMPK activation stimulates myofibrillar protein degradation and expression of atrophy-related ubiquitin ligases by increasing FOXO transcription factors in C2C12 myotubes. Biosci Biotechnol Biochem 71(7):1650-1656.

Nedachi T, Kadotani A, Ariga M, Katagiri H, Kanzaki M. 2008. Ambient glucose levels qualify the potency of insulin myogenic actions by regulating SIRT1 and FoxO3a in C2C12 myocytes. Am J Physiol Endocrinol Metab 294(4):E668-678.

Newhouse K, Hsuan SL, Chang SH, Cai B, Wang Y, Xia Z. 2004. Rotenone-induced apoptosis is mediated by p38 and JNK MAP kinases in human dopaminergic SH-SY5Y cells. Toxicol Sci 79(1):137-146.

Nikiforov A, Kulikova V, Ziegler M. 2015. The human NAD metabolome: Functions, metabolism and compartmentalization. Crit Rev Biochem Mol Biol:1-14.

Novellasdemunt L, Bultot L, Manzano A, Ventura F, Rosa JL, Vertommen D, Rider MH, Navarro-Sabate A, Bartrons R. 2013. PFKFB3 activation in cancer cells by the p38/MK2 pathway in response to stress stimuli. Biochem J 452(3):531-543.

O'Neill HM. 2013. AMPK and Exercise: Glucose Uptake and Insulin Sensitivity. Diabetes Metab J 37(1):1-21.

O'Neill HM, Maarbjerg SJ, Crane JD, Jeppesen J, Jorgensen SB, Schertzer JD, Shyroka O, Kiens B, van Denderen BJ, Tarnopolsky MA, Kemp BE, Richter EA, Steinberg GR. 2011. AMP-activated protein kinase (AMPK) beta1beta2 muscle null mice reveal an essential role for AMPK in maintaining mitochondrial content and glucose uptake during exercise. Proc Natl Acad Sci U S A 108(38):16092-16097.

Ortenblad N, Nielsen J. 2015. Muscle glycogen and cell function - Location, location, location. Scand J Med Sci Sports 25 Suppl 4:34-40.

Ozcan S, Dover J, Johnston M. 1998. Glucose sensing and signaling by two glucose receptors in the yeast Saccharomyces cerevisiae. EMBO J 17(9):2566-2573.

Pedersen BK, Saltin B. 2015. Exercise as medicine - evidence for prescribing exercise as therapy in 26 different chronic diseases. Scand J Med Sci Sports 25 Suppl 3:1-72.

Pehmoller C, Treebak JT, Birk JB, Chen S, Mackintosh C, Hardie DG, Richter EA, Wojtaszewski JF. 2009. Genetic disruption of AMPK signaling abolishes both contraction- and insulin-stimulated TBC1D1 phosphorylation and 14-3-3 binding in mouse skeletal muscle. Am J Physiol Endocrinol Metab 297(3):E665-675.

Pelletier A, Joly E, Prentki M, Coderre L. 2005. Adenosine 5'-monophosphate-activated protein kinase and p38 mitogen-activated protein kinase participate in the stimulation of glucose uptake by dinitrophenol in adult cardiomyocytes. Endocrinology 146(5):2285-2294.

Pesce MA, Bodourian SH, Nicholson JF. 1975. Rapid kinetic measurement of lactate in plasma with a centrifugal analyzer. Clin Chem 21(13):1932-1934.

Peters SJ, Harris RA, Heigenhauser GJ, Spriet LL. 2001. Muscle fiber type comparison of PDH kinase activity and isoform expression in fed and fasted rats. Am J Physiol Regul Integr Comp Physiol 280(3):R661-668.

Pilegaard H, Saltin B, Neufer PD. 2003. Exercise induces transient transcriptional activation of the PGC-1alpha gene in human skeletal muscle. J Physiol 546(Pt 3):851-858.

Pittelli M, Formentini L, Faraco G, Lapucci A, Rapizzi E, Cialdai F, Romano G, Moneti G, Moroni F, Chiarugi A. 2010. Inhibition of nicotinamide phosphoribosyltransferase: cellular bioenergetics reveals a mitochondrial insensitive NAD pool. J Biol Chem 285(44):34106-34114.

Powers SK, Nelson WB, Hudson MB. 2011. Exercise-induced oxidative stress in humans: cause and consequences. Free Radic Biol Med 51(5):942-950.

Prosser BL, Ward CW, Lederer WJ. 2011. X-ROS signaling: rapid mechano-chemo transduction in heart. Science 333(6048):1440-1445.

Rardin MJ, Wiley SE, Naviaux RK, Murphy AN, Dixon JE. 2009. Monitoring phosphorylation of the pyruvate dehydrogenase complex. Anal Biochem 389(2):157-164.

Revollo JR, Grimm AA, Imai S. 2004. The NAD biosynthesis pathway mediated by nicotinamide phosphoribosyltransferase regulates Sir2 activity in mammalian cells. J Biol Chem 279(49):50754-50763.

Richter EA, Hargreaves M. 2013. Exercise, GLUT4, and skeletal muscle glucose uptake. Physiol Rev 93(3):993-1017.

Rocha M, Diaz-Morales N, Rovira-Llopis S, Escribano-Lopez I, Banuls C, Hernandez-Mijares A, Diamanti-Kandarakis E, Victor VM. 2016. Mitochondrial dysfunction and endoplasmic reticulum stress in diabetes. Curr Pharm Des.

Rodgers JT, Lerin C, Haas W, Gygi SP, Spiegelman BM, Puigserver P. 2005. Nutrient control of glucose homeostasis through a complex of PGC-1alpha and SIRT1. Nature 434(7029):113-118.

Rohas LM, St-Pierre J, Uldry M, Jager S, Handschin C, Spiegelman BM. 2007. A fundamental system of cellular energy homeostasis regulated by PGC-1alpha. Proc Natl Acad Sci U S A 104(19):7933-7938.

Romanello V, Guadagnin E, Gomes L, Roder I, Sandri C, Petersen Y, Milan G, Masiero E, Del Piccolo P, Foretz M, Scorrano L, Rudolf R, Sandri M. 2010. Mitochondrial fission and remodelling contributes to muscle atrophy. EMBO J 29(10):1774-1785.

Ryall JG, Dell'Orso S, Derfoul A, Juan A, Zare H, Feng X, Clermont D, Koulnis M, Gutierrez-Cruz G, Fulco M, Sartorelli V. 2015. The NAD(+)-dependent SIRT1 deacetylase translates a metabolic switch into regulatory epigenetics in skeletal muscle stem cells. Cell Stem Cell 16(2):171-183.

Sahlin K. 1985. NADH in human skeletal muscle during short-term intense exercise. Pflugers Arch 403(2):193-196.

Sahlin K, Gorski J, Edstrom L. 1990. Influence of ATP turnover and metabolite changes on IMP formation and glycolysis in rat skeletal muscle. Am J Physiol 259(3 Pt 1):C409-412.

Sahlin K, Katz A, Henriksson J. 1987. Redox state and lactate accumulation in human skeletal muscle during dynamic exercise. Biochem J 245(2):551-556.

Sasaki T, Nakata R, Inoue H, Shimizu M, Inoue J, Sato R. 2014. Role of AMPK and PPARgamma1 in exercise-induced lipoprotein lipase in skeletal muscle. Am J Physiol Endocrinol Metab 306(9):E1085-1092.

Sauve AA, Wolberger C, Schramm VL, Boeke JD. 2006. The biochemistry of sirtuins. Annu Rev Biochem 75:435-465.

Schiaffino S, Reggiani C. 2011. Fiber types in mammalian skeletal muscles. Physiol Rev 91(4):1447-1531.

Schmitz JP, Groenendaal W, Wessels B, Wiseman RW, Hilbers PA, Nicolay K, Prompers JJ, Jeneson JA, van Riel NA. 2013. Combined in vivo and in silico investigations of activation of glycolysis in contracting skeletal muscle. Am J Physiol Cell Physiol 304(2):C180-193.

Semenza GL. 2000. HIF-1: mediator of physiological and pathophysiological responses to hypoxia. J Appl Physiol (1985) 88(4):1474-1480.

Seo KS, Park JH, Heo JY, Jing K, Han J, Min KN, Kim C, Koh GY, Lim K, Kang GY, Uee Lee J, Yim YH, Shong M, Kwak TH, Kweon GR. 2015. SIRT2 regulates tumour hypoxia response by promoting HIF-1alpha hydroxylation. Oncogene 34(11):1354-1362.

Shimokawa T, Kato M, Ezaki O, Hashimoto S. 1998. Transcriptional regulation of muscle-specific genes during myoblast differentiation. Biochem Biophys Res Commun 246(1):287-292.

Slot IG, Schols AM, Vosse BA, Kelders MC, Gosker HR. 2014. Hypoxia differentially regulates muscle oxidative fiber type and metabolism in a HIF-1alpha-dependent manner. Cell Signal 26(9):1837-1845.

Slysz J, Stultz J, Burr JF. 2015. The efficacy of blood flow restricted exercise: A systematic review & meta-analysis. J Sci Med Sport.

Somwar R, Kim DY, Sweeney G, Huang C, Niu W, Lador C, Ramlal T, Klip A. 2001. GLUT4 translocation precedes the stimulation of glucose uptake by insulin in muscle cells: potential activation of GLUT4 via p38 mitogen-activated protein kinase. Biochem J 359(Pt 3):639-649.

Somwar R, Koterski S, Sweeney G, Sciotti R, Djuric S, Berg C, Trevillyan J, Scherer PE, Rondinone CM, Klip A. 2002. A dominant-negative p38 MAPK mutant and novel selective inhibitors of p38 MAPK reduce insulin-stimulated glucose uptake in 3T3-L1 adipocytes without affecting GLUT4 translocation. J Biol Chem 277(52):50386-50395.

Somwar R, Perreault M, Kapur S, Taha C, Sweeney G, Ramlal T, Kim DY, Keen J, Cote CH, Klip A, Marette A. 2000. Activation of p38 mitogen-activated protein kinase alpha and beta by insulin and contraction in rat skeletal muscle: potential role in the stimulation of glucose transport. Diabetes 49(11):1794-1800.

Spriet LL, Howlett RA, Heigenhauser GJ. 2000. An enzymatic approach to lactate production in human skeletal muscle during exercise. Med Sci Sports Exerc 32(4):756-763.

St-Pierre J, Buckingham JA, Roebuck SJ, Brand MD. 2002. Topology of superoxide production from different sites in the mitochondrial electron transport chain. J Biol Chem 277(47):44784-44790.

Sugden MC, Holness MJ. 2006. Mechanisms underlying regulation of the expression and activities of the mammalian pyruvate dehydrogenase kinases. Arch Physiol Biochem 112(3):139-149.

Susztak K, Raff AC, Schiffer M, Bottinger EP. 2006. Glucose-induced reactive oxygen species cause apoptosis of podocytes and podocyte depletion at the onset of diabetic nephropathy. Diabetes 55(1):225-233.

Sweeney G, Somwar R, Ramlal T, Volchuk A, Ueyama A, Klip A. 1999. An inhibitor of p38 mitogen-activated protein kinase prevents insulin-stimulated glucose transport but not glucose transporter translocation in 3T3-L1 adipocytes and L6 myotubes. J Biol Chem 274(15):10071-10078.

Team R-C. 2015. R: A language and environment for statistical computing. R Foundation for Statistical Computing. Vienna.

Thevis M, Schanzer W. 2016. Emerging drugs affecting skeletal muscle function and mitochondrial biogenesis - Potential implications for sports drug testing programs. Rapid Commun Mass Spectrom 30(5):635-651.

Thorens B, Mueckler M. 2010. Glucose transporters in the 21st Century. Am J Physiol Endocrinol Metab 298(2):E141-145.

Thorstensson A, Sjodin B, Karlsson J. 1975. Enzyme activities and muscle strength after "sprint training" in man. Acta Physiol Scand 94(3):313-318.

Turban S, Beardmore VA, Carr JM, Sakamoto K, Hajduch E, Arthur JS, Hundal HS. 2005. Insulin-stimulated glucose uptake does not require p38 mitogen-activated protein kinase in adipose tissue or skeletal muscle. Diabetes 54(11):3161-3168.

Ussher JR, Jaswal JS, Lopaschuk GD. 2012. Pyridine nucleotide regulation of cardiac intermediary metabolism. Circ Res 111(5):628-641.

Van Noorden CJ, Butcher RG. 1989. The involvement of superoxide anions in the nitro blue tetrazolium chloride reduction mediated by NADH and phenazine methosulfate. Anal Biochem 176(1):170-174.

Vichaiwong K, Purohit S, An D, Toyoda T, Jessen N, Hirshman MF, Goodyear LJ. 2010. Contraction regulates site-specific phosphorylation of TBC1D1 in skeletal muscle. Biochem J 431(2):311-320.

Volkov AN, van Nuland NA. 2012. Electron transfer interactome of cytochrome C. PLoS Comput Biol 8(12):e1002807.

WADA. 2016. Prohibited List.4.

Wagenknecht B, Lieberman M. 1991. Adenine nucleotide degradation in cultured chick heart muscle cells. Mol Cell Biochem 107(2):119-125.

Wagner TC, Scott MD. 1994. Single extraction method for the spectrophotometric quantification of oxidized and reduced pyridine nucleotides in erythrocytes. Anal Biochem 222(2):417-426.

Weiss S, Rossi R, Pellegrino MA, Bottinelli R, Geeves MA. 2001. Differing ADP release rates from myosin heavy chain isoforms define the shortening velocity of skeletal muscle fibers. J Biol Chem 276(49):45902-45908.

Williamson DH, Lund P, Krebs HA. 1967. The redox state of free nicotinamide-adenine dinucleotide in the cytoplasm and mitochondria of rat liver. Biochem J 103(2):514-527.

Wojtaszewski JF, Higaki Y, Hirshman MF, Michael MD, Dufresne SD, Kahn CR, Goodyear LJ. 1999. Exercise modulates postreceptor insulin signaling and glucose transport in muscle-specific insulin receptor knockout mice. J Clin Invest 104(9):1257-1264.

Xi X, Han J, Zhang JZ. 2001. Stimulation of glucose transport by AMP-activated protein kinase via activation of p38 mitogen-activated protein kinase. J Biol Chem 276(44):41029-41034.

Xie Z, Dong Y, Zhang M, Cui MZ, Cohen RA, Riek U, Neumann D, Schlattner U, Zou MH. 2006. Activation of protein kinase C zeta by peroxynitrite regulates LKB1-dependent AMP-activated protein kinase in cultured endothelial cells. J Biol Chem 281(10):6366-6375.

Yamamoto T, Byun J, Zhai P, Ikeda Y, Oka S, Sadoshima J. 2014. Nicotinamide mononucleotide, an intermediate of NAD+ synthesis, protects the heart from ischemia and reperfusion. PLoS One 9(6):e98972.

Yang T, Chan NY, Sauve AA. 2007. Syntheses of nicotinamide riboside and derivatives: effective agents for increasing nicotinamide adenine dinucleotide concentrations in mammalian cells. J Med Chem 50(26):6458-6461.

Ying W. 2008. NAD+/NADH and NADP+/NADPH in cellular functions and cell death: regulation and biological consequences. Antioxid Redox Signal 10(2):179-206.

Yoshino J, Mills KF, Yoon MJ, Imai S. 2011. Nicotinamide mononucleotide, a key NAD(+) intermediate, treats the pathophysiology of diet- and age-induced diabetes in mice. Cell Metab 14(4):528-536.

Yu PB, Hong CC, Sachidanandan C, Babitt JL, Deng DY, Hoyng SA, Lin HY, Bloch KD, Peterson RT. 2008. Dorsomorphin inhibits BMP signals required for embryogenesis and iron metabolism. Nat Chem Biol 4(1):33-41.

Zhang X, Rojas JC, Gonzalez-Lima F. 2006. Methylene blue prevents neurodegeneration caused by rotenone in the retina. Neurotox Res 9(1):47-57.

Zmijewski JW, Banerjee S, Bae H, Friggeri A, Lazarowski ER, Abraham E. 2010. Exposure to hydrogen peroxide induces oxidation and activation of AMP-activated protein kinase. J Biol Chem 285(43):33154-33164.

Zong H, Ren JM, Young LH, Pypaert M, Mu J, Birnbaum MJ, Shulman GI. 2002. AMP kinase is required for mitochondrial biogenesis in skeletal muscle in response to chronic energy deprivation. Proc Natl Acad Sci U S A 99(25):15983-15987.

VITA

Chia George Hsu

George was born in Taipei, Taiwan. He received a B.S. in Chemistry from National Cheng Kung University in 2001, where he was a president of the NCKU bodybuilding club. He received a M.A. in Exercise science from National Taiwan Sport University. Beginning in 2004 he spent 5 years as an assistant researcher at National Sports Training Center in Kaohsiung, Taiwan before coming to Georgia Tech to pursue a doctorate in Applied Physiology.